Title
Tying Trophic Ecology with Chemical Pollution in California Coastal Ecosystems

Author
Bezerra, Moises Fernandes

Publication Date
2021

Peer reviewed|Thesis/dissertation

Tying Trophic Ecology with Chemical Pollution in California Coastal Ecosystems

By

MOISES FERNANDES BEZERRA
DISSERTATION

Submitted in partial satisfaction of the requirements for the degree of

DOCTOR OF PHILOSOPHY

in

Joint Doctoral Program in Ecology

in the

OFFICE OF GRADUATE STUDIES

of the

UNIVERSITY OF CALIFORNIA

DAVIS

Approved:

Chun-Ta Lai, Chair

John Largier

Andrew Whitehead

2021

Acknowledgements

Firstly, I would like to express my sincere gratitude to my advisor Prof. Chun-Ta Lai for the collaboration while conducting my Ph.D study and related research, for his patience, and motivation.

Besides my advisor, I would like to thank the rest of my thesis committee: Prof. John Largier, and Prof. Andrew Whitehead, for their insightful comments and encouragement, but also for the hard question which incented me to widen my research from various perspectives.

My sincere thanks also goes to Dr. Jeff Seminoff, Dr. John Largier, Dr. Darel Slotton, and Dr. Eunha Hoh, who provided me an opportunity to join their team, and who gave access to the laboratory and research facilities. Without they precious support it would not be possible to conduct this research.

Last but not the least, I would like to thank my family: my wife, my son, and my parents for supporting me spiritually throughout pursuing this goal and writing this dissertation.

ABSTRACT

Batoids are animals of the Chondrichthyan group comprising stingrays, skates and guitarfishes. In California coast, batoids, such as bat-rays, shovelnose guitarfish and round stingrays, inhabits coastal areas that can be impacted by overfishing, habitat degradation and pollution. These animals play the role of mesopredators and can have large effect on the structure and function of benthic communities. Paradoxically, habitat use and feeding ecology of batoid species are poorly understood as well as their exposure risk and accumulation patterns of contaminants, such as Hg. Considering that most batoids has a life-cycle strongly associated to bottom sediments of benthic habitats, which is an important site deposition and partitioning processes for many pollutants, these animals might be in risk of higher exposure to these pollutants and exposed to deleterious effects. This research aims to describe the habitat use of batoids species occurring in San Diego Bay, Southern California, and Tomales Bay, Central California, and assess their exposure levels to pollutants. In chapter 1, I present an extensive systematic review of the scientific literature on the fate of trace metals and POPs in batoids with the goal of describing the current state of environmental contamination in batoid. In chapter 2, I describe trophic interactions of three sympatric batoid species inhabiting an urbanized estuary using carbon ($\delta^{13}C$) and nitrogen ($\delta^{15}N$) stable isotopes and total Hg (THg) as ecological tracers. I also assess THg accumulation in two populations of *Myliobatis californica* while accounting for changes in trophic structure, diet sources, and contamination background. In chapter 3, I describe and compare Hg bioaccumulation and biomagnification between two estuarine food-webs in California coast assessing temporal and spatila variation in Hg levels, and which factors best explain these variations.

INTRODUCTION

Batoids are fishes of the Chondrichthyes group comprising stingrays, skates and guitarfishes (Ebert and Compagno, 2007; Fowler et al., 2005). In California coast, batoids, such as bat-rays, shovelnose guitarfish and round stingrays, inhabits coastal areas that can be impacted by overfishing, habitat degradation and pollution. These animals are benthic top predators and can potentially play important role in trophic dynamics of benthic communities (Myers et al., 2007). Although overexploitation and habitat degradation are shown as the two biggest threats to elasmobranch populations (Dulvy et al., 2014), coastal and oceanic pollution can potentially be another important factor contributing to population disruption.

Trophic ecology of batoids is poorly understood compared to sharks and teleost fishes (Vaudo and Heithaus, 2012). Diets vary regionally in many coastal batoid species, especially those with wide distributions. A few studies have addressed feeding ecology of batoids in California coast. In Humboldt Bay and Tomales Bay (TB), the diet of Bat-rays (*Myliobatis californica*) is shown to consist predominantly of benthic invertebrates with main prey items differing between locations potentially due to an opportunist/generalist behavior and distinct prey item composition (Gray et al., 1997; Matern et al., 2000; Ridge, 1963). Foraging strategy of this species consist on resuspending mud flat sediments seeking for infauna and epibenthic invertebrates (Gray et al., 1997; Matern et al., 2000). Batoid diet vary among species, among size classes within the same species and among individuals in the same foraging location, especially for species with generalist and opportunist feeding behaviors (Babel, 1967; Valadez-Gonzalez et al., 2001). The generalist and opportunist foraging behavior of these species explain their diet variation among habitats comprising different benthic fauna.

Environmental pollution is a worldwide concern and evaluating contamination impacts using only measurements in water, air and sediment samples are challenging. Pollutants have varied persistence and mobility on the environment, with specific affinities to different elements, which makes it difficult to

follow their fate without a comprehensive understanding of local geochemistry dynamics and using biological components in the assessment (Manahan, 2010).

Many pollutants tend to bioaccumulate in living organisms resulting in an increase of its concentrations in consumers occupying higher trophic levels of the food web (i.e.biomagnification) (Muto et al., 2014). Therefore, in systems where top predators (i.e. sharks; mackerel) are historically overexploited with their abundance reduced, mesopredators have the potential to provide valuable information as bioindicators of environmental pollution (Allen et al., 2002; Jackson et al., 2001; Myers et al., 2007).

In southern California, bays and estuaries provide valuable ecological services to a variety of marine organisms. These areas are vital in the life cycle of an incredible diversity of species by providing protected shelters against predation, nursery habitats, food sources and strategic reproduction sites (Dale et al., 2011; Gray et al., 1997; Szoboszlai et al., 2015). As a coastal zone under an arid climate, ecological features such as hydrography, water physico-chemistry and fish assemblage are controlled by marine drivers due to the limited freshwater inputs common in this region (Allen et al., 2006). Consequently, these ecosystems often present low trophic complexity, where marine mesopredators can regulate food web structure and in which batoids have significant importance (Barría et al., 2015; Farrugia et al., 2014, 2011; Matern et al., 2000). From the perspective of the integrated Hg monitoring program proposed by Evers et al., (2008), batoids can be classified as bioindicators of contamination in coastal areas, especially in bays and estuaries. Batoids are ubiquitous and abundant in many coastal zones worldwide with many species being used for human consumption (Gassel et al., 2013). Batoids generally feed on secondary and above trophic levels, which increase their exposure and accumulation of pollutants through diet.

The present study is divided in three chapters, each aiming to address a fundamental question regarding batoids trophic ecology and contamination. In chapter 1, I ask: is chemical pollution a cause of concern in batoids? Using a systematic literature review and meta-analysis, I describe the major pollutants found in this elasmobranch group and identify areas and species with contamination concerns. In chapter 2, I ask: how trophic interaction and habitat use affect Hg uptake in batoids? Using multiple ecological tracers and

Bayesian statistical models, I characterize trophic interactions, diet proportions, and contamination niches of three sympatric batoid species in an urbanized estuary in California coast. In Chapter 3, I ask: do Hg levels and biomagnification vary temporally and spatially in aquatic biota of two estuaries with distinct Hg backgrounds and sources? Using Hg levels quantified in mollusks, crustaceans, elasmobranchs, and teleost fishes across multiple decades from two study sites, I identify patterns and trends in Hg accumulation, and estimate biomagnification rates for batoids' food webs.

CHAPTER 1 - Trace Metals and Persistent Organic Pollutants Contamination in Batoids (Chondrichthyes: Batoidea): A Systematic Review.

M.F. Bezerra et al. / *Environmental Pollution* 248 (2019) 684 – 695

Environmental Pollution 248 (2019) 684–695

Contents lists available at ScienceDirect

Environmental Pollution

journal homepage: www.elsevier.com/locate/envpol

Trace metals and persistent organic pollutants contamination in batoids (Chondrichthyes: Batoidea): A systematic review☆

Moises F. Bezerra [a, c, *], Luiz D. Lacerda [b], Chun-Ta Lai [a]

[a] Department of Biology, San Diego State University, San Diego, CA, 92182-4614, USA
[b] Instituto de Ciências do Mar, Universidade Federal do Ceará, Fortaleza, CE, 60165-081, Brazil
[c] Graduate Group in Ecology, University of California Davis, Davis, CA, 95616, USA

Abstract

Batoids (Chondrichthyes: Batoidea; e.g. stingrays, skates, and guitarfish) comprise more than 55% of elasmobranch taxa and represent ecologically important predators in benthic and pelagic habitats. Although overexploitation and habitat degradation are the two biggest threats to batoid populations, coastal and oceanic pollution is also a pervasive potential threat. In this systematic review, we compile published scientific literature on trace metals and persistent organic pollutants (POPs) contamination in elasmobranch species of the Batoidea superorder and present contamination patterns, exposure effects, and potential human exposure risks to most reported contaminants. We found batoids to accumulate a wide range of trace metals, including mercury (Hg), arsenic (As), lead (Pb), copper (Cu), cadmium (Cd) and zinc (Zn). Accumulation of POPs is reported for chlordanes, dichlorodiphenyltrichloroethane (DDT), polychlorinated biphenyl (PCB), dieldrin, Heptachlor epoxide, hexachlorobenzene and perfluoroalkyl substances (PFAS). Hg levels in muscle tissue were significantly different among oceanic basins and habitats, consistent with previous global assessments of Hg oceanic background levels. Some batoid species presented Hg levels higher than large pelagic teleost fishes and comparable to sharks. Ecological traits such as, bottom feeding, upper trophic position and elasmobranch-specific physiology and metabolism are discussed as potential factors associated with Hg uptake and accumulation in batoids. Some species exceeded USEPA's maximum contamination safety limits in edible tissues for Hg, As and ΣPCBs. For most trace metals and POPs, there is a lack of studies focusing on contamination levels in batoids. We recommend future research increasing reporting on POPs and trace metals besides Hg in batoids to further investigate the role of Elasmobranch as a bioindicator for marine pollution.

Introduction

Increased nutrient loads, solid waste discharges, oil spills, untreated sewage, radioactive wastes and chemical discharges by industries and urban run-off are all pervasive threats to oceanic and coastal ecosystems (Derraik, 2002; Kitsiou and Karydis, 2011; Vikas and Dwarakish, 2015). Among these, trace metal and persistent organic pollutant (POP) contamination from anthropogenic sources is one of the most widespread human footprints in the Anthropocene (Gałuszka et al., 2014). Anthropogenic activities can alter natural geochemical background and cycling of these elements, increasing uptake of toxic compounds by primary producers and building up along the food web resulting in deleterious effects on aquatic biota (Chopra et al., 2011; de Souza Machado et al., 2016; El-Shahawi et al., 2010; Gałuszka et al., 2014).

Trace metals are metallic elements found in trace amounts in the environment that can be either an essential nutrient (e.g. iron (Fe), zinc (Zn), selenium (Se)) or a toxicant (e.g. mercury (Hg), lead (Pb), cadmium (Cd), arsenic (As)), depending on their concentrations in organisms and/or their specific role in biological metabolism (e.g. copper (Cu) is an essential trace metal because of its role in respiratory proteins found in the Mollusca and Arthropoda) (Morel and Price, 2007). POPs such as, polychlorinated biphenyls (PCBs), chlordanes (CHLs) and dichlorodiphenyl-trichloroethane (DDT) are toxic chemicals, resistant to biodegradation and have no known function in biological metabolism. These pollutants are often found accumulating in aquatic biota with a tendency of biomagnification in the food web (Jones and de Voogt, 1999).

Chronic and acute exposure to non-essential trace metals have been studied in many teleost fish species and are known to cause a reduction in reproductive success, immunosuppression and oxidative stress to tissue cells (Baatrup, 1991; Rajeshkumar et al., 2013; Vieira et al., 2009). Similarly, chronic and acute exposures to POPs are hypothesized in association with impaired development, reduced reproductive success and increased carcinogenic effect in many aquatic organisms (Harmon, 2015). Therefore, environmental exposure to trace metals and POPs has the potential to indirectly impact entire populations

and communities through the cascading effects of impaired metabolic and reproductive functions of organisms exposed to these pollutants (Fleeger et al., 2003).

Elasmobranchs (e.g. sharks, rays, chimeras) are highly susceptible to accumulation of environmental pollution, in general, due to their intrinsic biological and ecological traits (e.g. slow growth, late maturation, low reproductive output) (Dulvy et al., 2017, 2008; Pierce and Bennett, 2010). Although overexploitation and habitat degradation are suggested as the most significant threats to elasmobranch populations (Dulvy et al., 2014), coastal and oceanic pollution represent a potential additional threat with unknown consequences to this taxonomic group. Similar to teleost fishes, elasmobranchs accumulate water-borne pollutants but likely to a larger extent, as observed for some trace metals, such as silver and copper, under controlled laboratory experiments (De Boeck et al., 2001; Grosell et al., 2003; Webb and Wood, 2000). Paradoxically, there are few numbers of studies investigating trace metal and POP contamination in elasmobranch, and fewer publications focusing only on batoids (Gelsleichter and Walker, 2010).

The term batoids is used here to identify cartilaginous fish encompassing the superorder Batoidea which is further sub-divided in four orders: Rajiformes, with suborder of Rhinobatoidei (guitarfishes) and Rajoidea (skates), Pristiformes (sawfishes), Torpediniformes (electric rays), and Myliobatiformes (stingrays) (Aschliman, 2011; Ebert and Compagno, 2007). These organisms differ from sharks by their dorso-ventrally flattened body morphology conferring them a widespread distribution in coastal and oceanic environments, most commonly found in benthic and demersal habitats. Some batoid species play crucial ecological functions in their food webs by directly (e.g. predation) or indirectly (e.g. bioturbation) structuring benthic communities (Bornatowski et al., 2014; Myers et al., 2007; Pierce et al., 2011). Their life history is directly linked to the bottom substrate where trace metals and organic contaminants often accumulate, increasing their exposure potential (de Souza Machado et al., 2016).

In this paper, we conduct an extensive systematic review of the scientific literature on the fate of trace metals and POPs in batoids. Our purpose is to present a general view of contamination in batoid taxa that

could help understanding distribution of pervasive pollutants in marine ecosystems. To guide this review, we aim to address the following questions: 1. What are the most common contaminants found in batoids? How do batoid's contamination level differs from teleost fishes occupying similar habitats? 2. Are there geographical differences in contaminant levels found in batoid tissues? 3. What is human's risk of exposure to contaminants through consumption of batoids?

Material and methods

The present review identifies research papers related to marine pollution in batoids by adopting a systematic quantitative framework proposed by Pickering & Byrne (2014). Selection criteria included papers published in the English language and institutional reports that provided detailed results of pollutant levels in any batoid species throughout the world. Academic theses, dissertations, and monographs were considered in our discussion but were not included in our meta-analysis as these are not broadly available online and often not subjected to a peer-review process. Online databases such as, Web of Science; Science Direct; Scopus; and Google Scholar, were searched using the following keywords: '*batoids'* '*contamination'* '*copper'* '*elasmobranch'* '*guitarfish'* '*mercury'* '*myliobatodei'* '*organic compounds'* '*pollution'* 'POPs' '*rhinobatodei'* '*rajoidei'* '*rajiformes'* '*skates'* '*stingray'* '*trace metal'* '*torpedinoidei'*. Keywords were used in combination or as a search refining term to improve result outputs. Additional searches were conducted in the reference list of papers to identify studies published in regional journals not included in the mentioned database. Literature surveyed included published papers available at mentioned databases by December 2017.

General recorded information included year, journal, authors, study area, study title, species reported, species size class, sample size, tissue type, pollutant type, biological parameters measured, contamination trends reported, relationship with biological parameters, knowledge gaps highlighted, and additional notes. For trace metals, 24.8% of the results surveyed were reported on a dry weight basis for Hg levels. Because concentrations were commonly reported on a wet weight basis, we converted those reported on a

dry weight using the respective tissue moisture content and reported all the Hg concentrations on a wet weight basis in this study. POPs are reported on a lipid weight basis.

We calculated contamination ranges of contaminants using average levels reported in the literature and separated them in 6 independent groups. We used information reported in the respective paper to organize data into groups based on taxa (e.g. sub-order; family; genera and species), area of study (e.g. Barents Sea, China Sea, Laccadive Sea, Mediterranean, North Atlantic, North Pacific, North Sea, South Atlantic and South Pacific) and sex. We also separated species into groups based on preferred prey items (e.g. crustacea, crustacea/fish, fish, invertebrates, mollusk, and zooplankton), habitat zones (e.g. benthic, benthopelagic, and pelagic) and life stage (e.g. adult and juvenile) (Table S3). In addition, we assigned trophic positions to the recorded batoid species based on stomach content and stable isotope ratios previously published in the literature (Barría et al., 2015; Borrell et al., 2011; Ebert and Bizzarro, 2007; Jacobsen and Bennett, 2013; Yemışken et al., 2017)

We followed U.S. EPA and U.S. FDA's published criteria of maximum safety consumption for assessing chemical contaminant data to assess human exposure risk by batoid consumption (Depew et al., 2012; Scheuhammer et al., 2015; USEPA, 2000). A complete list of recorded papers is available in Table S1.

Statistical analysis

A descriptive statistical approach was used to identify patterns that emerged from the data. Explanatory factors tested included taxonomic groups (e.g. sub-order; family; genera and species), oceanic areas of study (e.g. Barents Sea, Laccadive Sea, Mediterranean, North Atlantic, North Pacific, North Sea, South Atlantic and South Pacific), main prey items (e.g. Crustacea, Crustacea/fish, fish, invertebrates, mollusk and zooplankton), habitat zones (e.g. benthopelagic, demersal and pelagic), life stages (e.g. adult and juvenile) and sex. When not provided by recorded papers, information about species feeding habits and life history was obtained from the literature. We performed parametric (e.g. ANOVA, Student's t) and nonparametric (e.g. Kruskal-Wallis) tests to identify significant differences among groups. We used

Generalized Linear Models – GLMs (family = Gamma) to consider factors better explaining Hg concentration variations, and examined potential confounding effects from interactions between the factors "Oceanic area", "Habitat", "Sub order", and "Main prey item. Statistical significance was set at $\alpha = 0.5$. All analysis and plots were conducted using RStudio software (R Core Team, 2017).

Results

A total of 47 publications were published between 1981 and December 2017 reporting levels of trace metal and/or POPs in batoids (Fig. 1.1). A total of 65 batoid species were reported including 25 genera from the suborders Myliobatoidei (35 species), Rajoidei (18 species), Rhinobatoidei (8 species), Torpedinoidei (3 species) and Platyrhinoidei (1 species). Major coastal and oceanic areas identified include the North Pacific Ocean (11 papers), Mediterranean Sea and North Atlantic Ocean (10 papers each), South Pacific Ocean (5 papers), China Sea, North Sea, Barents Sea and South Atlantic Ocean (2 papers each) and Laccadive Sea (1 paper). The vast majority of papers reported exclusively trace metal contamination in batoid species (35 papers). Organic contaminants were reported in 10 papers and 2 studies reported both contaminant types. Trace metal and POPs results will be presented and discussed separately. A detailed list of batoids species surveyed in this study is presented as supplementary material, along with the type of contaminants, study areas and their references (see Table S1).

A variety of tissues has been used to quantify contaminants in batoids, including brachial plate, blood, embryo, eggs, fins, gills, gut, intestine, kidney, liver, muscle, ova, and yolk. Muscle and liver tissues were the most common matrices of analysis being reported in 83% (n = 39) and 47% (n = 22) of studies, respectively. The genus *Raja* is the most represented batoid taxon, being reported in 36% (n = 17) of papers reviewed in this study. Other highly represented genera are *Dasyatis* (note this genera has recently been revised – Last et al., (2016)) and *Myliobatis* being reported in 23% (n = 11) and 17% (n = 8), respectively. The species *Raja clavata*, also known as Thornback ray, is the most reported batoid species, represented in 21% (n = 10) of papers. This species has a wide distribution range occurring in the North and South Eastern Atlantic, the Southwest Indian Ocean and the Mediterranean Sea. We found reported

contamination levels for this species mainly in the Mediterranean Sea, but also in North Sea and North Atlantic sites.

Trace metal contamination in batoids

Twenty-seven trace metals were reported in batoids (Tab. S1.1). Among these, mercury (Hg) was the most reported contaminant comprising 84% of papers (n = 31) followed by cadmium (Cd) and lead (Pb) (n = 11; 31%), zinc (Zn) (n = 10; 29%), copper (Cu) (n = 9; 26%) and arsenic (As) (n = 7; 20%). Contamination levels of most reported trace metals in muscle and liver tissues of batoids are shown in Table 1.1 along with species presenting the lowest and highest levels. Other trace metals were reported in less than 15% of papers ($n \leq 5$) including chromium (Cr), manganese (Mn), cobalt (Co), iron (Fe), nickel (Ni), selenium (Se), rubidium (Rb), strontium (Sr), palladium (Pd), rhodium (Rh), platinum (Pt), vanadium (V), bismuth (Bi), tin (Sn), antimony (Sb), barium (Ba), thallium (Tl), indium (In), molybdenum (Mo) and silver (Ag).

Due to a very limited number of studies available, we did not observe a clear global trend for most of trace metals except for Hg. Therefore, we focus most of our trace metal contamination discussion primarily on Hg levels. Clear trends of Hg contamination were observed among oceanic basins and animal sizes. Hg levels are discussed here on a wet-weight basis. Hg distributions were significantly different among oceanic basins (Kruskal Wallis chi squared = 51.4; $p < 0.001$) with the Mediterranean Sea presenting consistently higher Hg levels (Fig. 1. 3). Hg levels in muscle tissue of batoid species ranged from 0.086 to 2.42 μg Hg g^{-1} in the Mediterranean Sea (559 specimens of 10 species), 0.011 to 1.1 μg Hg g^{-1} in the North Pacific (347 specimens of 20 species), 0.039 to 0.265 μg Hg g^{-1} in the North Atlantic (416 specimens of 6 species), 0.039 to 0.129 μg Hg g^{-1} in the North Sea (49 specimens of 2 species), 0.096 to 0.350 μg Hg g^{-1} in the Barents Sea (13 specimens of 2 species), 0.004 to 2.05 μg Hg g^{-1} in the South Pacific (39 specimens of 8 species), 0.83 to 0.430 μg Hg g^{-1} in the South Atlantic (number of specimens not available; 3 species), 0.019 μg Hg g^{-1} in the Laccadive Sea (15 specimens of 1 species), and 0.040 μg Hg g^{-1} in the China Sea (5 specimens: 1 species). Species were pooled together regardless of

their feeding habits and trophic levels to observe how Hg levels varied in areas with different contamination backgrounds.

We have found no significant differences on average trophic position among oceanic basins (Kruskal-Wallis chi-squared = 4.776, df = 3, p-value = 0.189). The Mediterranean Sea dataset included benthic and pelagic species with an average trophic position of 3.43 ± 0.4. The North Pacific basin dataset included benthic and pelagic species with an average trophic position 3.48 ± 0.4. The North Atlantic basin dataset included benthic and benthopelagic species with an average trophic position of 3.57 ± 0.5. The South Pacific basin dataset included pelagic and benthic species with an average trophic position of 3.47 ± 0.4. In addition, all these oceanic basins shared species of the same genera (i.e. *Dasyatis*, *Myliobatis*, *Raja*, *Torpedo*).

Hg levels in adult specimens were significantly higher compared to juveniles (Student's $t = 3.5$; $p < 0.001$; $df = 1$). Hg concentrations were also significantly different among prey items with "Crustacea" presenting higher concentration compared to "Zooplankton" (GLM, t value = 2.045., $p = 0.04$; Fig. 1. 2a). In contrast, no significant differences were found among sub-orders and foraging habitat (GLM, $p > 0.1$) or between genders (Student's $t = -1.19$; $p = 0.2$; $df = 1$) (Fig. 1. 2).

Persistent Organic Pollutants (POPs) contamination in batoids

There were only 11 papers reporting POPs in batoids. Reported POPs include dichlorodiphenyltrichloroethane (DDTs), chlordanes (CHLs), polychlorinated biphenyls (PCBs), perfluoralkyl substances (PFAS) and polybrominated diphenyl ethers (PBDEs). PCBs, CHLs, and DDTs were the most reported contaminants accounting for 63% of papers in this category (n = 7). PFAS were reported in only two papers but in more species than any other POPs surveyed. The most analyzed tissue was liver accounting for 81% of papers in this category (n= 9). Other reported tissues include muscle, eggs, and embryo. Species were captured from four oceanic basins including the North Atlantic (2

species), the Mediterranean Sea (3 species), the North Pacific (2 species) and the South Pacific (6 species).

Total PCB levels in liver ranged from 0.2 to 9.5 $\mu g.g^{-1}$ lipid weight (2 species; 274 specimens) (Lyons et al., 2014; Weijs et al., 2015), 0.02 to 0.07 $\mu g.g^{-1}$ lipid weight for ΣDDTs (4 species; 261 specimens) (Lyons et al., 2014; Miskiewicz and Gibbs, 1994) and 0.02 to 2.5 $\mu g.g^{-1}$ lipid weight for ΣCHLs (5 species; 276 specimens) (Lyons et al., 2014; Miskiewicz and Gibbs, 1994; Weijs et al., 2015). POP levels in muscle tissue were reported in only four papers and varied from 0.005 to 3.16 $\mu g.g^{-1}$ for total PCBs (6 species; 50 specimens) (Gassel et al., 2013; Johnson-Restrepo et al., 2005; Storelli, 2008). DDTs and CHLs were reported in muscle tissue of one species (e.g. *Rhinobatos productus*) and varied from 0.002 to 0.004 $\mu g.g^{-1}$ of DDTs and non-detectable for CHLs (Gassel et al., 2013). PFAS levels were reported in muscle tissue of one specimen of *Dasyatis americana* (Senthil Kumar et al., 2009).

The highest total PCB levels found in batoids were reported in livers of *Urobatis halleri* (4.5 ± 2.4 $\mu g.g^{-1}$; n = 208) from Seal Beach, USA (Lyons et al., 2014). The highest mean values of total CHLs were found in livers of *Urolophus kapalensis, Aptychotrema rostrata* and *Myliobatis australis* (2.52 $\mu g.g^{-1}$; 1.02 $\mu g.g^{-1}$ and 0.99 $\mu g.g^{-1}$, respectively), all captured in the coast of Sidney, Australia (Miskiewicz and Gibbs, 1994). *M. australis* also presented the highest total DDTs levels (1.48 ± 5.17 $\mu g.g^{-1}$) (Miskiewicz and Gibbs, 1994). The highest total PFAS concentrations in batoids were found in livers of *D americana* (mean of 0.033 $\mu g.g^{-1}$; n = 2) and *Neotrygon kuhlii* (0.018 ± 0.027 $\mu g.g^{-1}$; n = 35) captured at the coasts of Georgia, USA, and Sidney, AUS respectively (Baduel et al., 2014; Senthil Kumar et al., 2009).

Exposure effects of POPs and trace metal on batoids

We found only five studies reporting the effects of trace metals and POPs contamination on batoids. Assessed contaminants included trace metals (e.g. Cu and Sn) (Dwivedi and Trombetta, 2006; Grosell et al., 2003), an organometallic compound (e.g. tributyltin oxide -TBTO) (Dwivedi and Trombetta, 2006) and persistent organic pollutants (e.g. DDTs, PCBs and CHLs) (Gelsleichter et al., 2006; Lyons et al.,

2014; Sawyna et al., 2017). Effects of pollutants were measured through the use of biomarkers (e.g. Na/K-ATPase activity in gill, rectal gland and intestine; EROD activity in liver; enzyme-linked immunosorbent assay (ELISA); CYP1A, heme-oxygenase (HO–1) and Hsp70 proteins expression; lipid peroxidation marker 4-hydroxynonenol) and non-biomarker parameters (e.g. total ammonia, Cl^{-}, Na^{+} and Mg^{+} in plasma; immune cell counts; morphological measures of reproductive and respiratory organs; hormone levels; and embryo development).

Discussion

The research field of environmental contamination in batoids has received relatively less attention considering that earliest papers were mainly opportunistic studies (i.e. capturing batoids as a bycatch rather than a target species) without asking specific questions about this taxonomic group. That aspect changed in the last decade, with more studies exclusively targeting batoid species to address questions concerning aspects of this taxonomic group. Likely, that shift built on our better understanding of food web function (e.g. trophic interactions associated with ecosystem stability (Gorman and Emmerson, 2009), trophic cascades in food web dynamics (Polis et al., 2000) and the potential role of elasmobranchs in ecosystem stability (i.e. top-down trophic cascades, mesopredator release) (Myers et al., 2007). Studies of environmental contamination in batoids, however, remain relatively limited. This review provides a status quo of pollutant levels in the batoid taxonomic group.

Trace metal accumulation in batoids

Relatively few studies have investigated the impacts of marine pollution in elasmobranchs (Gelsleichter and Walker, 2010), despite the fact that exposure experiments showed these organisms could be more susceptible to accumulation of and toxicity effects imposed by trace metals. As an example, some species of sharks and skates were found to be 10 times more sensitive to toxicity effects from silver exposure (De Boeck et al., 2001; Webb and Wood, 2000) and accumulated 13 times more copper in gill tissues

compared to teleost fish (Grosell et al., 2003). However, there has not been a systematic review that reports trace metals concentrations found in batoids worldwide.

Based on the reported Hg levels in batoids and teleost fishes, our survey revealed that average Hg concentrations were consistently higher in batoids compared to teleost fishes at similar trophic levels and, in some instances, comparable to levels found in top pelagic and benthic predators. In the Gulf of California, average Hg levels from 9 batoid species were found similar to those from 7 large pelagic teleosts (García-Hernández et al., 2007). When comparing fish of similar size, *D. longa*, *Dasyatis brevis* , and *Rhinoptera steindachnerii* presented higher, though not statistically significant, average Hg levels than those in the pelagic Indo-Pacific sailfish (*Istiophorus platypterus*), Blue marlin (*Makaira mazara*) and Wahoo (*Acanthocybium solandri*). These pelagic fishes are predators known to accumulate Hg to a great extent due to their upper-level position in the food web (Perelman et al., 2017; Rosas-Alayola et al., 2002). Hg levels in batoids were in the same range compared to four grouper species inhabiting the deep-water or shallow hard bottom reefs (García-Hernández et al., 2007). In another study, a remarkable result was found where *U. halleri*, a medium size invertebrate forager, presented the highest Hg levels among 40 fish species of teleost and elasmobranchs (Jonathan et al., 2015). These authors attributed this high Hg levels to the proximity to bottom sediments and intrinsic physiological traits in elasmobranch taxa.

Denton and Breck, (1981) reported average Hg levels in the demersal batoids *G. australis, Himantura uarnak, Rynchobatus dijiddensis* from northeastern Australia. Similar levels were found in teleost fishes of all comparable sizes, all of which were benthic carnivorous predators. In southeast Australia, a similar pattern was also found for *M. australis, Urolophus sp. A. rostrata* (Gibbs and Miskiewicz, 1995). In the Mediterranean Sea, specimens of *Raja* genus presented Hg levels comparable to demersal top predators (e.g. *Lophius budegassa, Lepidopus caudatus* and *Conger conger*) but lower than pelagic top predator *Thunnus alalunga* (Storelli et al., 2003b; Storelli, 2008). These findings suggest batoids inherit specific traits that are subject to accumulation of Hg in a greater extent than teleost fishes sharing similar diet and habitats. However, that hypothesis has not been tested and needs further investigation.

It is accepted that trophic position and feeding behavior are two common factors strongly related to Hg accumulation (Hall et al., 1997). Animal physiology and metabolism control elimination process and the accumulation rate of contaminants (Bradley et al., 2017; Trudel and Rasmussen, 1997). These are likely explanations for the apparent higher Hg levels in batoids relative to teleost with comparable diets. Organisms with a long lifespan associated with slow growth rates are known to present increased Hg levels in older/larger individuals (Dang and Wang, 2012). In addition, elasmobranchs present relatively large lipid-rich livers which result in greater bioaccumulation of lipophilic compounds that eventually accrues in muscle tissues due to sulfhydryl groups association to amino acids (Gelsleichter and Walker, 2010).

Geographic variation of Hg levels batoids

Among reported trace metals, Hg was the only element with enough information to assess accumulation and distribution patterns in batoids from different areas.

Figure 1.3 shows the comparison of Hg concentration in batoid species grouped by oceanic basins presenting at least ten Hg observations. Each area is composed of species feeding on various preys (e.g. crustacea, fish, mollusks, and zooplankton) in the benthic, benthopelagic, and pelagic habitats. The intra-basin variability in habitat and main prey items is not strong enough to mask the observed differences among ocean basins. The Mediterranean Sea is a semi-enclosed, Hg-enriched basin, a part of what was known as the Hg mineral belt (Rajar et al., 2007). Riverine inputs and anthropogenic emissions are the main sources of Hg in this basin (AMAP/UNEP, 2013). Rytuba (2003) showed that Mediterranean Sea coastal areas consistently accumulate recently formed submarine deposits enriched in Hg. Average Hg level in *Torpedo* and *Raja* genera in the Mediterranean Sea are four and three times higher, respectively, compared to the Pacific coast of Costa Rica. Sandoval-Herrera et al. (2016) attributed these differences to the deeper distribution of *Torpedo* population in the Mediterranean Sea (200 – 500 m depth compared to 50 - 250 m in Costa Rica). Net production of methylated Hg forms occurs primarily in deep hypoxic waters and was found to be higher in the Mediterranean Sea compared to North Pacific basin (Horvat et

al., 2003; Sunderland et al., 2009). Moreover, foraging strategy may also explain the Hg content in marine fish. Lacerda et al., (2017) observed that prey type ingested, rather than depth-specific methyl-Hg production, can explain the higher Hg levels found in tuna species feeding at different depths in the Equatorial Atlantic Ocean. This is because deeper water populations are mostly composed of carnivorous species, whereas non-carnivorous prey species predominate in surface waters in their study areas.

Two of the highest Hg levels surveyed in the present study were found in the Gulf of Trieste, Northern Adriatic Sea, an area heavily impacted by Hg mining contamination (Horvat et al., 2014). These authors found that the piscivorous species *Pteroplatytrygon violacea* presented average Hg levels roughly 4 times higher than *Pteromylaeus bovinus* foraging on benthic invertebrates in the same area. Even higher average Hg levels were found in demersal fish consumer *Torpedo nobiliana* from southern Adriatic Sea (Storelli et al., 2002b) despite the fact that Hg mining activities have had relatively small impacts in this area compared to northern Adriatic. In this case, differences in prey preference (deep-water vs. surface water preys) are likely the main driver of observed Hg contents. Also, these authors emphasize that predators closely associated with sediment and consuming a large amount of benthic fish are more susceptible to Hg accumulation than consumers of pelagic fish or benthic invertebrates (Storelli et al., 2002b, 1998). In general, high regional Hg backgrounds and foraging in favor of benthic fish preys are likely causes of high Hg levels in batoid species in these areas.

High average Hg levels were also observed in batoids from sites in the North Pacific basin (Fig. 1. 3), which includes sites in Costa Rica coast, Gulf of California and Baja in Mexico and Southern/Central California coast in the US. The highest Hg concentration in batoid species in this oceanic basin was observed in *Dasyatis longa* from Gulf of California (1.2 $\mu g.g^{-1}$ w.w.) (Ruelas-Inzunza et al., 2013) though it was based on a single specimen. In contrast, García-Hernández et al., (2007) in the same area found an average Hg level of 0.7 ± 0.26 $\mu g.g^{-1}$ w.w. for *D. longa* and with other batoid species presenting lower average Hg levels. The Gulf of California is impacted by a number of anthropogenic Hg sources, in order of importance, including gold mining and refining, Hg mining and refining, chloralkali industry, copper

smelting, residential combustion of wood, carboelectric plants and oil refining (Páez-Osuna et al., 2017). That shows there is an important source of Hg to this region, but trophic position and foraging habitat of local biota likely have major role in Hg accumulation as evidenced by the large variability among batoids species and teleost fishes with different life history traits (Escobar-Sanchez et al., 2014; García-Hernández et al., 2007; Ruelas-Inzunza et al., 2008).

The South Pacific and North Atlantic basins presented lower Hg levels on average compared to the Mediterranean and the North Pacific basins (Fig. 1. 3). All but one batoid species analyzed presented Hg levels lower than 0.24 $\mu g.g^{-1}$. In one large female *Rhinobatos armatus* (>2m of body length) from Cleveland Bay, Australia, an extremely high Hg level (2.1 $\mu g.g^{-1}$ w.w.) was found, which was comparable to the level found in sharks with similar sizes from the same area (Denton and Breck, 1981).

The observed differences among oceanic basins are consistent with previous surveys of global Hg budgets in oceanic waters (Mason et al., 2012; Sunderland et al., 2009). However, results shown in Figure 1.3 should be interpreted with caution because in our analysis, areas were not represented by the same species nor equal number of observations. Future studies need to consider potential interaction effects between interspecific variability in Hg uptake and locations once data become readily available.

We further categorized specimens into juvenile and adult groups when size information was available. We did this by following criteria that separately consider minimum sizes of maturation for each species (Araújo et al., 2016; Babel, 1967; Bizzarro et al., 2007; Cicia et al., 2009; Clarke et al., 2014; Cuevas-Zimbrón et al., 2011; Gadig et al., 2003; Jacobsen et al., 2009; Kyne and Bennett, 2002; López-García et al., 2012; McCully et al., 2012; Oddone and Velasco, 2004; Ramirez Mosqueda et al., 2012; Saglam and Ak, 2012; Smith et al., 2007; Timmons and Bray, 1997; Yeldan et al., 2009). This was consistent with previous findings where positive relationships between Hg levels and animal size have been reported in batoids (Escobar-Sanchez et al., 2014; Gutiérrez-Mejía et al., 2009; Law and Singh, 1991; Lyons et al., 2017; Sandoval-Herrera et al., 2016). All these authors show that habitat use and ontogenetic diet shifts are the major factors explaining this positive correlation.

Ontogenetic shifts are common in elasmobranchs which often is complemented by changing foraging habitat and feeding behavior (Brickle et al., 2003; Grubbs, 2010). Adults present slower metabolism and lower elimination rates of metals compared to juveniles (Gutiérrez-Mejía et al., 2009). Finally, adult elasmobranchs tend to feed on larger preys and in higher quantities (Jacobsen and Bennett, 2013) which also contribute to greater bioaccumulation and higher Hg concentrations.

Human exposure risk

Essential and non-essential trace metals in batoids, except As and Hg, were found below maximum contamination safety limits for seafood consumption (USEPA, 2000). The maximum contamination limit established for inorganic As is 0.13 $\mu g.g^{-1}$ in edible fish tissues (USEPA, 2000). This is the most conservative limit to avoid potential toxic effects induced by As inorganic forms (e.g. arsenite – As(III) and arsenate – As(V)). In the present survey, the average total As in muscle tissues of batoids was 20.9 ± 19.6 $\mu g.g^{-1}$ w.w. (Table 1.1), which is above the safety threshold. However, total As includes organic and inorganic fractions of this element. A major fraction of total As is in harmless organic As forms (e.g. arsenobetaine, arsenocholine, and tetramethylarsonium ion). De Gieter et al., (2002) assessed As speciation in 29 fish species from the North Sea and found an inorganic fraction variation from <1% to 9%. Among these fishes, elasmobranchs (e.g. *Scyliorhinus canicular* and *R. clavata*) presented two of the three highest levels of total As. Nevertheless, the inorganic fraction in these species was less than ~2%, the lowest fraction among all fish species studied by these authors. Assuming an inorganic fraction as low as 2% and an average total As concentration of 20.9 $\mu g.g^{-1}$, we calculated that batoids surveyed in our study present 0.418 $\mu g.g^{-1}$ of inorganic As, which is roughly 3 times higher than the safety threshold established by USEPA.

In comparison, toxic effects associated with Hg contamination comes from exposure to its organic form, methylmercury (Methyl-Hg), rather than Hg inorganic forms (e.g. Hg^{2+} and Hg^{0}) (Mason et al., 2012). The great affinity of Methyl-Hg to lipids results in long-term accumulations in biological tissues and deleterious effects from exposure even to relatively low environmental concentrations (Depew et al.,

2012; Fitzgerald et al., 2007). In the present study, the proportion of Methyl-Hg in surveyed batoids ranged from 71.6% to 100% (with a mean of 92.8 ± 9.4%) in muscle, 48% to 100% (78 ± 20.8%) in liver and 71% to 90% (83.8 ± 7.6%) in gill tissues (Baeyens et al., 2003; Horvat et al., 2014; Storelli et al., 2003b, 2003a, 2002b). The proportion of organic Hg in fish is largely related to feeding habit and age (de Pinho et al., 2002), but also strongly influenced by background levels (Lacerda et al., 2014), local geochemistry nature of Hg-associated particles (Lacerda et al., 2007) and phytoplankton assimilation processes occurring in the base of the food web (Mason et al., 1995). Reported Methyl-Hg levels in batoids were comparable with upper-level predatory fishes, such as tuna (Storelli et al., 2002a), mackerel (Hajeb et al., 2010) and sharks (De Carvalho et al., 2014). Therefore, we assume a large proportion of the total Hg in batoids compiled in the present study is Methyl-Hg and, thus toxic to the animal and its consumers.

The maximum total Hg contamination limits for safety consumption is 1.0 μg Hg g^{-1} for predatory fish species (FAO/WHO, 2011; USEPA, 2000). Average Hg concentration found in the present study was below this limit (0.34 ± 0.43 μg.g^{-1} w.w.). However, Hg levels varied greatly among batoid species (Fig. 1. 4), with 18% of surveyed species presenting average Hg levels above the safety limit. Among those, *Leucoraja circulares, P. bovinus, R. clavata, Raja miraleus, Raja oxyrhynchus,* and *T. nobiliana* were captured in the Mediterranean Sea; *D. longa* and *Torpedo peruana*, were captured in the North Pacific; and *R. armatus* was captured in the South Pacific.

Although the worldwide safety limit of 1.0 μg Hg g^{-1} targets to protect humans against Hg exposure, having Hg levels below that threshold does not mean neither the animal nor human consumers are free of risk of experiencing toxicity effects. Recent assessments of Hg toxicity in fish estimated a lowest observable adverse effect level (LOAEL) of about 0.5 μg Hg g^{-1} w.w. in muscle tissues of freshwater and marine fish (Depew et al., 2012; Dillon et al., 2010; Scheuhammer et al., 2015). That means deleterious effects to the fish has been observed under Hg concentrations at this level. Moreover, surveys in the Amazon region observed an impairment of visual capability in a riverine human population with no direct

contact with Hg contamination (e.g. gold mining) (Feitosa-Santana et al., 2018). These communities have a diet largely based on fish presenting generally lower-than-LOAEL average Hg concentrations (Azevedo-Silva et al., 2016). If we consider a LOAEL of 0.5 μg Hg g^{-1}, 32% of batoid species surveyed in the present study are at potential risk of adverse effects which may also impair the health of human consumers.

POPs contamination

The very limited information on POPs contamination in batoids prevented us to observe potential trends with respect to oceanic basins, foraging habitat, gender or animal size. In general, animal size and lipid content are good predictors of PCB variations in some teleost fishes (Gewurtz et al., 2011; Rasmussen et al., 2014). However, positive correlations between animal size and PCB levels is not always observed and trophic ecology seems to be another important factor. As an example, a positive relationship between PCBs levels and animal size has been observed more consistently in upper-level consumers, but not in lower level consumers in freshwater fish species (Gewurtz et al., 2011). In the batoid species *U. halleri*, PCBs, DDTs and CHLs concentrations were shown to increase with size but with different slopes in males (higher) and females (lower) which the authors discuss as a result of maternal offloading of contaminants as an elimination route in females (Lyons et al., 2014; Lyons and Lowe, 2013). A similar result was observed in dolphins where PCBs levels increased with age in males but not in females, highlighting maternal offloading as an important depuration pathway of POPs (Wells et al., 2005). In addition, POP accumulation in *U. halleri* were found to vary by location, sex and age suggesting that similar to Hg, several factors influence POP uptake and accumulation patterns in this species and likely other batoids (Lyons et al., 2014).

Regarding food safety, US EPA's (2000) recommends maximum limits (expressed in a wet weight basis for edible tissues) of 0.38 $mg.kg^{-1}$, 0.94 $mg.kg^{-1}$ and 9.4 $mg.kg^{-1}$, for total PCBs, DDTs and CHLs, respectively. In the present survey, DDT and CHL levels were always below the safety limits. However, 87.5% of total PCB levels in liver tissue surveyed in the present study exceeded this safety limit. Those

samples were juvenile and adult specimens of *U. halleri* from Southern California coast and *D. sabina* from Florida coastal lagoons in the USA (Lyons et al., 2014; Sawyna et al., 2017; Weijs et al., 2015). For edible tissues, such as muscle, 50% of total PCBs levels surveyed in the present study exceeded the safety limits for human consumption (Gassel et al., 2013; Johnson-Restrepo et al., 2005; Storelli, 2008). In Southern California coastal areas, 12 fish species, including batoid species *R. productus*, are currently under restricted consumption advisory due to PCBs contamination (OEHHA, 2009). Weijs et al. (2015) also reported high PCB levels in both liver and muscle tissues of shark species (e.g. *Carcharhinus leucas, Negaprion brevirostris* and *Sphyrna tiburo*) in Florida's coastal lagoons. They found that POPs were more commonly observed in species of higher trophic levels while low trophic level species (e.g. *D. sabina*) had fewer compounds detected. They attributed these differences to a combination of factors including biomagnification, species-specific feeding ecologies and diet, and metabolic traits of sharks and rays.

Johnson-Restrepo et al., (2005) found average ΣPCB levels in *D. sabina* to be higher than in silver perch (*Bairdiella chrysoura*, carnivorous diet) and striped mullet (*Mugil cephalus*, herbivore diet) but lower than spotted seatrout (*Cynoscion nebulosus*, carnivorous diet), red drum (*Sciaenops ocellatus*, carnivorous diet), and hardhead catfish (*Ariopsis felis*, carnivorous diet). In general, our survey suggest that, compared to teleosts, batoids are particularly subjected to accumulation of contaminants mostly due to their close association with sediments, but also because of their feeding ecology associated to varied prey types and elasmobranch physiology that seems to favor accumulation of contaminants (De Boeck et al., 2001; Grosell et al., 2003; Webb and Wood, 2000). However, that hypothesis was not tested in the present study and requires further investigations.

An assessment of PFAS contamination, which has no established maximum safety limit for fish consumption, showed that levels in *D. americana* are among the highest of a fish assemblage including predator teleost fishes and sharks (Senthil Kumar et al., 2009). Among PFA substances, Perfluorooctane sulfonate (PFOS) is one of the most widely detected in biological samples (Houde et al., 2006) and was

the main compound found in livers of batoid species surveyed in the present study (Baduel et al., 2014; Senthil Kumar et al., 2009).

Considering POP levels in muscle tissues, Johnson-Restrepo et al. (2005) reported PCB levels in *D. americana* as among the lowest of all organisms including teleost fishes, sharks, and dolphins. These authors highlight that organochlorine uptake is associated to feeding behavior and habitat use, while contaminant accumulation is a tissue-specific process controlled by the metabolic and physiological traits of the organism. This general principle can explain higher POP levels in batoids liver compared to muscle tissues (Johnson-Restrepo et al., 2005; Senthil Kumar et al., 2009).

Information on POP contamination levels in batoids is very limited and values are reported over a wide range. Table S1.2 shows specific congeners/compounds in reported POP levels in batoids. This table presents an example of the complexity in reporting POPs, making it very difficult for cross comparison among studies. For instance, PCB is the most reported organic contaminant in batoids. However, studies do not always report comparable PCB congeners. PCBs are synthetic chlorinated aromatic hydrocarbons composed of one to ten chlorine atoms resulting in 209 compounds with different molecular configuration and toxicity. Among these, twelve dioxin-like compounds (77, 81, 105, 114, 118, 123, 126, 156, 157, 167, 169, 189) are recognized as the most toxic to biota (U.S. EPA, 2008). Therefore, direct comparisons among species and areas for total PCB levels summed from varied congeners mixtures may lead to unclear or misleading results (Batang et al., 2016). In the present survey, compound-specific PCB levels were rarely reported and total PCB levels varied greatly among studies. In addition, levels of CHLs and DDTs are sometimes summed together and presented as total pesticides concentrations which further complicate comparisons among studies.

Exposure effects of POPs and trace metal on batoids

The clearnosed skate, *Leucoraja erinacea,* and the Yellow stingray, *Urolophus jamaicensis,* were the only batoid species in which acute exposure was assessed (Dwivedi and Trombetta, 2006; Grosell et al., 2003).

In *R. erinacea*, acute exposure to Cu produced alterations of plasma total ammonia but had no effect on plasma electrolytes or Na/K- ATPase enzyme activity (Grosell et al., 2003). In contrast, in *U. jamaicensis*, acute exposure to TBTO resulted in altered behavior and produced stress responses measured by Hsp70 and HO1 proteins expression (Dwivedi and Trombetta, 2006). Two other species, the Atlantic stingray, *Dasyatis sabina* (former *Dasyatis sabina*), and the Round stingray, *U. halleri*, were used to assess the exposure effects of PCBs, DDTs, CHLs and other chlorinated contaminants in the wild. In *U. halleri*, increased EROD and CYP1A enzymes activities corresponded to higher levels of organochlorine compounds (Lyons et al., 2014). Similar correspondence was also found for measured cell proliferation and phagocytosis in whole blood (Sawyna et al., 2017). In contrast, despite the high organochlorine accumulation found in *D. sabina* specimens from two contaminated coastal lakes, the authors found no evidence of impaired reproductive parameters and no clear association with the observed endocrine dysfunction (Gelsleichter et al., 2006). Clearly, there is a need for more research on exposure effects of trace metal and POPs in batoid species as the limited evidence shows contrasting results for trace metal and POPs exposure. Future studies should employ comparable biomarkers such as, leukocytes counting and/or EROD activity and CYP1A mRNA expression to allow interpretation of exposure effects across species. In addition, to better represent real conditions, studies should focus on effects of chronic exposure to environmentally relevant levels of pervasive contaminants, including Hg, As and PCBs, that were observed in the present survey to exceed the action limits in many batoid species.

Conclusion

We found batoids accumulating a wide range of trace metals, including mercury (Hg), arsenic (As), lead (Pb), copper (Cu), cadmium (Cd) and zinc (Zn) in our survey. These findings likely represent a common pattern in the upper trophic position of most batoid species in coastal and demersal habitats. Mercury is the most reported contaminant in batoids ranging from moderate to high levels in edible tissues. We found notable differences in batoids Hg levels when the aggregated data were compared among: 1) ocean basins, 2) main prey items, and 3) foraging habitats. Batoids of high Hg levels were mostly associated

with habitats affected by natural Hg-rich backgrounds and anthropogenic Hg emissions. These findings were consistent with global Hg budgets in oceanic waters (Mason et al., 2012; Sunderland et al., 2009). Unfortunately, a very limited number of published studies prohibited us from performing meaningful statistical analysis on other trace metals and POPs. Future studies should be encouraged to report contamination loadings in batoids including trace metals besides Hg.

The published data on POPs contamination in batoid taxa are still very limited and for the most part, inconsistent in the way data were reported to draw general patterns. Our findings point to increased susceptibility of contaminant accumulation in batoids because of elasmobranch-specific physiological/metabolic traits that apparently enhance the accumulation of lipophilic contaminants. This hypothesis has not been tested and needs further investigation in future studies.

Regarding human exposure to contaminants by consumption of batoids, our survey showed that contamination levels are generally below recommended safety limits for most contaminants in most species reported. It is advisable, however, to use caution when consuming batoids inhabiting contaminated areas as some species surveyed in the present study were observed to accumulate above-the-limit levels of Hg, As and ΣPCB.

Table 1.1 – Contamination levels ($\mu g.g^{-1}$) of most reported trace metals in muscle and liver tissues of batoids. Concentration means were calculated from levels reported in the literature and are shown on a wet weight basis.

Trace metal [d]	Tissue (n)	Mean ± SE (range)	Total species reported	Species with lowest / highest levels
Hg	Muscle [a] (n = 122)	0.35 ± 0.43 (< L.D.[c] – 2.4)	48	*Manta alfredi* / *Torpedo nobiliana*
	Liver [b] (n = 29)	0.32 ± 0.79 (0.01 – 4.4)	19	*Raja clavata* / *Rhinobatos armatus*
As	Muscle [a] (n = 61)	20.9 ± 19.6 (0.1 – 94)	10	*Manta alfredi* / *Pteromylaeus bovinus*
	Liver (n =29)	7.4 ± 3.5 (2.4 – 16.5)	5	*Pteromylaeus bovinus*
Pb	Muscle [a] (n = 51)	0.31 ± 0.24 (0.01 – 1.1)	19	*Aptychotrema rostrata* / *Manta alfredi*
	Liver (n = 17)	0.76 ± 0.38 (0.03 – 1.3)	12	*Raja fyllae* / *Gymnura altavela*
Cu	Muscle [a] (n = 23)	0.74 ± 0.43 (0.12 – 1.4)	16	*Aptychotrema rostrate* / *Raja radula*
	Liver [b] (n = 18)	5.24 ± 5.51 (1.1 – 16.5)	11	*Dasyatis pastinaca* / *Raja clavata*
Cd	Muscle [a] (n = 55)	0.06 ± 0.06 (0.03 – 0.2)	21	*Myliobatis australis* / *Mobula japanica*
	Liver [b] (n = 19)	0.32 ± 0.23 (0.1 – 0.8)	12	*Raja clavata*
Zn	Muscle [a] (n = 25)	7.2 ± 2.8 (1.7 – 9.1)	18	*Rhynchobatus australiae* / *Raja miraletus*
	Liver [b] (n = 18)	14.4 ± 6.2 (5.7 – 29.9)	11	*Dasyatis pastinaca* / *Raja clavata*

[a] Muscle concentrations were converted to wet weight assuming a moisture content of 74% (Escobar-Sánchez et al., 2016).

[b] Liver concentrations were converted to wet weight assuming genus-specific moisture content (Sellami et al., 2018; Tufan et al., 2013).

[c] Limit of detection (L.D.) = 0.004 $\mu g.g^{-1}$ (Ooi et al., 2015).

[d] See Table S1 for included references.

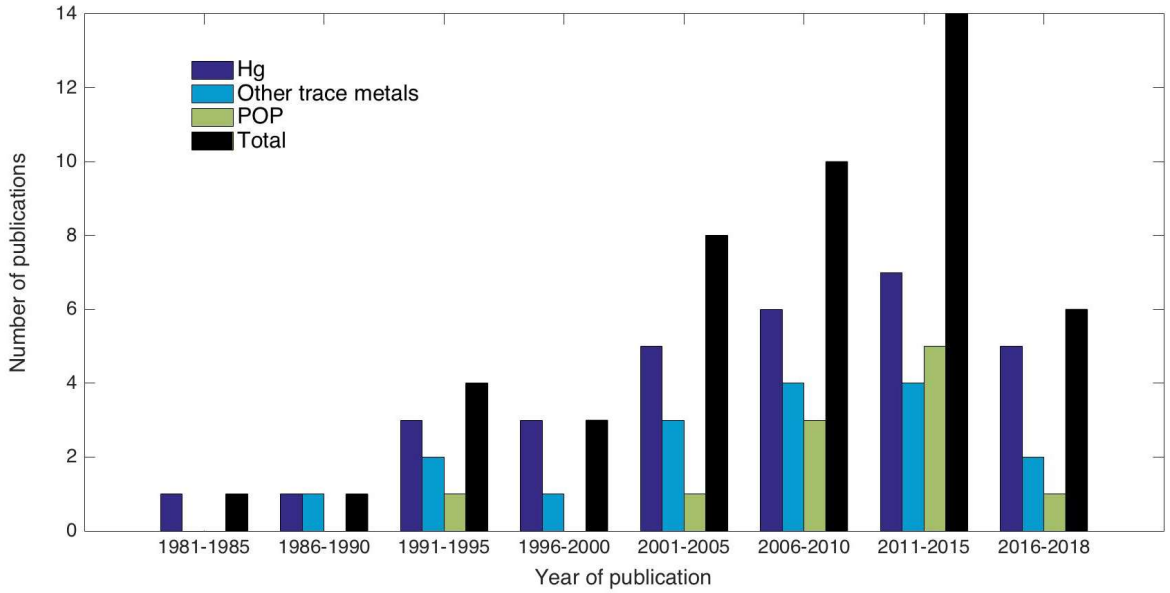

Figure 1.1 – Number of studies on environmental contamination in batoids categorized by type of contaminant reported. Black bars denote total number of papers published at the respective year period.

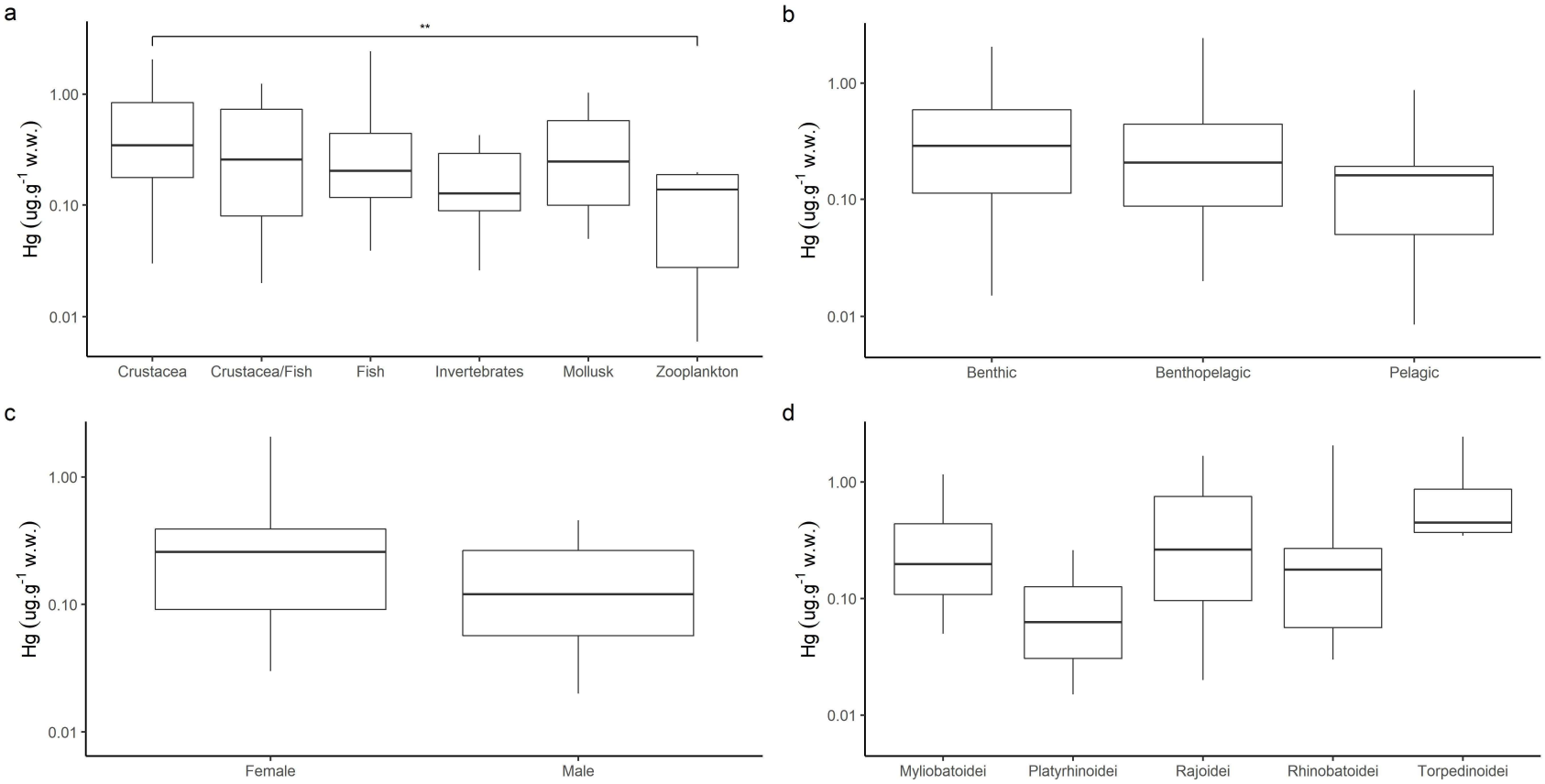

Figure 1. 2 – Boxplot of Hg levels in batoids categorized by (a) main prey item, (b) foraging habitat, (c) sex and (d) sub-order. Asterisks denotes statistical significant differences (**0.01).

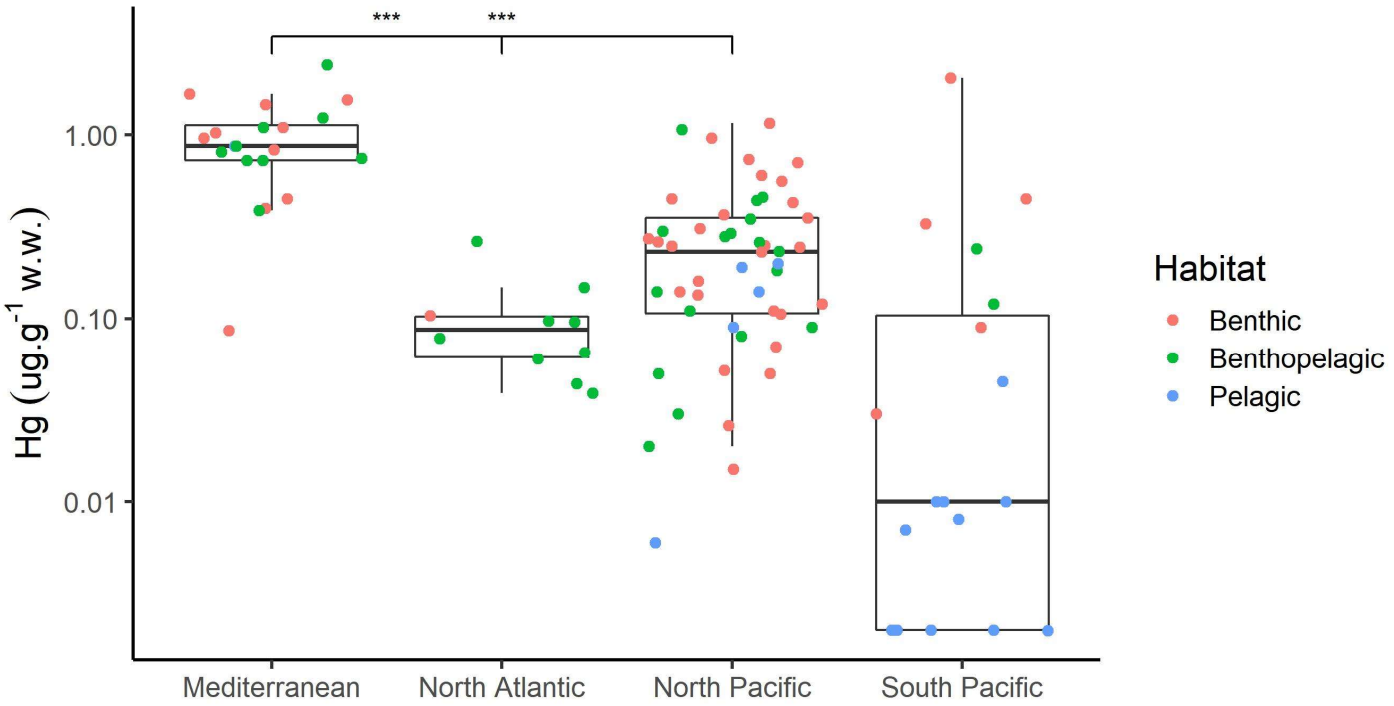

Figure 1. 3 – Boxplot of Hg concentration in muscles of batoid species from major ocean basins. Pooled data include all reported species from each region. Asterisks indicate statistically significant differences (***0.001).

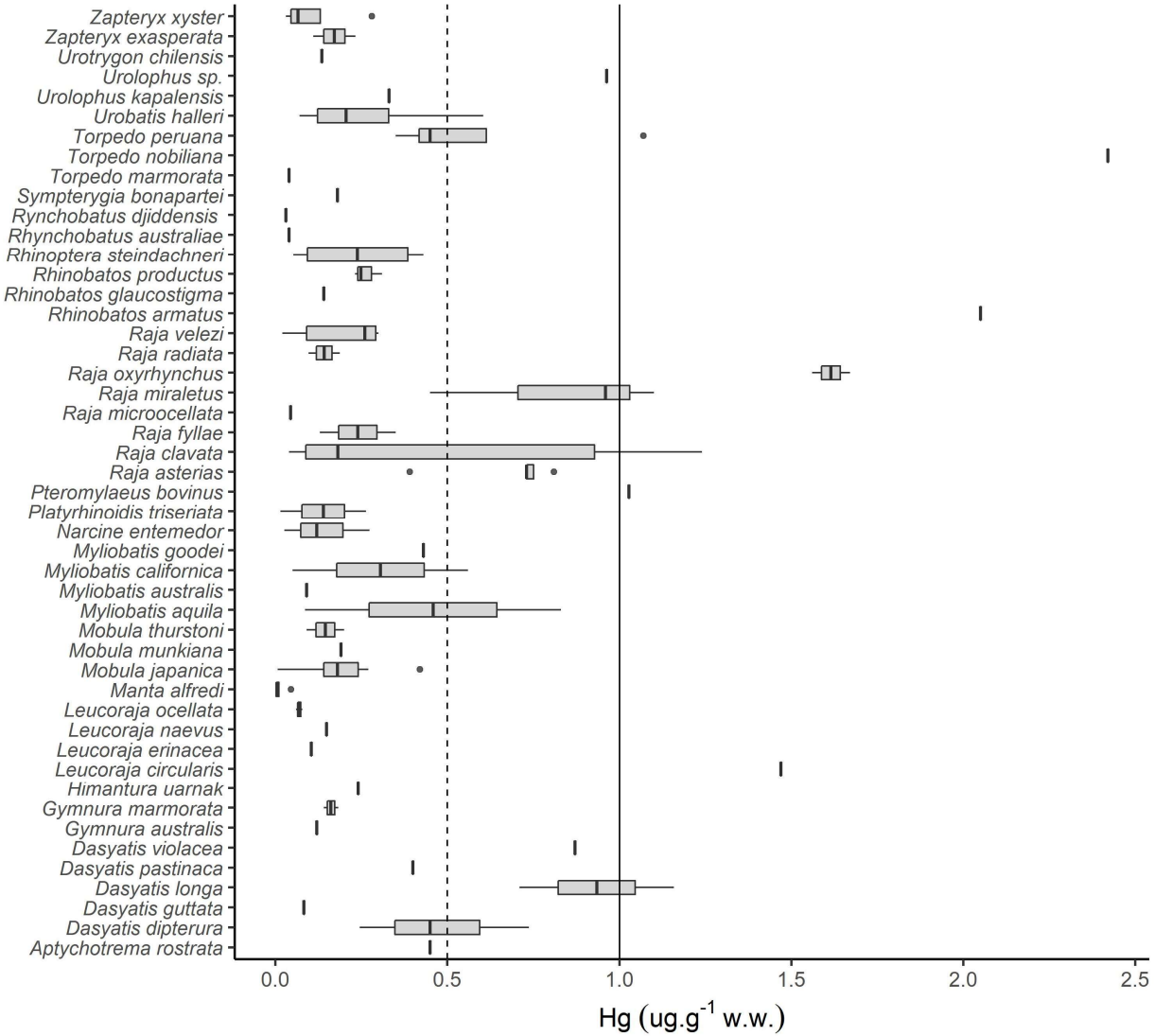

Figure 1. 4 – Hg contamination range reported in batoid species worldwide. The solid line indicates US EPA's recommendation for maximum safety consumption. The dashed line indicates the lowest observable adverse effect level (LOAEL) for freshwater and marine fish (Depew et al., 2012; Dillon et al., 2010; Scheuhammer et al., 2015).

References

AMAP/UNEP, 2013. Technical Background Report for the Global Mercury Assessment. Arct. Monit. Assess. Program. 263.

Araújo, P.R. V, Oddone, M.C., Velasco, G., 2016. Reproductive biology of the stingrays, Myliobatis goodei and Myliobatis ridens (Chondrichthyes: Myliobatidae), in southern Brazil. J. Fish Biol. 89, 1043–1067. https://doi.org/10.1111/jfb.13015

Aschliman, N.C., 2011. The Batoid Tree Of Life: Recovering the patterns and timing of the evolution of skate, rays and allies (Chondrichthyes : Batoidea). Florida State Univ. Res. Repos. Florida State University.

Azevedo-Silva, C.E., Almeida, R., Carvalho, D.P., Ometto, J.P.H.B., de Camargo, P.B., Dorneles, P.R., Azeredo, A., Bastos, W.R., Malm, O., Torres, J.P.M., 2016. Mercury biomagnification and the trophic structure of the ichthyofauna from a remote lake in the Brazilian Amazon. Environ. Res. 151, 286–296. https://doi.org/10.1016/j.envres.2016.07.035

Baatrup, E., 1991. Structural and functional effects of heavy metals on the nervous system, including sense organs, of fish. Comp. Biochem. Physiol. Part C Comp. Pharmacol. 100, 253–257. https://doi.org/10.1016/0742-8413(91)90163-N

Babel, J.S., 1967. Reproduction, life history, and ecology of the round stingray, Urolophus halleri Cooper. Fish Bull. 1–104.

Baduel, C., Lai, F.Y., Townsend, K., Mueller, J.F., 2014. Size and age-concentration relationships for perfluoroalkyl substances in stingray livers from eastern Australia. Sci. Total Environ. 496, 523–530. https://doi.org/10.1016/j.scitotenv.2014.07.010

Baeyens, W., Leermakers, M., Papina, T., Saprykin, A., Brion, N., Noyen, J., De Gieter, M., Elskens, M., Goeyens, L., 2003. Bioconcentration and biomagnification of mercury and methylmercury in North

Sea and Scheldt Estuary. Arch. Environ. Contam. Toxicol. 45, 498–508. https://doi.org/s00244-003-2136-4

Barría, C., Coll, M., Navarro, J., 2015. Unravelling the ecological role and trophic relationships of uncommon and threatened elasmobranchs in the western Mediterranean Sea. Mar. Ecol. Prog. Ser. 539, 225–240. https://doi.org/10.3354/meps11494

Batang, Z.B., Alikunhi, N., Gochfeld, M., Burger, J., Al-Jahdali, R., Al-Jahdali, H., Aziz, M.A.M., Al-Jebreen, D., Al-Suwailem, A., 2016. Congener-specific levels and patterns of polychlorinated biphenyls in edible fish tissue from the central Red Sea coast of Saudi Arabia. Sci. Total Environ. 572, 915–925. https://doi.org/10.1016/j.scitotenv.2016.07.207

Bizzarro, J.J., Smith, W.D., Márquez-Farías, J.F., Hueter, R.E., 2007. Artisanal fisheries and reproductive biology of the golden cownose ray, Rhinoptera steindachneri Evermann and Jenkins, 1891, in the northern Mexican Pacific. Fish. Res. 84, 137–146. https://doi.org/10.1016/j.fishres.2006.10.016

Bornatowski, H., Navia, A.F., Braga, R.R., Abilhoa, V., Correa, M.F.M., 2014. Ecological importance of sharks and rays in a structural foodweb analysis in southern Brazil. ICES J. Mar. Sci. 71, 1586–1592. https://doi.org/10.1093/icesjms/fsu025

Borrell, A., Cardona, L., Kumarran, R.P., Aguilar, A., 2011. Trophic ecology of elasmobranchs caught off Gujarat, India, as inferred from stable isotopes. ICES J. Mar. Sci. 68, 547–554. https://doi.org/10.1093/icesjms/fsq170

Bradley, M.A., Barst, B.D., Basu, N., 2017. A review of mercury bioavailability in humans and fish. Int. J. Environ. Res. Public Health 14. https://doi.org/10.3390/ijerph14020169

Brickle, P., Laptikhovsky, V., Pompert, J., Bishop, A., 2003. Ontogenetic changes in the feeding habits and dietary overlap between three abundant rajid species on the Falkland Islands' shelf. J. Mar. Biol. Assoc. United Kingdom 83, 1119–1125. https://doi.org/10.1017/S0025315403008373h

Chopra, A.K., Sharma, M.K., Chamoli, S., 2011. Bioaccumulation of organochlorine pesticides in aquatic system-an overview. Environ. Monit. Assess. 173, 905–916. https://doi.org/10.1007/s10661-010-1433-4

Cicia, A.M., Driggers, W.B., Ingram, G.W., Kneebone, J., Tsang, P.C.W., Koester, D.M., Sulikowski, J.A., 2009. Size and age estimates at sexual maturity for the little skate Leucoraja erinacea from the western Gulf of Maine, U.S.A. J. Fish Biol. 75, 1648–1666. https://doi.org/10.1111/j.1095-8649.2009.02392.x

Clarke, T.M., Espinoza, M., Wehrtmann, I.S., 2014. Reproductive ecology of demersal elasmobranchs from a data-deficient fishery, Pacific of Costa Rica, Central America. Fish. Res. 157, 96–105. https://doi.org/10.1016/j.fishres.2014.04.003

Cuevas-Zimbrón, E., Pérez-Jiménez, J.C., Méndez-Loeza, I., 2011. Spatial and seasonal variation in a target fishery for spotted eagle ray Aetobatus narinari in the southern Gulf of Mexico. Fish. Sci. 77, 723–730. https://doi.org/10.1007/s12562-011-0389-9

Dang, F., Wang, W.X., 2012. Why mercury concentration increases with fish size? Biokinetic explanation. Environ. Pollut. 163, 192–198. https://doi.org/10.1016/j.envpol.2011.12.026

De Boeck, G., Grosell, M., Wood, C., 2001. Sensitivity of the spiny dogfish (Squalus acanthias) to waterborne silver exposure. Aquat. Toxicol. 54, 261–275. https://doi.org/10.1016/S0166-445X(00)00180-6

De Carvalho, G.G.A., Degaspari, I.A.M., Branco, V., Canário, J., De Amorim, A.F., Kennedy, V.H., Ferreira, J.R., 2014. Assessment of total and organic mercury levels in blue sharks (Prionace glauca) from the south and southeastern Brazilian coast. Biol. Trace Elem. Res. 159, 128–134. https://doi.org/10.1007/s12011-014-9995-6

De Gieter, M., Leermakers, M., Van Ryssen, R., Noyen, J., Goeyens, L., Baeyens, W., 2002. Total and

toxic arsenic levels in North Sea fish. Arch. Environ. Contam. Toxicol. 43, 406–417. https://doi.org/10.1007/s00244-002-1193-4

de Pinho, A.P., Guimarães, J.R.D., Martins, A.S., Costa, P.A.S., Olavo, G., Valentin, J., 2002. Total mercury in muscle tissue of five shark species from Brazilian Offshore waters: Effects of feeding habit, sex, and length. Environ. Res. 89, 250–258. https://doi.org/10.1006/enrs.2002.4365

de Souza Machado, A.A., Spencer, K., Kloas, W., Toffolon, M., Zarfl, C., 2016. Metal fate and effects in estuaries: A review and conceptual model for better understanding of toxicity. Sci. Total Environ. 541, 268–281. https://doi.org/10.1016/j.scitotenv.2015.09.045

Denton, G.R.., Breck, W.., 1981. Mercury in tropical marine organisms from north Queensland. Mar. Pollut. Bull. 12, 116–121. https://doi.org/10.1016/0025-326X(81)90439-2

Depew, D.C., Basu, N., Burgess, N.M., Campbell, L.M., Devlin, E.W., Drevnick, P.E., Hammerschmidt, C.R., Murphy, C.A., Sandheinrich, M.B., Wiener, J.G., 2012. Toxicity of dietary methylmercury to fish: Derivation of ecologically meaningful threshold concentrations. Environ. Toxicol. Chem. 31, 1536–1547. https://doi.org/10.1002/etc.1859

Derraik, J.G.B., 2002. The pollution of the marine environment by plastic debris: A review. Mar. Pollut. Bull. 44, 842–852. https://doi.org/10.1016/S0025-326X(02)00220-5

Dillon, T., Beckvar, N., Kern, J., 2010. Residue-based mercury dose–response in fish: An analysis using lethality-equivalent test endpoints. Environ. Toxicol. Chem. 29, 2559–2565. https://doi.org/10.1002/etc.314

Dulvy, N.K., Baum, J.K., Clarke, S., Compagno, L.J. V., Cortés, E., Domingo, A., Fordham, S., Fowler, S., Francis, M.P., Gibson, C., Martínez, J., Musick, J.A., Soldo, A., Stevens, J.D., Valenti, S., 2008. You can swim but you can't hide: the global status and conservation of oceanic pelagic sharks and rays. Aquat. Conserv. Mar. Freshw. Ecosyst. 18, 459–482. https://doi.org/10.1002/aqc.975

Dulvy, N.K., Fowler, S.L., Musick, J. a, Cavanagh, R.D., Kyne, M., Harrison, L.R., Carlson, J.K., Davidson, L.N.K., Sonja, V., 2014. Extinction risk and conservation of the world ' s sharks and rays. Elife 1–35. https://doi.org/10.7554/eLife.00590

Dulvy, N.K., Simpfendorfer, C.A., Davidson, L.N.K., Fordham, S. V., Bräutigam, A., Sant, G., Welch, D.J., 2017. Challenges and priorities in shark and ray conservation. Curr. Biol. 27, R565–R572. https://doi.org/10.1016/j.cub.2017.04.038

Dwivedi, J., Trombetta, L.D., 2006. Acute toxicity and bioaccumulation of tributyltin in tissues of Urolophus jamaicensis (Yellow Stingray). J. Toxicol. Environ. Heal. Part A 69, 1311–1323. https://doi.org/10.1080/15287390500356800

Ebert, D. a, Bizzarro, J.J., 2007. Standardized diet compositions and trophic levels of skates (Chondrichthyes: Rajiformes: Rajoidei). Dev. Environ. Biol. Fishes 80, 221–237. https://doi.org/10.1007/s10641-007-9227-4

Ebert, D.A., Compagno, L.J. V, 2007. Biodiversity and systematics of skates (Chondrichthyes: Rajiformes: Rajoidei). Environ. Biol. Fishes 80, 111–124. https://doi.org/10.1007/s10641-007-9247-0

El-Shahawi, M.S., Hamza, A., Bashammakh, A.S., Al-Saggaf, W.T., 2010. An overview on the accumulation, distribution, transformations, toxicity and analytical methods for the monitoring of persistent organic pollutants. Talanta 80, 1587–1597. https://doi.org/10.1016/j.talanta.2009.09.055

Escobar-Sánchez, O., Ruelas-Inzunza, J., Moreno-Sánchez, X.G., Romo-Piñera, A.K., Frías-Espericueta, M.G., 2016. Mercury concentrations in Pacific Angel sharks (Squatina californica) and prey fishes from Southern Gulf of California, Mexico. Bull. Environ. Contam. Toxicol. 96, 15–19. https://doi.org/10.1007/s00128-015-1708-0

Escobar-Sanchez, O., Ruelas-Inzunza, J., Patron-Gomez, J.C., Corro-Espinosa, D., 2014. Mercury levels

in myliobatid stingrays (Batoidea) from the Gulf of California: tissue distribution and health risk assessment. Environ. Monit. Assess. 186, 1931–1937. https://doi.org/10.1007/s10661-013-3506-7

FAO/WHO, 2011. Working document for information and use in discussions related to contaminants and toxins in the GSCTFF., Joint Fao/Who Food Standards Programme Codex Committee On Contaminants In Foods: Fifth session. https://doi.org/10.3768/rtipress.2014.rb.0007.1405

Feitosa-Santana, C., Souza, G. da S., Sirius, E.V.P., Rodrigues, A.R., Cortes, M.I.T., Silveira, L.C. de L., Ventura, D.F., 2018. Color vision impairment with low-level methylmercury exposure of an Amazonian population – Brazil. Neurotoxicology 66, 179–184. https://doi.org/10.1016/j.neuro.2018.01.010

Fitzgerald, W.F., Lamborg, C.H., Hammerschmidt, C.R., 2007. Marine biogeochemical cycling of mercury. Chem. Rev. 107, 641–662. https://doi.org/10.1021/cr050353m

Fleeger, J.W., Carman, K.R., Nisbet, R.M., 2003. Indirect effects of contaminants in aquatic ecosystems. Sci. Total Environ. 317, 207–233. https://doi.org/10.1016/S0048-9697(03)00141-4

Gadig, O.B.F., Namora, R.C., dos Santos Motta, F., 2003. Occurrence of the bentfin devil ray, Mobula thurstoni (Chondrichthyes: Mobulidae), in the western Atlantic. J. Mar. Biol. Assoc. UK 83, 869–870. https://doi.org/10.1017/S0025315403007914h

Gałuszka, A., Migaszewski, Z.M., Zalasiewicz, J., 2014. Assessing the Anthropocene with geochemical methods. Geol. Soc. London, Spec. Publ. 395, 221–238. https://doi.org/10.1144/SP395.5

García-Hernández, J., Cadena-Cárdenas, L., Betancourt-Lozano, M., García-De-La-Parra, L.M., García-Rico, L., Márquez-Farías, F., 2007. Total mercury content found in edible tissues of top predator fish from the Gulf of California, Mexico. Toxicol. Environ. Chem. 89, 507–522. https://doi.org/10.1080/02772240601165594

Gassel, M., Brodberg, R.K., Bangia, K., 2013. Health Advisory and Guidelines for Eating Fish From San

Diego Bay (San Diego County). Special Report from the Office of Environmental Health Hazard Assessment California Environmental Protection Agency. San Diego, California.

Gelsleichter, J., Walker, C.J., 2010. Pollutant exposure and effects in sharks and their relatives., in: Carrier, J.C., Musick, J.A., Heithaus, M.R. (Eds.), Sharks And Their Relatives II: Biodiversity, Adaptive Physiology, And Conservation. CRC Press, pp. 491–537. https://doi.org/10.1201/9781420080483

Gelsleichter, J., Walsh, C.J., Szabo, N.J., Rasmussen, L.E.L., 2006. Organochlorine concentrations, reproductive physiology, and immune function in unique populations of freshwater Atlantic stingrays (Dasyatis sabina) from Florida's St. Johns River. Chemosphere 63, 1506–1522. https://doi.org/10.1016/j.chemosphere.2005.09.011

Gewurtz, S.B., Bhavsar, S.P., Fletcher, R., 2011. Influence of fish size and sex on mercury/PCB concentration: Importance for fish consumption advisories. Environ. Int. 37, 425–434. https://doi.org/10.1016/j.envint.2010.11.005

Gibbs, P.J., Miskiewicz, A.G., 1995. Heavy metals in fish near a major primary treatment sewage plant outfall. Mar. Pollut. Bull. 30, 667–674. https://doi.org/10.1016/0025-326X(95)00086-3

Gorman, E.J.O., Emmerson, M.C., 2009. Pertubations to trophic interactions Perturbations and the stability food webs of complex. Natl. Acad. Sci. 106, 13393–13398. https://doi.org/10.1073/pnas.0903682106

Grosell, M., Wood, C.M., Walsh, P.J., 2003. Copper homeostasis and toxicity in the elasmobranch Raja erinacea and the teleost Myoxocephalus octodecemspinosus during exposure to elevated water-borne copper. Comp. Biochem. Physiol. Part C Toxicol. Pharmacol. 135, 179–190. https://doi.org/10.1016/S1532-0456(03)00089-9

Grubbs, R.D., 2010. Ontogenetic shifts in movements and habitat use., in: Carrier, J. F., Musik. J. A. &

Heithaus, M. (Ed.), Sharks and Their Relatives II. Boca Raton, FL: CRC Press, pp. 319–341.

Gutiérrez-Mejía, E., Lares, M.L., Sosa-Nishizaki, O., 2009. Mercury and arsenic in muscle and liver of the golden cownose ray, rhinoptera steindachneri, evermann and jenkins, 1891, from the upper Gulf of California, México. Bull. Environ. Contam. Toxicol. 83, 230–234. https://doi.org/10.1007/s00128-009-9730-8

Hajeb, P., Jinap, S., Fatimah, A.B., Jamilah, B., 2010. Methylmercury in marine fish from malaysian waters and its relationship to total mercury content. Int. J. Environ. Anal. Chem. 90, 812–820. https://doi.org/10.1080/03067310903131941

Hall, B.D., Bodaly, R.A., Fudge, R.J.P., Rudd, J.W.M., Rosenberg, D.M., 1997. Food as the dominant pathway of methylmercury uptake by Fish. Water. Air. Soil Pollut. 100, 13–24. https://doi.org/10.1023/A:1018071406537

Harmon, S.M., 2015. The Toxicity of Persistent Organic Pollutants to Aquatic Organisms, in: Comprehensive Analytical Chemistry. Elsevier, pp. 587–613. https://doi.org/10.1016/B978-0-444-63299-9.00018-1

Horvat, M., Degenek, N., Lipej, L., Snoj Tratnik, J., Faganeli, J., 2014. Trophic transfer and accumulation of mercury in ray species in coastal waters affected by historic mercury mining (Gulf of Trieste, northern Adriatic Sea). Environ. Sci. Pollut. Res. 21, 4163–4176. https://doi.org/10.1007/s11356-013-2262-0

Horvat, M., Kotnik, J., Logar, M., Fajon, V., Zvonarić, T., Pirrone, N., 2003. Speciation of mercury in surface and deep-sea waters in the Mediterranean Sea. Atmos. Environ. 37. https://doi.org/10.1016/S1352-2310(03)00249-8

Houde, M., Martin, J.W., Letcher, R.J., Solomon, K.R., Muir, D.C.G., 2006. Biological monitoring of polyfluoroalkyl substances: A review. Environ. Sci. Technol. 40, 3463–3473.

https://doi.org/10.1021/es052580b

Jacobsen, I.P., Bennett, M.B., 2013. A comparative analysis of feeding and trophic level ecology in stingrays (Rajiformes; Myliobatoidei) and electric rays (Rajiformes: Torpedinoidei). PLoS One 8, e71348. https://doi.org/10.1371/journal.pone.0071348

Jacobsen, I.P., Johnson, J.W., Bennett, M.B., 2009. Diet and reproduction in the Australian butterfly ray Gymnura australis from northern and north-eastern Australia. J. Fish Biol. 75, 2475–2489. https://doi.org/10.1111/j.1095-8649.2009.02432.x

Johnson-Restrepo, B., Kannan, K., Addink, R., Adams, D.H., 2005. Polybrominated diphenyl ethers and polychlorinated biphenyls in a marine foodweb of coastal Florida. Environ. Sci. Technol. 39, 8243–8250. https://doi.org/10.1021/es051551y

Jonathan, M.P., Aurioles-Gamboa, D., Villegas, L.E.C., Bohórquez-Herrera, J., Hernández-Camacho, C.J., Sujitha, S.B., 2015. Metal concentrations in demersal fish species from Santa Maria Bay, Baja California Sur, Mexico (Pacific coast). Mar. Pollut. Bull. 99, 356–361. https://doi.org/10.1016/j.marpolbul.2015.07.032

Jones, K.C., de Voogt, P., 1999. Persistent organic pollutants (POPs): state of the science. Environ. Pollut. 100, 209–221. https://doi.org/10.1016/S0269-7491(99)00098-6

Kitsiou, D., Karydis, M., 2011. Coastal marine eutrophication assessment: A review on data analysis. Environ. Int. 37, 778–801. https://doi.org/10.1016/j.envint.2011.02.004

Kyne, P.M., Bennett, M.B., 2002. Diet of the eastern shovelnose ray, Aptychotrema rostrata (Shaw & Nodder, 1794), from Moreton Bay, Queensland, Australia. Mar. Freshw. Res. 53, 679–686. https://doi.org/10.1071/MF01040

Lacerda, L.D., Costa, B.G.B.C., Lopes, D.N., Oliveira, K., Bezerra, M.F., Bastos, W.R., 2014. Mercury in indigenous, introduced and farmed fish from the semiarid region of the Jaguaribe River Basin, NE

Brazil. Bull. Environ. Contam. Toxicol. 93, 31–35. https://doi.org/10.1007/s00128-014-1263-0

Lacerda, L.D., Goyanna, F., Bezerra, M.F., Silva, G.B., 2017. Mercury Concentrations in Tuna (Thunnus albacares and Thunnus obesus) from the Brazilian Equatorial Atlantic Ocean. Bull. Environ. Contam. Toxicol. 98, 149–155. https://doi.org/10.1007/s00128-016-2007-0

Lacerda, L.D., Santos, J.A., Campos, R.C., Gonçalves, R.A., Salles, R., 2007. Total-Hg and organic-Hg in Cephalopholis fulva (Linnaeus, 1758) from inshore and offshore waters of NE Brazil. Braz. J. Biol. 67, 493–498. https://doi.org/10.1590/S1519-69842007000300014

Last, P.R., Naylor, G.J.P., Manjaji-Matsumoto, B.M., 2016. A revised classification of the family Dasyatidae (Chondrichthyes: Myliobatiformes) based on new morphological and molecular insights. Zootaxa 4139, 345–368. https://doi.org/10.11646/zootaxa.4139.3.2

Law, A.T., Singh, A., 1991. Relationships between heavy metal content and body weight of fish from the Kelang estuary, Malaysia. Mar. Pollut. Bull. 22, 86–89. https://doi.org/10.1016/0025-326X(91)90143-G

López-García, J., Navia, A.F., Mejía-Falla, P.A., Rubio, E.A., 2012. Feeding habits and trophic ecology of Dasyatis longa (Elasmobranchii: Myliobatiformes): Sexual, temporal and ontogenetic effects. J. Fish Biol. 80, 1563–1579. https://doi.org/10.1111/j.1095-8649.2012.03239.x

Lyons, K., Carlisle, A.B., Lowe, C.G., 2017. Influence of ontogeny and environmental exposure on mercury accumulation in muscle and liver of male Round Stingrays. Mar. Environ. Res. 130, 30–37. https://doi.org/10.1016/j.marenvres.2017.07.004

Lyons, K., Lavado, R., Schlenk, D., Lowe, C.G., 2014. Bioaccumulation of organochlorine contaminants and ethoxyresorufin-o-deethylase activity in southern California round stingrays (Urobatis halleri) exposed to planar aromatic compounds. Environ. Toxicol. Chem. 33, 1380–1390. https://doi.org/10.1002/etc.2564

Lyons, K., Lowe, C.G., 2013. Mechanisms of maternal transfer of organochlorine contaminants and mercury in the common thresher shark (*Alopias vulpinus*). Can. J. Fish. Aquat. Sci. 70, 1667–1672. https://doi.org/10.1139/cjfas-2013-0222

Mason, R.P., Choi, A.L., Fitzgerald, W.F., Hammerschmidt, C.R., Lamborg, C.H., Soerensen, A.L., Sunderland, E.M., 2012. Mercury biogeochemical cycling in the ocean and policy implications. Environ. Res. 119, 101–17. https://doi.org/10.1016/j.envres.2012.03.013

Mason, R.P., Reinfelder, J.R., Morel, F.M.M., 1995. Bioaccumulation of mercury and methylmercury. Water, Air, Soil Pollut. 80, 915–921. https://doi.org/10.1007/BF01189744

McCully, S.R., Scott, F., Ellis, J.R., 2012. Lengths at maturity and conversion factors for skates (Rajidae) around the British Isles, with an analysis of data in the literature. ICES J. Mar. Sci. 69, 1812–1822. https://doi.org/10.1093/icesjms/fss150

Miskiewicz, A.G., Gibbs, P.J., 1994. Organochlorine pesticides and hexachlorobenzene in tissues of fish and invertebrates caught near a sewage outfall. Environ. Pollut. 84, 269–277. https://doi.org/10.1016/0269-7491(94)90138-4

Morel, F.M.M., Price, N.M., 2007. The Biogeochemical Cycles of Trace Metals. Science (80-.). 944, 944–948. https://doi.org/10.1126/science.1083545

Myers, R.A., Baum, J.K., Shepherd, T.D., Powers, S.P., Peterson, C.H., 2007. Cascading Effects of the Loss of Apex Predatory Sharks from a Coastal Ocean. Science (80-.). 315, 1846–1850. https://doi.org/10.1126/science.1138657

Oddone, M.C., Velasco, G., 2004. Size at maturity of the smallnose fanskate Sympterygia bonapartii (M??ller & Henle, 1841) (Pisces, Elasmobranchii, Rajidae) in the SW Atlantic. ICES J. Mar. Sci. 61, 293–296. https://doi.org/10.1016/j.icesjms.2003.11.004

OEHHA, 2009. Safe Eating Guidelines For Fish From Coastal Areas of Southern California: Ventura

Harbor toand Safe Eating Guidelines for Fish from Coastal Areas of Southern California: Ventura Harbor to San Mateo Point.

Ooi, M.S.M., Townsend, K.A., Bennett, M.B., Richardson, A.J., Fernando, D., Villa, C.A., Gaus, C., 2015. Levels of arsenic, cadmium, lead and mercury in the branchial plate and muscle tissue of mobulid rays. Mar. Pollut. Bull. 94, 251–259. https://doi.org/10.1016/j.marpolbul.2015.02.005

Páez-Osuna, F., Álvarez-Borrego, S., Ruiz-Fernández, A.C., García-Hernández, J., Jara-Marini, M.E., Bergés-Tiznado, M.E., Piñón-Gimate, A., Alonso-Rodríguez, R., Soto-Jiménez, M.F., Frías-Espericueta, M.G., Ruelas-Inzunza, J.R., Green-Ruiz, C.R., Osuna-Martínez, C.C., Sanchez-Cabeza, J.A., 2017. Environmental status of the Gulf of California: A pollution review. Earth-Science Rev. 166, 181–205. https://doi.org/10.1016/j.earscirev.2017.01.014

Perelman, J.N., Schmidt, K.N., Haro, I., Tibbetts, I.R., Zischke, M.T., 2017. Feeding dynamics, consumption rates and daily ration of wahoo Acanthocybium solandri in Indo-Pacific waters. J. Fish Biol. 90, 1842–1860. https://doi.org/10.1111/jfb.13270

Pickering, C., Byrne, J., 2014. The benefits of publishing systematic quantitative literature reviews for PhD candidates and other early-career researchers. High. Educ. Res. Dev. 33, 534–548. https://doi.org/10.1080/07294360.2013.841651

Pierce, S.J., Bennett, M.B., 2010. Destined to decline? Intrinsic susceptibility of the threatened estuary stingray to anthropogenic impacts. Mar. Freshw. Res. 61, 1468–1481. https://doi.org/10.1071/MF10073

Pierce, S.J., Scott-Holland, T.B., Bennett, M.B., 2011. Community Composition of Elasmobranch Fishes Utilizing Intertidal Sand Flats in Moreton Bay, Queensland, Australia [1]. Pacific Sci. 65, 235–247. https://doi.org/10.2984/65.2.235

Polis, G. a, Sears, A.L.W., Huxel, G.R., Strong, D.R., Maron, J., 2000. When is a trophic cascade a

trophic cascade? Integr. Vlsi J. 5347, 473–475. https://doi.org/10.1016/S0169-5347(00)01971-6

R Core Team, ., 2017. R: A Language and Environment for Statistical Computing.

Rajar, R., Cetina, M., Horvat, M., Zagar, D., 2007. Mass balance of mercury in the Mediterranean Sea. Mar. Chem. 107, 89–102. https://doi.org/10.1016/j.marchem.2006.10.001

Rajeshkumar, S., Mini, J., Munuswamy, N., 2013. Effects of heavy metals on antioxidants and expression of HSP70 in different tissues of Milk fish (Chanos chanos) of Kaattuppalli Island, Chennai, India. Ecotoxicol. Environ. Saf. 98, 8–18. https://doi.org/10.1016/j.ecoenv.2013.07.029

Ramirez Mosqueda, E., Perez Jimenez, J.C., Mendoza Carranza, M., 2012. Reproductive parameters of the southern stingray Dasyatis Americana in southern gulf of Mexico. Lat. Am. J. Aquat. Res. 40, 335–344. https://doi.org/10.3856/vol40-issue2-fulltext-8

Rasmussen, P.W., Schrank, C., Williams, M.C.W., 2014. Trends of PCB concentrations in Lake Michigan coho and chinook salmon, 1975-2010. J. Great Lakes Res. 40, 748–754. https://doi.org/10.1016/j.jglr.2014.05.011

Rosas-Alayola, J., Hernández-Herrera, A., Galvan-Magaña, F., Andres Abitia-Cárdenas, L., Muhlia-Melo, A.F., 2002. Diet composition of sailfish (Istiophorus platypterus) from the southern Gulf of California, Mexico. Fish. Res. 57, 185–195. https://doi.org/10.1016/S0165-7836(01)00344-7

Ruelas-Inzunza, J., Meza-López, G., Páez-Osuna, F., 2008. Mercury in fish that are of dietary importance from the coasts of Sinaloa (SE Gulf of California). J. Food Compos. Anal. 21, 211–218. https://doi.org/10.1016/j.jfca.2007.11.004

Rytuba, J.J., 2003. Mercury from mineral deposits and potential environmental impact. Environ. Geol. 43, 326–338. https://doi.org/10.1007/s00254-002-0629-5

Saglam, H., Ak, O., 2012. Reproductive biology of Raja clavata (Elasmobranchii: Rajidae) from Southern Black Sea coast around Turkey. Helgol. Mar. Res. 66, 117–126. https://doi.org/10.1007/s10152-

011-0252-5

Sandoval-Herrera, N.I., Vargas-Soto, J.S., Espinoza, M., Clarke, T.M., Fisk, A.T., Wehrtmann, I.S., 2016. Mercury levels in muscle tissue of four common elasmobranch species from the Pacific coast of Costa Rica, Central America. Reg. Stud. Mar. Sci. 3, 254–261. https://doi.org/10.1016/j.rsma.2015.11.011

Sawyna, J.M., Spivia, W.R., Radecki, K., Fraser, D.A., Lowe, C.G., 2017. Association between chronic organochlorine exposure and immunotoxicity in the round stingray (Urobatis halleri). Environ. Pollut. 223, 42–50. https://doi.org/10.1016/j.envpol.2016.12.019

Scheuhammer, A., Braune, B., Man, H., Frouin, H., Krey, A., Letcher, R., Loseto, L., Noël, M., Ostertag, S., Ross, P., Wayland, M., 2015. Recent progress on our understanding of the biological effects of mercury in fi sh and wildlife in the Canadian Arctic. Sci. Total Environ. 509–510, 91–103. https://doi.org/10.1016/j.scitotenv.2014.05.142

Sellami, M., Ben Rebah, F., Gargouri, Y., Miled, N., 2018. Lipid composition and antioxidant activity of liver oils from ray species living in Tunisian coasts. Arab. J. Chem. 11, 233–239. https://doi.org/10.1016/j.arabjc.2014.07.010

Senthil Kumar, K., Zushi, Y., Masunaga, S., Gilligan, M., Pride, C., Sajwan, K.S., 2009. Perfluorinated organic contaminants in sediment and aquatic wildlife, including sharks, from Georgia, USA. Mar. Pollut. Bull. 58, 621–629. https://doi.org/10.1016/j.marpolbul.2008.12.006

Smith, W.D., Cailliet, G.M., Melendez, E.M., 2007. Maturity and growth characteristics of a commercially exploited stingray, Dasyatis dipterura. Mar. Freshw. Res. 58, 54. https://doi.org/10.1071/MF06083

Storelli, M.M., 2008. Potential human health risks from metals (Hg, Cd, and Pb) and polychlorinated biphenyls (PCBs) via seafood consumption: Estimation of target hazard quotients (THQs) and toxic

equivalents (TEQs). Food Chem. Toxicol. 46, 2782–2788. https://doi.org/10.1016/j.fct.2008.05.011

Storelli, M.M., Giacominelli Stuffler, R., Marcotrigian, G.O., 2002a. Total and methylmercury residues in tuna-fish from the Mediterranean sea. Food Addit. Contam. 19, 715–721.

Storelli, M.M., Giacominelli Stuffler, R., Marcotrigiano, G.O., 2002b. Total and methylmercury residues in cartilaginous fish from Mediterranean Sea. Mar. Pollut. Bull. 44, 1354–1358. https://doi.org/10.1016/S0025-326X(02)00223-0

Storelli, M.M., Giacominelli Stuffler, R., Marcotrigiano, G.O., 1998. Total mercury in muscle of benthic and pelagic fish from the South Adriatic Sea (Italy). Food Addit. Contam. 15, 876–883. https://doi.org/10.1080/02652039809374724

Storelli, M.M., Giacominelli Stuffler, R., Storelli, A., D'Addabbo, R., Palermo, C., Marcotrigiano, G.O., 2003a. Survey of total mercury and methylmercury levels in edible fish from the Adriatic Sea. Food Addit. Contam. 20, 1114–1119. https://doi.org/10.1080/02652030310001622773

Storelli, M.M., Giacominelli Stuffler, R., Storelli, A., Marcotrigiano, G.O., 2003b. Total Mercury and Methylmercury Content in Edible Fish from the Mediterranean Sea. J. Food Prot. 66, 300–303. https://doi.org/10.4315/0362-028X-66.2.300

Sunderland, E.M., Krabbenhoft, D.P., Moreau, J.W., Strode, S.A., Landing, W.M., 2009. Mercury sources, distribution, and bioavailability in the North Pacific Ocean: Insights from data and models. Global Biogeochem. Cycles 23, 1–14. https://doi.org/10.1029/2008GB003425

Timmons, M., Bray, R.N., 1997. Age, growth, and sexual maturity of shovelnose guitarfish, Rhiinobatis productus (Ayres). Fish. Bull. 95, 349–359.

Trudel, M., Rasmussen, J.B., 1997. Modeling the elimination of mercury by fish. Environ. Sci. Technol. 31, 1716–1722. https://doi.org/10.1021/es960609t

Tufan, B., Koral, S., Köse, S., 2013. The Variations in Proximate Chemical Composition and Fatty Acid

Profile in Different Parts of the Thornback Ray (Raja clavata) Caught from Black Sea, Turkey. J. Aquat. Food Prod. Technol. 22, 83–95. https://doi.org/10.1080/10498850.2011.625593

U.S. EPA, 2008. Framework for application of the toxicity equivalence methodology for polychlorinated dioxins, furans, and biphenyls in ecological risk assessment. U.S.Environmental Prot. Agency, Off. Sci. Advis. Risk Assess. Forum, Washington, DC, EPA-100/R-08/004, June 2008. https://doi.org/EPA 1 0/R-0 /00

USEPA, 2000. Guidance for Assessing Chemical Contaminant Data for Use in Fish Advisories. Vol. 1: Fish Sampling and Analysis. EPA 823-B-00-007. Office of Science and Technology Office of Water U.S. Environmental Protection Agency Washington, DC.

Vieira, L.R., Gravato, C., Soares, A.M.V.M., Morgado, F., Guilhermino, L., 2009. Acute effects of copper and mercury on the estuarine fish Pomatoschistus microps: Linking biomarkers to behaviour. Chemosphere 76, 1416–1427. https://doi.org/10.1016/j.chemosphere.2009.06.005

Vikas, M., Dwarakish, G.S., 2015. Coastal Pollution: A Review. Aquat. Procedia 4, 381–388. https://doi.org/10.1016/j.aqpro.2015.02.051

Webb, N.A., Wood, C.M., 2000. Bioaccumulation and distribution of silver in four marine teleosts and two marine elasmobranchs: Influence of exposure duration, concentration, and salinity. Aquat. Toxicol. 49, 111–129. https://doi.org/10.1016/S0166-445X(99)00063-6

Weijs, L., Briels, N., Adams, D.H., Lepoint, G., Das, K., Blust, R., Covaci, A., 2015. Bioaccumulation of organohalogenated compounds in sharks and rays from the southeastern USA. Environ. Res. 137, 199–207. https://doi.org/10.1016/j.envres.2014.12.022

Wells, R.S., Tornero, V., Borrell, A., Aguilar, A., Rowles, T.K., Rhinehart, H.L., Hofmann, S., Jarman, W.M., Hohn, A.A., Sweeney, J.C., 2005. Integrating life-history and reproductive success data to examine potential relationships with organochlorine compounds for bottlenose dolphins (Tursiops

truncatus) in Sarasota Bay, Florida. Sci. Total Environ. 349, 106–119. https://doi.org/10.1016/j.scitotenv.2005.01.010

Yeldan, H., Avsar, D., Manaşirli, M., 2009. Age, growth and feeding of the common stingray (Dasyatis pastinaca, L., 1758) in the Cilician coastal basin, northeastern Mediterranean Sea. J. Appl. Ichthyol. 25, 98–102. https://doi.org/10.1111/j.1439-0426.2008.01075.x

Yemışken, E., Forero, M.G., Megalofonou, P., Eryilmaz, L., Navarro, J., 2017. Feeding habits of three Batoids in the Levantine Sea (north-eastern Mediterranean Sea) based on stomach content and isotopic data. J. Mar. Biol. Assoc. United Kingdom 1–8. https://doi.org/10.1017/S002531541700073X

CHAPTER 1 – SUPPLEMENTAL MATERIAL

Table S1.1 – List of batoids species along with analyzed pollutant, area of study and references.

Species	Pollutants [a]		Study area	References
Aetobatus narinari	POPs	PFASs	South Pacific	(Baduel et al., 2014)
Aptychotrema rostrata	POPs	HCB, CHLs, DDTs, Dieldrin	South Pacific	(Gibbs and Miskiewicz, 1995; Miskiewicz and Gibbs, 1994)
	Trace metals	Hg, As, Cd, Pb, Cr, Cu, Zn, Se		
Bathyraja spinicauda	Trace metals	Hg, Cd, Pb, Cu, Ni, Zn	Barents Sea	(Zauke et al., 1999)
Dasyatis americana	POPs	PFASs	North Atlantic	(Senthil Kumar et al., 2009)
Dasyatis dipterura / brevi	Trace metals	Hg	North Pacific	(García-Hernández et al., 2007; Ruelas-Inzunza et al., 2013)
Dasyatis centroura	Trace metals	Cd, Pb, Co, Cr, Cu, Fe, Mn, Ni, Zn	Mediterranean	(Türkmen et al., 2014)
Dasyatis fluviorum	POPs	PFASs	South Pacific	(Baduel et al., 2014)
Dasyatis guttata	Trace metals	Hg	South Atlantic	(Lacerda et al., 2016)
Dasyatis longa	Trace metals	Hg	North Pacific	(García-Hernández et al., 2007; Ruelas-Inzunza et al., 2013)
Dasyatis pastinaca	Trace metals	Hg, As, Cd, Pb, Co, Cr, Cu, Fe, Mn, Ni, Zn	Mediterranean	(Horvat et al., 2014; Türkmen et al., 2014, 2013)
Dasyatis sabina	POPs	PCBs, CHLs, DDTs, Dieldrin	North Atlantic	(Gelsleichter et al., 2006; Johnson-Restrepo et al., 2005; Weijs et al., 2015)
Dasyatis violacea	Trace metals	Hg	Mediterranean	(Horvat et al., 2014)
Gymnura altavela	Trace metals	Cd, Pb, Co, Cr, Cu, Fe, Mn, Ni, Zn	Mediterranean	(Türkmen et al., 2013)
Gymnura australis	Trace metals	Hg	South Pacific	(Denton and Breck, 1981)
Gymnura marmorata	Trace metals	Hg	North Pacific	(García-Hernández et al., 2007; Ruelas-Inzunza et al., 2013)
Himantura astra	POPs	PFASs	South Pacific	(Baduel et al., 2014)
Himantura toshi	POPs	PFASs	South Pacific	(Baduel et al., 2014)
Himantura uarnak	POPs	PFASs	South Pacific	(Baduel et al., 2014; Denton and Breck, 1981)
	Trace metals	Hg		
Leucoraja circularis	Trace metals	Hg	Mediterranean	(Storelli et al., 1998)
Leucoraja erinacea	Trace metals	Hg, As	North Atlantic	(Taylor et al., 2014)
Leucoraja naevus	Trace metals	Hg	North Atlantic	(Chouvelon et al., 2012)
Leucoraja ocellata	Trace metals	Hg	North Atlantic	(Taylor et al., 2014; USEPA, 2013)
Manta alfredi	Trace metals	Hg, As, Cd, Pb	South Pacific	(Ooi et al., 2015)
Manta birostris	Trace metals	Pt, Pd, Rh	North Atlantic	(Essumang, 2010)
Mobula japanica	Trace metals	Hg, As, Cd, Pb	Laccadive Sea North Pacific	(Escobar-Sanchez et al., 2014; Ooi et al., 2015)
Mobula munkiana	Trace metals	Hg	North Pacific	(Escobar-Sanchez et al., 2014)
s	Trace metals	Hg	North Pacific	(Escobar-Sanchez et al., 2014)
Myliobatis aquila	Trace metals	Hg, As	Mediterranean	(Horvat et al., 2014; Šlejkovec et al., 2014; Storelli et al., 2002)
Myliobatis australis	POPs	HCB, CHLs, DDTs, Dieldrin	South Pacific	(Gibbs and Miskiewicz, 1995; Miskiewicz and Gibbs, 1994)
	Trace metals	Hg, As, Cd, Pb, Cr, Cu, Zn, Se		
Myliobatis californica	Trace metals	Hg	North Pacific	(García-Hernández et al., 2007; Johnson et al., 2009)

Table S1.1 – Cont.

Species	Pollutants [a]		Study area	References
Myliobatis goodei	Trace metals	Hg, Cd, Zn	South Atlantic	(Marcovecchio et al., 1988)
Narcine entemedor	Trace metals	Hg	North Pacific	(García-Hernández et al., 2007; Ruelas-Inzunza et al., 2013)
Neotrygon kuhlii	POPs	PFASs	South Pacific	(Baduel et al., 2014)
Platyrhinoidis triseriata	Trace metals	Hg	North Pacific	(van Hees and Ebert, 2017)
Pteromylaeus bovinus	Trace metals	Hg, As, Cd, Pb, Co, Cr, Cu, Fe, Mn, Ni, Zn	Mediterranean	(Horvat et al., 2014; Šlejkovec et al., 2014; Türkmen et al., 2013)
Pteroplatytrygon violacea	Trace metals	As	Mediterranean	(Šlejkovec et al., 2014)
Raja asterias	Trace metals	Hg	Mediterranean	(Storelli, 2008; Storelli et al., 2007, 2003a, 2003b, 1998)
Raja clavata	POPs	PCBs	Mediterranean, North Sea and North Atlantic	(Baeyens et al., 2003; Chouvelon et al., 2012; De Gieter et al., 2002; Dixon and Jones, 1994; Storelli, 2008; Storelli et al., 2003b, 1998; Torres et al., 2016; Türkmen et al., 2014, 2013)
	Trace metals	Hg, As, Cd, Pb, Co, Cr, Co, Fe, Mn, Ni, Zn, Se, Rb, Sr		
Raja fyllae	Trace metals	Hg, Cd, Pb, Cu, Ni, Zn	North Sea Barents Sea	(Mormede and Davies, 2001; Zauke et al., 1999)
Raja kenojei	Trace metals	Hg, As, Cd, Pb, Co, Cr, Cu, Mn, Zn, V, Se, Rb, Sr, Mo, Ag, In, Sn, Sb, Cs, Ba, Tl, Bi	North Pacific	(Asante et al., 2008)
Raja kwangtungensis	Trace metals	Hg, As, Cd, Pb, Co, Cr, Cu, Mn, Zn, V, Se, Rb, Sr, Mo, Ag, In, Sn, Sb, Cs, Ba, Tl, Bi	North Pacific	(Asante et al., 2008)
Raja microocellata	Trace metals	Hg	North Atlantic	(Chouvelon et al., 2012)
Raja miraletus	POPs	PCBs	Mediterranean	(Storelli, 2008; Storelli et al., 2003b, 1998, Türkmen et al., 2014, 2013)
	Trace metals	Hg, As, Cd, Pb, Co, Cr, Co, Cu, Fe, Mn, Ni, Zn		
Raja oxyrhynchus	Trace metals	Hg	Mediterranean	(Storelli et al., 2003b, 1998)
Raja radiata	Trace metals	Hg, Cd, Pb, Cu, Ni, Zn	Barents Sea	(Joiris et al., 1997; Zauke et al., 1999)
Raja radula	Trace metals	Cd, Pb, Co, Cr, Cu, Fe, Mn, Ni, Zn	Mediterranean	(Türkmen et al., 2014, 2013)
Raja velezi	Trace metals	Hg	North Pacific	(Ruelas-Inzunza et al., 2013; Sandoval-Herrera et al., 2016)
Rhinobatos armatus	Trace metals	Hg	South Pacific	(Denton and Breck, 1981)
Rhinobatos glaucostigma	Trace metals	Hg	North Pacific	(García-Hernández et al., 2007)
Rhinobatos productus	POPs	PCBs, CHLs, DDTs	North Pacific	(García-Hernández et al., 2007; Gassel et al., 2013; Ruelas-Inzunza et al., 2013)
	Trace metals	Hg, As		
Rhinoptera steindachneri	Trace metals	Hg, As	North Pacific	(Escobar-Sanchez et al., 2014; García-Hernández et al., 2007; Gutiérrez-Mejía et al., 2009)
Rhynchobatus australiae	Trace metals	Hg, Cd, Pb, Cu, Zn	China Sea	(Ong and Gan, 2017)
Rynchobatus djiddensis	Trace metals	Hg	South Pacific	(Denton and Breck, 1981)
Sympterygia bonapartei	Trace metals	Hg, Cd, Zn	South Atlantic	(Marcovecchio et al., 1988)
Torpedo marmorata	Trace metals	Hg, Cd, Pb, Co, Cr, Cu, Fe, Mn, Ni, Zn	Mediterranean North Atlantic	(Chouvelon et al., 2012; Türkmen et al., 2014)

Table S1.1 – Cont.

Species	Pollutants [a]		Study area	References
Torpedo nobiliana	Trace metals	Hg, Cd, Pb, Co, Cr, Cu, Fe, Mn, Ni, Zn	Mediterranean	(Storelli et al., 2002; Türkmen et al., 2014)
Torpedo peruana	Trace metals	Hg	North Pacific	(Sandoval-Herrera et al., 2016)
Urobatis halleri	POPs	PCBs, CHLs, DDTs	North Pacific	(Gassel et al., 2013; Jonathan et al., 2015; Lyons et al., 2017, 2014; Lyons and Lowe, 2013; Ruelas-Inzunza et al., 2013; Sawyna et al., 2017)
	Trace metals	Hg		
Urolophus sp.	Trace metals	Hg	North Pacific	(Ruelas-Inzunza et al., 2013)
Urolophus kapalensis	POPs	HCB, CHLs, DDTs, Dieldrin	South Pacific	(Gibbs and Miskiewicz, 1995; Miskiewicz and Gibbs, 1994)
	Trace metals	Hg, As, Cd, Pb, Cr, Cu, Zn, Se		
Urotrygon chilensis	Trace metals	Hg	North Pacific	(Ruelas-Inzunza et al., 2013)
Zapteryx exasperata	Trace metals	Hg	North Pacific	(García-Hernández et al., 2007; Ruelas-Inzunza et al., 2013)
Zapteryx xyster	Trace metals	Hg	North Pacific	(Sandoval-Herrera et al., 2016)

[a] Pollutant acronym - Perfluoroalkyl substances (PFASs); hexachlorobenzene (HCB); Chlordanes (CHLs); dichlorodiphenyltrichloroethane (DDTs); polychlorinated biphenyls (PCBs).

Table S1.2 – Specific POPs compounds and/or congener groups analyzed in batoids.

	Congener group (ID#) or Compound name	References
PCBs	Tri (18, 28); tetra (44, 47, 49, 52, 66, 74); penta (87, 95, 99, 101, 105, 110, 118); hexa (128, 132, 138, 146, 149, 151, 153, 156, 167); hepta (170, 171, 172, 174, 177, 180, 183, 187); octa (194, 195, 196, 199, 203); nona (206); deca (209).	(Weijs et al., 2015)
	Tri (28, 31, 33); tetra (44, 49, 52, 56, 66, 70, 74, 81); penta (87, 97, 99, 101, 105, 110, 114, 118, 123, 126); hexa (128, 138, 141, 149, 153, 156, 157, 158, 167, 169); hepta (170, 174, 177, 180, 183, 187, 189); octa (194, 195, 201); nona (206); deca (209).	(Lyons et al., 2014)
	Tri (28); tetra (56, 60, 66, 70, 74); penta (99, 101, 105, 110, 118); hexa (128, 138, 141, 149, 153, 156, 157, 158, 167); hepta (170, 174, 180, 183, 187, 189); octa (194, 195, 199, 200, 201); nona (207); deca (209).	(Sawyna et al., 2017)
	[a] Tri; tetra; penta; hexa; hepta; octa; nona.	(Lyons and Lowe, 2013)
	[a] Tri; tetra; penta; hexa; hepta; octa; nona; deca.	(Johnson-Restrepo et al., 2005)
	Not specified.	(Gelsleichter et al., 2006)
DDTs	*o,p'*-DDE; *p,p'*-DDE; *o,p'*-DDD; *p,p'*-DDD; *o,p'*-DDT; *p,p'*-DDT	(Gelsleichter et al., 2006; Lyons et al., 2014; Lyons and Lowe, 2013; Weijs et al., 2015)
	p,p'-DDE; *p,p'*-DDD; *p,p'*-DDT	(Miskiewicz and Gibbs, 1994)
	o,p'-DDE	(Sawyna et al., 2017)
CHLs	Oxychlordane; trans-chlordane; cis-chlordane; trans-nonachlor.	(Lyons et al., 2014)
	Oxychlordane; trans-chlordane; cis-chlordane.	(Lyons and Lowe, 2013)
	Oxychlordane; trans-chlordane; cis-chlordane; heptachlor; heptachlor epoxide; cis-nonachlor; trans-nonachlor.	(Gelsleichter et al., 2006)
	Oxychlordane; heptachlor; heptachlor epoxide.	(Miskiewicz and Gibbs, 1994)
	Hexachlorobenzene; trans-chlordane; cis-chlordane; cis-nonachlor; trans-nonachlor.	(Sawyna et al., 2017)
PFASs	Perfluorohexanoate (PFHxA); perfluoroheptanoate (PFHpA); perfluorooctanoate (PFOA); perfluorononanoate (PFNA); perfluorodecanoate (PFDA); perfluoroundecanoate (PFUnDA); perfluorododecanoate (PFDoDA); perfluorotridecanoate (PFTrDA); perfluorohexanesulfonate (PFHxS); perfluorooctane sulfonate (PFOS).	(Baduel et al., 2014)
	Perfluorohexanoate (PFHxA); perfluoroheptanoate (PFHpA); perfluorooctanoate (PFOA); perfluorononanoate (PFNA); perfluorododecanoate (PFDoDA); perfluorohexanesulfonate (PFHxS); Perfluorooctane sulfonate (PFOS); perfluorooctane sulfonate isomer (Is-PFOS); perfluorobutanesulfonate (PFBS); tetrahydroperfluorooctanesulfonate (THPFOS); perfluorodecanesulfonate (PFDS); perfluoropentanoic acid (PFPeA); perfluoroundecanoic acid (PFUnA); perfluorododecanoic acid (PFDoA); n-ethylperfluoro-1-octanesulfonamidoacetic acid (N-EtFOSAA); n-methylperfluoro-1-octanesulfonamidoacetic acid (N-MeFOSAA); 2H-perfluoro-2-octenoic acid (6:2 FTUCA); 2H-perfluoro-2-decenoic acid (8:2 FTUCA); 2H-perfluoro-2-dodecenoic acid (10:2 FTUCA); perfluoroheptanesulfonate (PFHpS); perfluoropentanesulfonate (PFPeS); perfluorononanesulfonate (PFNS).	(Senthil Kumar et al., 2009)

[a] Congener identification number not specified.

Table S1.3 –Habitat zone and main prey items of batoid species included in statistical analysis

Species	Main prey item	Habitat zone	References
Dasyatis guttata	Crustacea	benthic	(Jacobsen and Bennett, 2013)
Dasyatis longa	Crustacea	benthic	(Jacobsen and Bennett, 2013)
Dasyatis pastinaca	Crustacea	benthic	(Jacobsen and Bennett, 2013)
Dasyatis violacea	Fish	Pelagic	(Jacobsen and Bennett, 2013; Lipej et al., 2013)
Gymnura australis	Fish	Benthopelagic	(Jacobsen et al., 2009; Jacobsen and Bennett, 2013)
Gymnura marmorata	Fish	Benthopelagic	(Jacobsen and Bennett, 2013)
Himantura uarnak	Fish	Benthopelagic	(Jacobsen and Bennett, 2013)
Hypanus dipterura	Crustacea	Benthic	(Jacobsen and Bennett, 2013)
Manta alfredi	Zooplankton	Pelagic	(Couturier, 2013)
Mobula japanica	Zooplankton	Pelagic	(Jacobsen and Bennett, 2013; Rohner et al., 2017)
Mobula munkiana	Zooplankton	Pelagic	(Jacobsen and Bennett, 2013; Rohner et al., 2017)
Mobula thurstoni	Zooplankton	Pelagic	(Jacobsen and Bennett, 2013; Rohner et al., 2017)
Myliobatis aquila	Mollusk	Benthic	(Jacobsen and Bennett, 2013; Jardas et al., 2004)
Myliobatis australis	Mollusk	Benthic	(Jacobsen and Bennett, 2013; Sommerville et al., 2011)
Myliobatis californica	Mollusk	Benthic	(Gray et al., 1997; Jacobsen and Bennett, 2013)
Myliobatis goodei	Mollusk	Benthic	(Molina and Lopez Cazorla, 2015)
Pteromylaeus bovinus	Mollusk	Benthic	(Jacobsen and Bennett, 2013)
Rhinoptera steindachneri	Invertebrate[a]	Benthic	(Bizzarro, 2005; Jacobsen and Bennett, 2013)
Urobatis halleri	Crustacea	Benthic	(Jacobsen and Bennett, 2013)
Urolophus kapalensis	Crustacea	Benthic	(Jacobsen and Bennett, 2013)
Urotrygon chilensis	Invertebrate[a]	Benthic	(Jacobsen and Bennett, 2013)
Leucoraja erinacea	Crustacea	Benthic	(Ebert and Bizzarro, 2007)
Leucoraja naevus	Fish	Benthopelagic	(Barría et al., 2015)
Leucoraja ocellata	Fish	Benthopelagic	(Ebert and Bizzarro, 2007)
Narcine entemedor	Invertebrate[a]	Benthic	(Jacobsen and Bennett, 2013)
Raja asterias	Crustacea/Fish	Benthopelagic	(Yemışken et al., 2017)
Leucoraja circularis	Crustacea	Benthic	(Stehmann and Bürkel, 1984)
Raja clavata	Crustacea/Fish	Benthopelagic	(Yemışken et al., 2017)
Raja fyllae	Crustacea	Benthic	(Ebert and Bizzarro, 2007)

[a] Invertebrates (other than elsewhere specified), includes unidentified invertebrates and insects.

Table S1.3 – Cont.

Species	Main prey item	Habitat zone	References
Raja microocellata	Crustacea/Fish	Benthopelagic	(Ebert and Bizzarro, 2007)
Raja miraletus	Crustacea	Benthic	(Ebert and Bizzarro, 2007)
Raja oxyrhynchus	Crustacea	Benthic	(Anastasopoulou et al., 2018)
Raja radiata	Crustacea/Fish	Benthopelagic	(Dolgov, 2005)
Raja velezi	Crustacea/Fish	Benthopelagic	(Espinoza et al., 2012)
Sympterygia bonapartei	Mollusk	Benthic	(Penchaszadeh et al., 2006)
Aptychotrema rostrata	Crustacea	Benthic	(Kyne and Bennett, 2002)
Rhinobatos armatus	Crustacea	Benthic	(Vaudo, 2011)
Rhinobatos glaucostigma	Crustacea	Benthic	(Lara-Mendoza et al., 2015)
Rhinobatos productus	Crustacea	Benthic	(Valenzuela-Quiñonez et al., 2017)
Rynchobatus djiddensis	Crustacea	Benthic	(Borrell et al., 2011)
Rhynchobatus australiae	Crustacea	Benthic	(Last et al., 2010)
Zapteryx exasperata	Fish	Benthopelagic	(Blanco-Parra et al., 2012)
Zapteryx xyster	Crustacea/Fish	Benthopelagic	(Espinoza et al., 2013)
Torpedo marmorata	Fish	Benthopelagic	(Barría et al., 2015)
Torpedo nobiliana	Fish	Benthopelagic	(Barría et al., 2015)
Torpedo peruana	Fish	Benthopelagic	(Espinoza et al., 2015)

Table S1.4 – Generalized Linear Models (Gamma distribution) of Hg concentration in batoids explained by oceanic basin of occurrence ("Area"), main prey item in diet ("Prey"), foraging habitat ("Habitat"), and taxonomic classification ("Sub order"). Models are ranked by Akaike Information Criterion (AIC). Best models are shown first.

Gamma model	**AIC**	**ΔAIC**
~ Area + Prey	-58.1	0
~ Area + Habitat + Prey	-56.4	1.7
~ Area + Prey + Sub order	-55.9	2.2
~ Area + Habitat + Prey + Sub order	-55.7	2.4
~ Area + Habitat	-41.9	16.2
~ Area + Habitat + Sub order	-39.2	18.9
~ Prey + Sub order	-37.6	20.5
~ Prey	-33	25.1
~ Habitat + Prey	-31.7	26.4
~ Area	-31.4	26.7
~ Area + Sub order	-27.8	30.3
~ Habitat + Sub order	-19.1	39
~ Habitat	-16	42.1
~ Sub order	-2.8	55.3

Appendix S1 – List of literature cited in tables S1.1 and S1.3.

Anastasopoulou, A., Mytilineou, C., Smith, C.J., Papadopoulou, K.N., 2018. Crustacean prey in the diet of fishes from deep waters of the Eastern Ionian Sea. J. Mar. Biol. Assoc. United Kingdom 1–9. https://doi.org/10.1017/S0025315417001977

Asante, K.A., Agusa, T., Mochizuki, H., Ramu, K., Inoue, S., Kubodera, T., Takahashi, S., Subramanian, A., Tanabe, S., 2008. Trace elements and stable isotopes (d13C and d15N) in shallow and deep-water organisms from the East China Sea. Environ. Pollut. 156, 862–873. https://doi.org/10.1016/j.envpol.2008.05.020

Baduel, C., Lai, F.Y., Townsend, K., Mueller, J.F., 2014. Size and age-concentration relationships for perfluoroalkyl substances in stingray livers from eastern Australia. Sci. Total Environ. 496, 523–530. https://doi.org/10.1016/j.scitotenv.2014.07.010

Baeyens, W., Leermakers, M., Papina, T., Saprykin, A., Brion, N., Noyen, J., De Gieter, M., Elskens, M., Goeyens, L., 2003. Bioconcentration and biomagnification of mercury and methylmercury in North Sea and Scheldt Estuary. Arch. Environ. Contam. Toxicol. 45, 498–508. https://doi.org/s00244-003-2136-4

Barría, C., Coll, M., Navarro, J., 2015. Unravelling the ecological role and trophic relationships of uncommon and threatened elasmobranchs in the western Mediterranean Sea. Mar. Ecol. Prog. Ser. 539, 225–240. https://doi.org/10.3354/meps11494

Bizzarro, J., 2005. Fishery Biology and Feeding Ecology of Rays in Bahía Almejas, Mexico. Master Thesis. San Francisco State University. https://doi.org/10.1017/CBO9781107415324.004

Blanco-Parra, M. del P., Galván-Magaña, F., Márquez-Farías, J.F., Niño-Torres, C.A., 2012. Feeding ecology and trophic level of the banded guitarfish, Zapteryx exasperata, inferred from stable isotopes and stomach contents analysis. Environ. Biol. Fishes 95, 65–77.

https://doi.org/10.1007/s10641-011-9862-7

Borrell, A., Cardona, L., Kumarran, R.P., Aguilar, A., 2011. Trophic ecology of elasmobranchs caught off Gujarat, India, as inferred from stable isotopes. ICES J. Mar. Sci. 68, 547–554. https://doi.org/10.1093/icesjms/fsq170

Chouvelon, T., Spitz, J., Caurant, F., Mèndez-Fernandez, P., Autier, J., Lassus-Débat, a., Chappuis, a., Bustamante, P., 2012. Enhanced bioaccumulation of mercury in deep-sea fauna from the Bay of Biscay (north-east Atlantic) in relation to trophic positions identified by analysis of carbon and nitrogen stable isotopes. Deep. Res. Part I Oceanogr. Res. Pap. 65, 113–124. https://doi.org/10.1016/j.dsr.2012.02.010

Couturier, L.I.E., 2013. " Population ecology and biology of the reef manta ray Manta alfredi in eastern Australia ." 2013.

De Gieter, M., Leermakers, M., Van Ryssen, R., Noyen, J., Goeyens, L., Baeyens, W., 2002. Total and toxic arsenic levels in North Sea fish. Arch. Environ. Contam. Toxicol. 43, 406–417. https://doi.org/10.1007/s00244-002-1193-4

Denton, G.R.., Breck, W.., 1981. Mercury in tropical marine organisms from north Queensland. Mar. Pollut. Bull. 12, 116–121. https://doi.org/10.1016/0025-326X(81)90439-2

Dixon, R., Jones, B., 1994. Mercury Concentrations in Stomach Contents and Muscle of Five Fish Species from the North East Coast of England. Mar. Pollut. Bull. 28, 741–745. https://doi.org/10.1016/0025-326X(94)90333-6

Dolgov, A. V., 2005. Feeding and food consumption by the Barents Sea skates. J. Northwest Atl. Fish. Sci. 35, 495–503. https://doi.org/10.2960/J.v35.m523

Ebert, D. a, Bizzarro, J.J., 2007. Standardized diet compositions and trophic levels of skates (Chondrichthyes: Rajiformes: Rajoidei). Dev. Environ. Biol. Fishes 80, 221–237.

https://doi.org/10.1007/s10641-007-9227-4

Escobar-Sanchez, O., Ruelas-Inzunza, J., Patron-Gomez, J.C., Corro-Espinosa, D., 2014. Mercury levels in myliobatid stingrays (Batoidea) from the Gulf of California: tissue distribution and health risk assessment. Environ. Monit. Assess. 186, 1931–1937. https://doi.org/10.1007/s10661-013-3506-7

Espinoza, M., Clarke, T.M., Villalobos-Rojas, F., Wehrtmann, I.S., 2013. Diet composition and diel feeding behaviour of the banded guitarfish Zapteryx xyster along the Pacific coast of Costa Rica, Central America. J. Fish Biol. 82, 286–305. https://doi.org/10.1111/j.1095-8649.2012.03488.x

Espinoza, M., Clarke, T.M., Villalobos-Rojas, F., Wehrtmann, I.S., 2012. Ontogenetic dietary shifts and feeding ecology of the rasptail skate Raja velezi and the brown smoothhound shark Mustelus henlei along the Pacific coast of Costa Rica, Central America. J. Fish Biol. 81, 1578–1595. https://doi.org/10.1111/j.1095-8649.2012.03410.x

Espinoza, M., Munroe, S.E.M., Clarke, T.M., Fisk, A.T., Wehrtmann, I.S., 2015. Feeding ecology of common demersal elasmobranch species in the Pacific coast of Costa Rica inferred from stable isotope and stomach content analyses. J. Exp. Mar. Bio. Ecol. 470, 12–25. https://doi.org/10.1016/j.jembe.2015.04.021

Essumang, D.K., 2010. First determination of the levels of platinum group metals in manta birostris (Manta Ray) caught along the ghanaian coastline. Bull. Environ. Contam. Toxicol. 84, 720–725. https://doi.org/10.1007/s00128-010-0019-8

García-Hernández, J., Cadena-Cárdenas, L., Betancourt-Lozano, M., García-De-La-Parra, L.M., García-Rico, L., Márquez-Farías, F., 2007. Total mercury content found in edible tissues of top predator fish from the Gulf of California, Mexico. Toxicol. Environ. Chem. 89, 507–522. https://doi.org/10.1080/02772240601165594

Gassel, M., Brodberg, R.K., Bangia, K., 2013. Health Advisory and Guidelines for Eating Fish From San

Diego Bay (San Diego County). Special Report from the Office of Environmental Health Hazard Assessment California Environmental Protection Agency. San Diego, California.

Gelsleichter, J., Walsh, C.J., Szabo, N.J., Rasmussen, L.E.L., 2006. Organochlorine concentrations, reproductive physiology, and immune function in unique populations of freshwater Atlantic stingrays (Dasyatis sabina) from Florida's St. Johns River. Chemosphere 63, 1506–1522. https://doi.org/10.1016/j.chemosphere.2005.09.011

Gibbs, P.J., Miskiewicz, A.G., 1995. Heavy metals in fish near a major primary treatment sewage plant outfall. Mar. Pollut. Bull. 30, 667–674. https://doi.org/10.1016/0025-326X(95)00086-3

Gray, A.E., Mulligan, T.J., Hannah, R.W., 1997. Food habits, occurrence, and population structure of the bat ray, *Myliobatis californica*, in Humboldt Bay, California. Environ. Biol. Fishes 49, 227–238.

Gutiérrez-Mejía, E., Lares, M.L., Sosa-Nishizaki, O., 2009. Mercury and arsenic in muscle and liver of the golden cownose ray, rhinoptera steindachneri, evermann and jenkins, 1891, from the upper Gulf of California, México. Bull. Environ. Contam. Toxicol. 83, 230–234. https://doi.org/10.1007/s00128-009-9730-8

Horvat, M., Degenek, N., Lipej, L., Snoj Tratnik, J., Faganeli, J., 2014. Trophic transfer and accumulation of mercury in ray species in coastal waters affected by historic mercury mining (Gulf of Trieste, northern Adriatic Sea). Environ. Sci. Pollut. Res. 21, 4163–4176. https://doi.org/10.1007/s11356-013-2262-0

Jacobsen, I.P., Bennett, M.B., 2013. A comparative analysis of feeding and trophic level ecology in stingrays (Rajiformes; Myliobatoidei) and electric rays (Rajiformes: Torpedinoidei). PLoS One 8, e71348. https://doi.org/10.1371/journal.pone.0071348

Jacobsen, I.P., Johnson, J.W., Bennett, M.B., 2009. Diet and reproduction in the Australian butterfly ray Gymnura australis from northern and north-eastern Australia. J. Fish Biol. 75, 2475–2489.

https://doi.org/10.1111/j.1095-8649.2009.02432.x

Jardas, I., Santic, M., Pallaoro, A., 2004. Diet composition of the eagle ray, Myliobatis aquila (Chondrichthyes: Myliobatidae), in the Eastern Adriatic Sea. Cybium 28, 372–374.

Johnson-Restrepo, B., Kannan, K., Addink, R., Adams, D.H., 2005. Polybrominated diphenyl ethers and polychlorinated biphenyls in a marine foodweb of coastal Florida. Environ. Sci. Technol. 39, 8243–8250. https://doi.org/10.1021/es051551y

Johnson, B.E., Esser, B.K., Whyte, D.C., Ganguli, P.M., Austin, C.M., Hunt, J.R., 2009. Mercury accumulation and attenuation at a rapidly forming delta with a point source of mining waste. Sci. Total Environ. 407, 5056–5070. https://doi.org/10.1016/j.scitotenv.2009.05.025

Joiris, C.R., Ali, I.B., Holsbeek, L., Kanuya-Kinoti, M., Tekele-Michael, Y., 1997. Total and organic mercury in Greenland and Barents Seas demersal fish. Bull. Environ. Contam. Toxicol. 58, 101–7.

Jonathan, M.P., Aurioles-Gamboa, D., Villegas, L.E.C., Bohórquez-Herrera, J., Hernández-Camacho, C.J., Sujitha, S.B., 2015. Metal concentrations in demersal fish species from Santa Maria Bay, Baja California Sur, Mexico (Pacific coast). Mar. Pollut. Bull. 99, 356–361. https://doi.org/10.1016/j.marpolbul.2015.07.032

Kyne, P.M., Bennett, M.B., 2002. Diet of the eastern shovelnose ray, Aptychotrema rostrata (Shaw & Nodder, 1794), from Moreton Bay, Queensland, Australia. Mar. Freshw. Res. 53, 679–686. https://doi.org/10.1071/MF01040

Lacerda, L.D., Bezerra, M.F., Costa, B.G.B., Braga, T.M.B., Goyanna, F.A.A., 2016. Mercury distribution in fish commercialized at the mucuripe market , Fortaleza , Ceará state , Brazil. Arq. Ciencias do Mar (Marine Sci. Arch. 49, 50–54.

Lara-Mendoza, R.E., Márquez-Farías, J.F., Román-Reyes, J.C., 2015. Feeding habits of the speckled guitarfish Rhinobatos glaucostigma (Elasmobranchii: Rhinobatidae). J. Fish Biol. 87, 311–322.

https://doi.org/10.1111/jfb.12720

Last, P.., White, W.., Pogonoski, J.., 2010. Sharks and Rays From Borneo. CSIRO Marine & Atmospheric Research.

Lipej, L., Mavrič, B., Paliska, D., Capapé, C., 2013. Feeding habits of the pelagic stingray Pteroplatytrygon violacea (Chondrichthyes: Dasyatidae) in the Adriatic Sea. J. Mar. Biol. Assoc. United Kingdom 93, 285–290. https://doi.org/10.1017/S0025315412000197

Lyons, K., Carlisle, A.B., Lowe, C.G., 2017. Influence of ontogeny and environmental exposure on mercury accumulation in muscle and liver of male Round Stingrays. Mar. Environ. Res. 130, 30–37. https://doi.org/10.1016/j.marenvres.2017.07.004

Lyons, K., Lavado, R., Schlenk, D., Lowe, C.G., 2014. Bioaccumulation of organochlorine contaminants and ethoxyresorufin-o-deethylase activity in southern California round stingrays (Urobatis halleri) exposed to planar aromatic compounds. Environ. Toxicol. Chem. 33, 1380–1390. https://doi.org/10.1002/etc.2564

Lyons, K., Lowe, C.G., 2013. Quantification of maternal offloading of organic contaminants in elasmobranchs using the histotrophic round stingray (urobatis halleri) as a model. Environ. Sci. Technol. 47, 12450–12458. https://doi.org/10.1021/es402347d

Marcovecchio, J.E., Moreno, V.J., Perez, A., 1988. Determination of heavy metal concentrations in biota of Bahia Blanca, Argentina. Sci. Total Environ. 75, 181–190. https://doi.org/10.1016/0048-9697(88)90031-9

Miskiewicz, A.G., Gibbs, P.J., 1994. Organochlorine pesticides and hexachlorobenzene in tissues of fish and invertebrates caught near a sewage outfall. Environ. Pollut. 84, 269–277. https://doi.org/10.1016/0269-7491(94)90138-4

Molina, J.M., Lopez Cazorla, A., 2015. Biology of Myliobatis goodei (Springer, 1939), a widely

distributed eagle ray, caught in northern Patagonia. J. Sea Res. 95, 106–114. https://doi.org/10.1016/j.seares.2014.09.006

Mormede, S., Davies, I.M., 2001. Trace elements in deep-water fish species from the rockall trough. Fish. Res. 51, 197–206. https://doi.org/10.1016/S0165-7836(01)00245-4

Ong, M.C., Gan, S.L., 2017. Assessment of metallic trace elements in the muscles and fins of four landed elasmobranchs from Kuala Terengganu Waters, Malaysia. Mar. Pollut. Bull. 124, 1001–1005. https://doi.org/10.1016/j.marpolbul.2017.08.019

Ooi, M.S.M., Townsend, K.A., Bennett, M.B., Richardson, A.J., Fernando, D., Villa, C.A., Gaus, C., 2015. Levels of arsenic, cadmium, lead and mercury in the branchial plate and muscle tissue of mobulid rays. Mar. Pollut. Bull. 94, 251–259. https://doi.org/10.1016/j.marpolbul.2015.02.005

Penchaszadeh, P.., Arrighetti, F., Cledon, M., Livore, J.., Botto, F., Iribarne, O.., 2006. Bivalve contribution to shallow sandy bottom food web off Mar Del Plata (Argentina): inference from stomach contents and stable isotope analysis. J. Shellfish Res. 25, 51–54. https://doi.org/10.2983/0730-8000(2006)25[51:BCTSSB]2.0.CO;2

Rohner, C.A., Burgess, K.B., Rambahiniarison, J.M., Stewart, J.D., Ponzo, A., Richardson, A.J., 2017. Mobulid rays feed on euphausiids in the Bohol Sea. R. Soc. Open Sci. 4, 161060. https://doi.org/10.1098/rsos.161060

Ruelas-Inzunza, J., Escobar-Sanchez, O., Patron-Gomez, J., Moreno-Sanchez, X.G., Murillo-Olmeda, A., Spanopoulos-Hernandez, M., Corro-Espinosa, D., 2013. Mercury in muscle and liver of ten ray species from Northwest Mexico. Mar. Pollut. Bull. 77, 434–436. https://doi.org/10.1016/j.marpolbul.2013.09.010

Sandoval-Herrera, N.I., Vargas-Soto, J.S., Espinoza, M., Clarke, T.M., Fisk, A.T., Wehrtmann, I.S., 2016. Mercury levels in muscle tissue of four common elasmobranch species from the Pacific coast of

Costa Rica, Central America. Reg. Stud. Mar. Sci. 3, 254–261. https://doi.org/10.1016/j.rsma.2015.11.011

Sawyna, J.M., Spivia, W.R., Radecki, K., Fraser, D.A., Lowe, C.G., 2017. Association between chronic organochlorine exposure and immunotoxicity in the round stingray (Urobatis halleri). Environ. Pollut. 223, 42–50. https://doi.org/10.1016/j.envpol.2016.12.019

Senthil Kumar, K., Zushi, Y., Masunaga, S., Gilligan, M., Pride, C., Sajwan, K.S., 2009. Perfluorinated organic contaminants in sediment and aquatic wildlife, including sharks, from Georgia, USA. Mar. Pollut. Bull. 58, 621–629. https://doi.org/10.1016/j.marpolbul.2008.12.006

Šlejkovec, Z., Stajnko, A., Falnoga, I., Lipej, L., Mazej, D., Horvat, M., Faganeli, J., 2014. Bioaccumulation of arsenic species in rays from the northern Adriatic Sea. Int. J. Mol. Sci. 15, 22073–22091. https://doi.org/10.3390/ijms151222073

Sommerville, E., Platell, M.E., White, W.T., Jones, A.A., Potter, I.C., 2011. Partitioning of food resources by four abundant, co-occurring elasmobranch species: Relationships between diet and both body size and season. Mar. Freshw. Res. 62, 54–65. https://doi.org/10.1071/MF10164

Stehmann, M., Bürkel, D.., 1984. Rajidae, in: Whitehead, M.L., Bauchot, J.C., Hureau, J., Nielsen, Tortonese, E. (Eds.), Fishes of the North-Eastern Atlantic and Mediterranean. UNESCO, Paris, pp. 163–196.

Storelli, M.M., 2008. Potential human health risks from metals (Hg, Cd, and Pb) and polychlorinated biphenyls (PCBs) via seafood consumption: Estimation of target hazard quotients (THQs) and toxic equivalents (TEQs). Food Chem. Toxicol. 46, 2782–2788. https://doi.org/10.1016/j.fct.2008.05.011

Storelli, M.M., Barone, G., Piscitelli, G., Marcotrigiano, G.O., 2007. Mercury in fish: concentration vs. fish size and estimates of mercury intake. Food Addit. Contam. 24, 1353–7. https://doi.org/10.1080/02652030701387197

Storelli, M.M., Giacominelli Stuffler, R., Marcotrigiano, G.O., 2002. Total and methylmercury residues in cartilaginous fish from Mediterranean Sea. Mar. Pollut. Bull. 44, 1354–1358. https://doi.org/10.1016/S0025-326X(02)00223-0

Storelli, M.M., Giacominelli Stuffler, R., Marcotrigiano, G.O., 1998. Total mercury in muscle of benthic and pelagic fish from the South Adriatic Sea (Italy). Food Addit. Contam. 15, 876–883. https://doi.org/10.1080/02652039809374724

Storelli, M.M., Giacominelli Stuffler, R., Storelli, A., D'Addabbo, R., Palermo, C., Marcotrigiano, G.O., 2003a. Survey of total mercury and methylmercury levels in edible fish from the Adriatic Sea. Food Addit. Contam. 20, 1114–1119. https://doi.org/10.1080/02652030310001622773

Storelli, M.M., Giacominelli Stuffler, R., Storelli, A., Marcotrigiano, G.O., 2003b. Total Mercury and Methylmercury Content in Edible Fish from the Mediterranean Sea. J. Food Prot. 66, 300–303. https://doi.org/10.4315/0362-028X-66.2.300

Taylor, D.L., Kutil, N.J., Malek, A.J., Collie, J.S., 2014. Mercury bioaccumulation in cartilaginous fishes from Southern New England coastal waters: Contamination from a trophic ecology and human health perspective. Mar. Environ. Res. 99, 20–33. https://doi.org/10.1016/j.marenvres.2014.05.009

Torres, P., Tristão da Cunha, R., Micaelo, C., Rodrigues, A. dos S., 2016. Bioaccumulation of metals and PCBs in Raja clavata. Sci. Total Environ. 573, 1021–1030. https://doi.org/10.1016/j.scitotenv.2016.08.187

Türkmen, M., Tepe, Y., Türkmen, A., Kemal Sangün, M., Ateş, A., Genç, E., 2013. Assessment of heavy metal contamination in various tissues of six ray species from İskenderun Bay, northeastern Mediterranean sea. Bull. Environ. Contam. Toxicol. 90, 702–707. https://doi.org/10.1007/s00128-013-0978-7

Türkmen, M., Türkmen, A., Tepe, Y., 2014. Comparison of Metal Levels in Different Tissues of Seven

Ray Species from Antalya Bay, Mediterranean Sea. Bull. Environ. Contam. Toxicol. 93, 159–164. https://doi.org/10.1007/s00128-014-1285-7

USEPA, 2013. Fish Tissue Analysis for Mercury and PCBs From a New York City Commercial Fish/seafood Market. EPA/600/R- 11/066F. Washington, DC, USA.

Valenzuela-Quiñonez, F., Galván-Magaña, F., Ebert, D.A., Aragón-Noriega, E.A., 2017. Feeding habits and trophic level of the shovelnose guitarfish (Pseudobatos productus) in the upper Gulf of California. J. Mar. Biol. Assoc. United Kingdom 1–10. https://doi.org/10.1017/S0025315417000832

van Hees, K.E., Ebert, D.A., 2017. An evaluation of mercury offloading in two Central California elasmobranchs. Sci. Total Environ. 590–591, 154–162. https://doi.org/10.1016/j.scitotenv.2017.02.191

Vaudo, J.J., 2011. Habitat Use and Foraging Ecology of a Batoid Community in Shark Bay, Western Australia. Florida International University. Electronic Theses and Dissertations.

Weijs, L., Briels, N., Adams, D.H., Lepoint, G., Das, K., Blust, R., Covaci, A., 2015. Bioaccumulation of organohalogenated compounds in sharks and rays from the southeastern USA. Environ. Res. 137, 199–207. https://doi.org/10.1016/j.envres.2014.12.022

Yemışken, E., Forero, M.G., Megalofonou, P., Eryilmaz, L., Navarro, J., 2017. Feeding habits of three Batoids in the Levantine Sea (north-eastern Mediterranean Sea) based on stomach content and isotopic data. J. Mar. Biol. Assoc. United Kingdom 1–8. https://doi.org/10.1017/S002531541700073X

Zauke, G.P., Savinov, V.M., Ritterhoff, J., Savinova, T., 1999. Heavy metals in fish from the Barents Sea (summer 1994). Sci. Total Environ. 227, 161–173. https://doi.org/10.1016/S0048-9697(99)00014-5

CHAPTER 2 – Trophic ecology of sympatric batoid species (Chondrichthyes: Batoidea) assessed by multiple biogeochemical tracers (δ13C, δ15N and total Hg)

M.F. Bezerra et al. / *Environmental Research* 199 (2021) 111398

Environmental Research 199 (2021) 111398

Contents lists available at ScienceDirect

Environmental Research

journal homepage: www.elsevier.com/locate/envres

Trophic ecology of sympatric batoid species (Chondrichthyes: Batoidea) assessed by multiple biogeochemical tracers ($\delta^{13}C$, $\delta^{15}N$ and total Hg)

M.F. Bezerra [a,*], J.A. Seminoff [b], G.E. Lemons [b], D.G. Slotton [c], K. Watanabe [d], C.T. Lai [a]

[a] Department of Biology, San Diego State University, San Diego, CA, USA
[b] NOAA-National Marine Fisheries Service, Southwest Fisheries Science Center, La Jolla, CA, USA
[c] Department of Environmental Science and Policy, University of California, Davis, CA, USA
[d] School of Public Health, San Diego State University, San Diego, CA, USA

Abstract

Aquatic pollution is known to reduce biodiversity and disrupt wildlife populations. Mercury (Hg) pollution is pervasive worldwide, contributing to the degradation of ecosystems, and causing deleterious effects to exposed organisms and populations. Batoids have a life history linked to the benthic substrate of coastal areas and occupy upper trophic levels. These combined with large bodies, long lifespan, and slow growth rates contributes to increased uptake and accumulation of Hg. However, mechanisms governing these associations are not well understood. Using multiple biogeochemical tracers ($\delta^{13}C$, $\delta^{15}N$ and total Hg), we describe trophic interactions of three sympatric batoid species inhabiting an urbanized estuary and identify diet sources that contribute to Hg accumulation and trophic position among these mesopredators. We also use the Bat-ray (*Myliobatis californica*) as a model species, to compare diet composition, trophic position, and isotopic niche between two populations in two Californian bays. Trophic plasticity in *M. californica* was characterized by isotopic niche, diet proportions, and trophic position estimates using Bayesian statistics. We found diet and local contamination background strongly associated with Hg accumulation, and Hg levels that exceed EPA water quality criterion (< 0.3 $\mu g.g^{-1}$ w.w.) in all studied species.

1. Introduction

Batoids are elasmobranch fishes comprising stingrays, skates and guitarfishes (Ebert and Compagno, 2007; Fowler et al., 2005). They inhabit the benthic and pelagic environments from shallow estuarine and coastal waters to the continental shelf regions with depths up to 3000 m (Frisk, 2010). Compared to sharks and teleost fishes, trophic ecology of batoids is poorly understood (Vaudo and Heithaus, 2012). Diet composition in nearshore batoid species can vary regionally. For example, diet of the Bat-ray (*Myliobatis californica*) and the Round stingray (*Urobatis halleri*) consist predominantly of benthic invertebrates but main prey items differ between populations (Gray et al., 1997; Matern et al., 2000; Ridge, 1963). These differences in diet composition resemble an opportunist/generalist foraging behavior in which prey availability and predator competition are important factors to determine the trophic niche of these animals.

Bays and estuaries are highly productive and oceanographically dynamic areas that offer abundant prey while commonly serving as nursery and foraging habitats to many nearshore batoid species (Babel, 1967; Farrugia et al., 2011; Gray et al., 1997; Heupel et al., 2007). These are arguably the most affected areas of the coastal zone, where anthropogenic perturbations change the structure and dynamics of biotic communities (Kennish, 2002). For elasmobranchs in general, population decrease worldwide is mainly associated with overexploitation and habitat degradation (Dulvy et al., 2014), but especially for nearshore species, pollution is an important threat contributing to disruption of populations (Tiktak et al., 2020).

Mercury (Hg) is a highly toxic pollutant, with natural and anthropogenic sources (UN Environment, 2019), that causes deleterious effects to exposed organisms, including reduced immunological response, decreased reproduction success, neurochemical alterations, and behavioral changes (Scheuhammer et al., 2015). Majority of Hg in fish is methylmercury, an organic compound that accumulates in organisms and biomagnifies through the food web, placing upper trophic level predators at greater risk of exposure to high concentrations (Wiener et al., 2003). Mercury is ubiquitous in marine ecosystems and an animal's diet is the most important route of uptake and accumulation (Hall et al., 1997). With a biogeochemical

cycle closely linked to the foraging ecology of animals, Hg has been often used as a dietary tracer in many aquatic organisms, including seabirds (Thorne et al., 2021), marine mammals (Das et al., 2003; Peterson et al., 2015), fishes (Di Beneditto et al., 2013), and elasmobranches (Le Croizier et al., 2019; Pinzone et al., 2019).

Stable isotope analysis (SIA) is a biogeochemical tool that uses the natural variation in stable isotopes ratios of elements in organisms to understand the ecology (e.g. foraging, migration, habitat use, etc.) of wild populations (Peterson and Fry, 1987). In particular, the ratio of nitrogen ($^{15}N/^{14}N$) and carbon ($^{13}C/^{12}C$) relative to a reference standard (hereafter $\delta^{15}N$ and $\delta^{13}C$, respectively) are most commonly used to examine trophic dynamics (Post et al., 2007; Yeakel et al., 2016). $\delta^{13}C$ changes very little as carbon moves through food webs (enrichment of ~0.5‰ – 1‰) and reflects the main sources of carbon and major pathways of energy transfer in the food-web (Bouillon et al., 2011; Peterson and Fry, 1987). $\delta^{15}N$ is typically enriched in consumers (~2‰ – 4‰) relative to their diet which can provide an estimate of trophic position and characterization of trophic niche (Hussey et al., 2010; Layman et al., 2007; Post, 2002).

In the present study, our goals are twofold: (1) To describe trophic interactions of three sympatric batoid species inhabiting an urbanized estuary using carbon ($\delta^{13}C$) and nitrogen ($\delta^{15}N$) stable isotopes and total Hg (hereafter referred as THg) as ecological tracers. (2) to assess THg accumulation in two populations of *Myliobatis californica* while accounting for changes in trophic structure, diet sources, and contamination background. Our study areas are San Diego Bay (SDB) and Tomales Bay (TB), two low-inflow estuaries with distinct fish assemblages and contamination background levels. We ask the following questions (1) How do sympatric batoid species co-exist with limited available food resources in SDB? We hypothesize that species with a generalist feeding behavior (e.g. *M. californica; Urobatis halleri*) are sharing the available food resources and, thus, should present similar isotopic values while *Rhinobatos productus,* with a specialized feeding behavior, should present distinct isotopic values. (2) Do THg levels vary among sympatric batoid species in SDB? If so, do prey-predator relationships explain these variations?

We hypothesize that THg levels will reflect the batoids' feeding behaviors, with generalist species presenting a wider range of variation and specialist species presenting a narrower range of THg levels; (3) How do isotopic values and THg accumulation in *M. californica* differ between SDB and TB estuaries? We hypothesize that, given the generalist feeding behavior of this species, isotopic values will be equally variable in both locations and, thus, no significant differences in trophic niche should be observed. In regards to THg contamination, given the known differences in Hg background exposure levels between locations, we expect these to be reflected in *M. californica* with greater levels in TB compared to SDB.

2. Materials and Methods

2.1. Study site description

San Diego Bay (SDB) is semi-enclosed embayment, located in Southern California, impacted by heavy metals pollution due to urban runoff, and long-term military and recreational boating activities (Deheyn and Latz, 2006; Lenihan et al., 1990; Maloney and Chan, 1859). These activities contributed for the legacy of Hg contamination in this area, and despite current environmental regulations requiring treatment of waste discharges, many upper trophic level organisms are currently listed in consumption advisory issued by the State of California's Office of Environmental Health Hazard Assessment (OEHHA) (OEHHA, 2018). SDB is home to an estimated 78 fish species, with the most numerically abundant being Northern Anchovy (*Engraulis mordax*), Topsmelt (*Atherinops affinis*) and Slough Anchovy (*Anchoa delicatissima*) (Allen et al., 2002). In terms of biomass, the Round Stingray (*U. halleri*) and the Bat-ray (*M. californica*) are among the most relevant species, representing over 30% of total fish biomass in the estuary (Allen et al., 2002).

Tomales Bay (TB) is a narrow and relatively shallow estuary located in Marin County, Central California. Similar to SDB, strong tidal influence occurs at the outer bay zones where tidal exchange controls physicochemical water characteristics while, in the inner zones the major drivers of water characteristics are runoff, evaporation and rainfall (Smith et al., 1991; Smith and Hollibaugh, 1997). Elasmobranch assemblage is composed mainly of sharks species, including *Mustelus henlei, Triakis semifasciata*, and

Squatina californica, with only one batoid species (*M. californica*) known to occur year round (Ackerman et al., 2000; Campos et al., 2009; Hopkins and Cech, 2003). The TB watershed is predominantly rural with relatively low human impacts. However, historical Hg mining activities in the Walker Creek tributary watershed are considered to be an important point source of Hg contributing to elevated concentrations in sediments and biota throughout the estuary (Johnson et al., 2009; Ridolfi et al., 2010). The Health Advisory and Guidelines recommend avoiding consumption of all elasmobranch species from this estuary (OEHHA, 2009).

2.2. Sample collection

Batoid specimens were captured in San Diego Bay (32°36'56"N; 117°06'02"W) in November 2016, June 2017, July 2018 and October 2019, and in Tomales Bay (38°09'04"N; 122°54'22"W) in June 2019 using entanglement nets and hook and line. Disc width (total length for *R. productus*), weight and sex (identified by presence/absence of claspers in males) were recorded for each individual. Muscle and skin tissue samples were collected with a non-lethal approach using 6 mm diameter biopsy punches from the dorsal area of both "wings" (in *R. productus*, samples were taken from ventral area of the pelvic region) and homogenized into a single sample per tissue per individual. As a result, we had limited amount of skin tissue mass to run Hg analysis. Hg analysis requires a sample mass of ~0.5 g which was only obtained for muscle tissues in this study. On the other hand, SIA requires only ~1 mg of sample mass, which enabled analysis of both muscle and skin tissues.

All animals were released in good health condition after the sampling efforts. Potential prey items (i.e. infaunal and benthic invertebrates) were collected from multiple sites in each study area using hand tools during low tide. These collections took place in 2019 and 2020 in both estuaries. All samples were kept on ice in the field and stored frozen (-20 ºC) in the laboratory. Upon analysis, all samples were freeze-dried for 24h – 48h and homogenized using a porcelain mortar and pestle. For potential prey and primary producers, composite samples were obtained by pooling sampled individuals into the following groups:

Filter-feeding mollusks, omnivorous crustaceans, omnivorous fish, and primary producers including eelgrass (*Zostera marina*) and marine macroalgae.

2.3. Isotopic background dataset

We used the $\delta^{13}C$ and $\delta^{15}N$ values in primary producers and invertebrates compiled in the NOAA SWFSC database to characterize the food web isotopic baseline in the San Diego Bay. These isotopic baseline values were used to re-construct each batoids' role in the food web and calculate trophic position and diet proportions.

2.4. Biogeochemical tracer analysis

Total mercury (THg) concentrations were determined in the muscle tissue of each individual batoid sampled and in the composite samples of potential prey using a dedicated Perkin Elmer Flow Injection Mercury System (FIMS) and Direct Mercury Analyzer (DMA-80 Milestone, Inc.), respectively, according to Slotton et al., (2004) and the EPA Method 7473 (US EPA, 2007). Calibration curves (n = 3) with an overall range varying from 0.5 to 200 ng Hg were established with a mean linearity coefficient (R^2) of 0.9998 ± 0.0001. We assured analytical quality (i.e. accuracy and reproducibility) of Hg measurements by using analytical blanks (every 10 samples) and certified reference materials (BCR-463, NRC DOLT-4, NRC DORM-3) in every analysis batch. Total Hg recovery ranged from 97.6% to 101.8% (100.8 ± 1.4%, n = 6) for BCR-463, 101.7% to 103.7% (102.5 ± 0.8%, n = 6) for NRC DOLT-4, and 88.0% to 97.7% (91.2 ± 3.7%, n = 12) for NRC DORM-3. The limit of detection is 0.002 $\mu g.g^{-1}$ dry weight (d.w.). All Hg concentrations are expressed as $\mu g.g^{-1}$ d.w.

Isotopic determination in muscle and skin tissues consisted of approximately 1.0 mg of tissue material loaded into sterilized tin capsules and analyzed by a continuous-flow isotope-ratio mass spectrometer in the Stable Isotope Laboratory at the University of Florida, Gainesville USA. All samples were analyzed for their $\delta^{13}C$, $\delta^{15}N$, %C, and %N values. A Carlo Erba NA 1500 Elemental Analyzer system interfaced via a ConFlo II device (Finningan MAT) to a Thermo Electron DeltaV Ad- vantage gas IRMS was used.

Prior to exiting the elemental analyzer, combustion gas was measured using a thermal conductivity detector to determine percent compositions. USGS40 standards (9.52 % N, 40.82% C) were used for calibration. Sample stable isotope ratios relative to the isotope standard are expressed in the following conventional delta (δ) notation in parts per thousand (‰).

$$\delta = [(R_{Sample}/R_{standard}) - 1] \times 1000 \quad (1)$$

where R_{sample} and $R_{standard}$ are the corresponding ratios of heavy to light isotopes ($^{13}C/^{12}C$ and $^{15}N/^{14}N$) in the sample and international standard (Air for nitrogen and Vienna Pee Dee Belemnite for carbon), respectively.

We use stable isotope ratios measured from the tissue samples to compare trophic niche widths between the sympatric batoid species in the present study. Bearhop et al., (2004) suggested the use of stable isotope variance as a measure of trophic niche width in consumer populations. In the case of carbon and nitrogen isotopes, the variation presented in the so-called isotopic niche width will be used to suggest the range of carbon source, forage location or diet components and the range of prey trophic levels, respectively. We use an open-source Bayesian stable isotope package to quantify the metrics of isotopic variance (discussed below).

2.5. Data analysis

All statistical analyses and plots were performed using R version 3.4.3 (R Core Team, 2017). Parametric assumptions of the data were tested using Shapiro Wilks and Levene's tests. We conducted parametric and non-parametric ANOVAs to examine the effects of location (SDB, TB), sex (male, female), and size class (juvenile, adult) on the $\delta^{13}C$ and $\delta^{15}N$ values and THg concentrations. To test for differences in $\delta^{13}C$ and $\delta^{15}N$ values between tissues, we conducted paired parametric and non-parametric (t tests and Wilcoxon rank test) tests. For factors with more than 2 levels, such as species (e.g. *M. californica, U. halleri,* and *R. productus;* for SDB only), non-parametric Kruskal Wallis and post hoc pairwise Wilcoxon Rank tests, with Holm corrections, were used to assess differences in $\delta^{13}C$ and $\delta^{15}N$ values and THg

concentrations. Parametric and non-parametric correlation tests (Person and Spearman) were conducted for all variable pairs (THg, $\delta^{13}C$, $\delta^{15}N$, and size (weight and length) in all species from SDB and TB. Using the Stable Isotope Bayesian Ellipses package (SIBER), we calculated isotopic niche space metrics (e.g. Total area (TA), $\delta^{13}C$ range, $\delta^{15}N$ range, and SEAc - standard ellipse area corrected for small sample size). The overlaps between SEAc of co-occurring species were calculated using the "maxLikOverlap" function (Jackson et al., 2011). Standard ellipses were also constructed using $\delta^{13}C$-Hg and $\delta^{15}N$-Hg pairs to provide complimentary information on species' trophic niches, referred here as contamination niche (Pinzone et al., 2019). Trophic levels of batoid species were estimated by the tRophicposition package (Quezada-Romegialli et al., 2018) using filter-feeding mollusks collected at each site as the N and C baselines (TP = 2). Three potential sources (mollusks, crustaceans, and polychaetes) were used to estimate prey contribution to batoid's diet using the SIAR package (Parnell et al., 2010). We employed multiple diet-tissue discrimination factors ($\Delta^{15}N = \delta^{15}N_{consumer} - \delta^{15}N_{prey}$ and $\Delta^{13}C = \delta^{13}C_{consumer} - \delta^{13}C_{prey}$) in our models and compared our results with the literature, including an elasmobranch-specific $\Delta^{15}N$ of 2.29 ± 0.22 ‰ and $\Delta^{13}C$ of 0.9 ± 0.33 ‰ reported by Hussey et al., (2010), and the generally used $\Delta^{15}N$ of 3.4 ± 0.98 ‰ and $\Delta^{13}C$ of 1 ± 0.5 ‰ reported by Post (2002). Statistical significance was defined as $p < 0.05$.

3. Results

Fifty-six individuals of four batoid species were sampled in SDB and TB, including *M. californica* (n = 41), *R. productus* (n = 4), *U. halleri* (n = 10), and *Gymnura marmorata* (n = 1). Only *M. californica* occurred and was sampled in both locations (n = 26 in SDB, and n = 15 in TB). All other species came from SDB. The *M. californica* specimens collected in SDB were all identified as juveniles (seven males, and 19 females) based on the classification method described in García-Rodríguez et al. (2020), while in TB we collected 6 adults (all males) and 9 juvenile (five females, four males) individuals. For *U. halleri*, two individuals were identified as adults following Hale and Lowe, (2008), while for *R. productus* three individuals were classified as adults (Villavicencio-Garayzar, 1993). None of the four studied species are

classified as vulnerable or threatened therefore not prioritized for conservation efforts according to the International Union for Conservation of Nature (IUCN) Red List of Threatened Species (IUCN, 2021).

3.1. $\delta^{13}C$ and $\delta^{15}N$ isotopic ranges, differences, and correlations

A representation of the SDB and TB food webs are presented in a $\delta^{13}C$ and $\delta^{15}N$ dual isotope space (mean ± SD) for each batoid species, and other ecological groups (e.g. omnivorous teleosts, omnivorous crustaceans, filter-feeding mollusks, polychaetes, and primary producers) (Fig. 2. 1). Mean muscle $\delta^{13}C$ values in SDB's batoids ranged from -17.24 ± 0.80 ‰ in *M. californica* to -16.17 ± 2.64 ‰ in *U. halleri*. Mean muscle $\delta^{15}N$ values ranged from 15.25 ± 0.76 ‰ in *M. californica* to 17.63 ± 0.65 ‰ in *R. productus*. In TB, $\delta^{13}C$ and $\delta^{15}N$ isotopic values in *M. californica* ranged from -17.4 ‰ to -13.0 ‰ (-14.86 ± 1.14 ‰), and from 13.9 ‰ to 16.8 ‰ (15.02 ± 0.98 ‰), respectively (Tab. 2. 1).

We found a small but significant difference in $\delta^{13}C$ and $\delta^{15}N$ isotopic values between skin and muscle tissues of *M. californica* from SDB ($\delta^{13}C$: paired t-test t = -12.25, df = 25, $p < 0.001$; $\delta^{15}N$: paired t-test t = 7.51, df = 25, $p = 0.002$). On average, muscle tissues for this species were depleted in $\delta^{13}C$ by 1.31 ‰ and enriched in $\delta^{15}N$ by 0.62 ‰ compared to skin tissues. Differences in isotopic values between tissues in *M. californica* from TB were significant for $\delta^{13}C$ (paired t-test t = -5.23, df = 14, $p < 0.001$), but not for $\delta^{15}N$ (paired Wilcoxon rank test V = 67, n = 15, $p = 0.72$).For *U. halleri* and *R. productus*, differences between tissues were not statistically significant for neither $\delta^{13}C$ nor $\delta^{15}N$ ($p > 0.05$) (Tab. S2.1).

We found significant differences in muscle $\delta^{15}N$ values among species in SDB (n = 406, Kruskal-Wallis H = 14.5, df = 2, $p < 0.001$) (Tab. S2.2). Post hoc pairwise comparisons detected a significant difference between *M. californica* and *R. productus* (Pairwise Wilcoxon Rank test: $p < 0.001$) and between *M. californica* and *U. halleri* ($p = 0.006$) (Tab. S2.2). We found no differences in muscle $\delta^{13}C$ isotopic values among species co-existing within SDB (ANOVA $F_{2, 37} = 2.06$, $p = 0.14$) (Tab. S2.3). In contrast, mean $\delta^{13}C$ isotopic values in muscle tissues of *M. californica* differed significantly between the two locations (ANOVA $F_{1, 39} = 61.32$, $p < 0.001$), with higher values in TB compared to SDB. We found no significant

differences in $\delta^{15}N$ isotopic values for this species between locations (ANOVA $F_{1, 39} = 0.23$, $p = 0.632$). In regards to size class, only *M. californica* in TB presented enough individuals from both size classes (e.g. juvenile and adult) to test for differences among variables. We observed no differences in $\delta^{13}C$ (ANOVA $F_{1, 13} = 0.001$, $p = 0.973$) or $\delta^{15}N$ (Mann-Whitney W = 25, n = 15, $p = 0.86$) values between juvenile and adults. In regards to sex, no differences were observed for any variable ($p > 0.28$) (Tab. S2.2 and S2.3). Isotopic values of $\delta^{13}C$ and $\delta^{15}N$ were not significantly correlated with size, sex nor between each other ($p > 0.21$) for all batoid species in SDB and TB, except for *M. californica* in SDB which presented a significant negative correlation between $\delta^{13}C$ and $\delta^{15}N$ values (Pearson r = -0.80, $p < 0.001$).

3.2. Total Hg accumulation, differences and correlations

Mean THg concentrations in SDB batoid species were 1.14 ± 0.33 $\mu g.g^{-1}$ in *M. californica*, 1.86 ± 0.65 $\mu g.g^{-1}$ in *R. productus*, and 0.54 ± 0.16 $\mu g.g^{-1}$ in *U. halleri* (Tab. 2. 1). We found significant differences in Hg concentration among species in SDB (n = 40, Kruskal-Wallis H = 22.4, df = 2, $p < 0.001$). Post hoc tests showed that Hg concentration in *U. halleri* were significantly lower compared to *M. californica* (Pairwise Wilcoxon Rank test: $p < 0.001$) and *R. productus* ($p = 0.004$), and significantly higher in *R. productus* compared to *M. californica* ($p = 0.04$ (Fig. 2.2). In TB, mean THg concentration in *M. californica* was 1.59 ± 0.42 $\mu g.g^{-1}$ and significantly higher compared to *M. californica* in SDB (ANOVA $F_{1, 39} = 14.8$, $p < 0.001$). We found no significant correlations ($p > 0.14$) between THg concentrations and any of the other variables (i.e. size, sex, $\delta^{13}C$, and $\delta^{15}N$) in all batoid species from both locations (Tab. 2. S4).

Niche differences among species characterized by isotopic and contamination measurements

Based on SIBER model results using $\delta^{13}C$ and $\delta^{15}N$ (Fig. 2. 3), *U. halleri* presented the largest isotopic niche represented by a SEAc of 16.21, while *R. productus* and M. *californica* presented SEAc of 6.34 and 1.20, respectively. Between locations, the isotopic niche was larger in TB compared to SDB with a SEAc of 4.31 and 1.20 found in *M. californica*, respectively. The isotopic niche for *U. halleri* had a modest

overlapping area, with 30% and 7% of its SEAc overlapping with *R. productus* and *M. californica*, respectively. By contrast, 77% of *R. productus* and 89% of *M. californica* isotopic niches overlapped with *U. halleri.* We observed no overlaps in the isotopic niche between *R. productus* and *M. californica*.

Contamination niche, based on T-Hg and $\delta^{15}N$ values (Fig. 2. 4A), was the largest in *R. productus* with SEAc area of 1.85. *M californica* and *U. halleri* presented similar contamination niche areas with SEAc of 0.82 and 0.88, respectively. We found no overlaps of THg-$\delta^{15}N$ contamination niche among batoid species. Similarly, based on T-Hg and $\delta^{13}C$ (Fig. 2. 4B), contamination niche was the largest in *R. productus* with SEAc area of 6.75, followed by *U. halleri* and *M. californica* with SEAc areas of 1.47 and 0.86, respectively. An overlapping area of THg-$\delta^{13}C$ contamination niche was observed only between *M. californica* and *R. productus*, where an overlapping area of 0.19 corresponded to 22% and 3% of SEAc, respectively.

3.3. Trophic position and diet proportions

Based on the tRophicposition model output using diet-tissue discrimination factors from Hussey et al., (2010) ($\Delta^{15}N = 2.29 \pm 0.22$ ‰ and $\Delta^{13}C = 0.9 \pm 0.33$ ‰), the estimated trophic position (TP) for *M. californica* was 3.4 and 3.0 in SDB and TB, respectively, with no significant differences between sites ($p = 0.79$). For *U. halleri, R. productus* and *G. marmorata*, estimated TP was 3.8, 4.2 and 3.5, respectively. We found no statistically significant differences in TP among batoid species ($p > 0.09$), except between *M. californica* and *R. productus* ($p = 0.019$). Using diet-tissue discrimination factors from Post, (2002) ($\Delta^{15}N = 3.4 \pm 0.98$ ‰ and $\Delta^{13}C = 1 \pm 0.5$ ‰), we found similar results of TP (3.5 for *U. halleri,* 3.8 for *R. productus,* 3.3 for *G. marmorata,* and 3.2 and 2.8 for *M. californica* in SDB and TB, respectively) which again, showed a significant difference between *M. californica* and *R. productus* ($p = 0.021$).

Based on SIAR model using diet-tissue discrimination factors from Hussey et al., (2010) (Fig. 2. 5), *M. californica* diet proportions in TB among the three potential sources were crustaceans (29.7 ± 10.9%), mollusks (24.8 ± 6.9%), and polychaetes (45.6 ± 11.6%). In contrast, *M. californica* from SDB fed mainly

on mollusk (81.1 ± 3%), with small contributions to the diet by crustaceans (6.8 ± 4.8%) and polychaetes (12.1 ± 5.9%). Using diet-tissue discrimination factors from Hussey et al., (2010), *U. halleri* diet proportion were crustaceans (23.9 ± 14%), mollusks (44.0 ± 13%), and polychaetes (31.9 ± 16.5%). We found *R. productus* feeding mainly on teleosts (59.1 ± 16%), with smaller contributions by crustaceans (17.5 ± 13.1%) and mollusks (23.4 ± 14.4%). Using diet-tissue discrimination factors from Post, (2002), we found similar results in source contribution for all species in both areas.

4. Discussion

Over the multiple years of this study, juvenile individuals of *M. californica* and *U. halleri* accounted for the large majority (94%) of captures in San Diego Bay (SDB). Although that alone does not characterize this area as a nursery habitat (Heupel et al., 2007), this area is clearly an important feeding ground for juvenile individuals of both species. Because of our small sample size for *R. productus* inferences at the population-level for this species should be considered with caution. This study reports new information on resource partitioning of sympatric batoid species at an early life stage, which has a large impact on the overall health of the adult populations (Cortés, 2002).

4.1. Stable Isotope differences in tissues

Stable isotope values in metabolically distinct tissues represent different time periods of feeding prior to sampling, and this time period is longer in tissues with slower metabolic turnover (MacNeil et al., 2006). A high-metabolism tissue, such as blood, reflects a shorter time period of feeding prior to sampling compared to slow-metabolism tissues, such as muscle and cartilage (Hobson and Clark, 1992; Logan and Lutcavage, 2010). There are only a few studies reporting differences in isotopic values among tissues of elasmobranchs. Differences among tissues is commonly associated with the different turnover rate of each tissue (Carlisle et al., 2012; Hussey et al., 2012).

In the present study, we found a small but consistent difference among all species, in $\delta^{13}C$ and $\delta^{15}N$ isotopic values between muscle and skin tissues. These differences result from distinct chemical

composition (e.g. carbohydrate, protein, lipid etc) that made of each tissue. Additionally, the isotopic variation measured among tissue types, reflects differences in the metabolic pathways and elemental turnover rates during the biosynthesis of each tissue type. In elasmobranches, stable isotope values in muscle tissues integrate over a year of diet (~488 days) (Logan and Lutcavage, 2010; MacNeil et al., 2006), while for skin/dermal tissues turnover rate is still unknown. Some authors speculate that skin/dermal tissue integrates elasmobranch diet from several months to a year (Carlisle et al., 2012; Marcus et al., 2019), which would place skin in a moderate place between fast (e.g. blood, liver) and slow (e.g. muscle, cartilage) turnover rates. If that is the case, considering our sampling occurred during Summer and Fall, differences between tissues observed in our study can be postulated as a result of different foraging strategies during colder seasons (e.g. Winter and early Spring), reflected by skin values, compared to warmer seasons (e.g. late Spring and Summer), reflected by muscle values. In fact, some batoid species are reported to have seasonal occurrence in many estuaries and bays along the California coast with higher occurrence observed during Spring and Summer compared to the Winter season (Gray et al., 1997; Jirik and Lowe, 2012). Therefore, it is reasonable to expect that isotopic values in these animals reflect feeding from inside and outside the bay.

In future studies, differences in isotopic composition between tissues can potentially be investigated using compound-specific isotope analysis of amino acids composing each tissue. This technique has been demonstrated as a powerful tool for estimating trophic positions in aquatic food webs (Chikaraishi et al., 2009), and may also be used to quantify various isotopic fractionation during the biosynthesis process that result in the observed bulk $\delta^{13}C$ and $\delta^{15}N$ disparity between skin and muscle tissues.

4.2. Stable isotope, diet and trophic position of sympatric batoid species

The wide range of $\delta^{13}C$ isotopic values found in batoid species from SDB suggest multiple sources of carbon to the base of the food web. Estuaries are complex and dynamic ecosystems presenting many sources of carbon, such as C3 and C4 plants, marine and estuarine phytoplankton, seagrasses, and benthic algae (Bouillon et al., 2011). Marine algae in SDB presented lower $\delta^{13}C$ values (-17.35 ± 4.07 ‰)

compared to eelgrass (-11.73 ± 1.74 ‰), which encompassed the variability observed in batoids. Additionally, batoids are known to occur in the estuary seasonally (Gray et al., 1997; Talent, 1985) and, thus, the wide range of $\delta^{13}C$ values can also be a result of feeding in areas outside the estuary with distinct isotopic ratios.

The multiple trophic levels of batoid species in the present study explain the observed variation in $\delta^{15}N$ isotopic values. The higher $\delta^{15}N$ values in *R. productus* suggest a diet with larger contribution by teleosts, which are generally in higher trophic positions compared to crustaceans and mollusks. Our diet mixing models suggested *R. productus* fed largely on fish (59.1 ± 16%) with smaller contributions from crustaceans and mollusk. Such specialized diet also resulted in a relatively small isotopic niche for this species (SEAc = 6.34). A stomach content study in another estuary along the California coast, reported *R. productus* feeding mainly on crustaceans but with a consistent contribution from fish to the diet of larger individuals (Talent, 1982). Similar results, based on stomach content and stable isotope analysis, were reported by Valenzuela-Quiñonez et al., (2017) studying the same species in the Gulf of California, Mexico. These authors found that crustaceans were the main prey for *R. productus* but with larger individuals of *R. productus* (> 83 cm of TL) having increased contribution of teleost fish (~25%) in their diet (Valenzuela-Quiñonez et al., 2017). Our results suggest that fish contribution to the diet of larger individuals can be significant even though our sample size of four individuals is not a good representation of the entire adult population. Regardless, our trophic models estimated a trophic position of 3.8 for this species, which is in close agreement with the value of 3.4 estimated for large individuals by Valenzuela-Quiñonez et al. (2017) using the same $\Delta^{15}N$ value ($\Delta^{15}N$ = 3.4% according to Post (2002)).

$\delta^{15}N$ isotopic values in *M. californica* also differed from other sympatric species. According to our mixing models, this species fed mainly on mollusks (81.1 ± 3%), which corresponds to the smallest isotopic niche (SEAc = 1.20) among our studied species. A similar diet contribution was also observed for this species in other estuaries along California coast, where clams were the most important item found in the stomachs of juvenile and adult individuals (Gray et al., 1997; Talent, 1982). This preference for low

trophic level prey is reflected by the lower trophic position (3.2) estimated for this species in the present study. To our knowledge, this is the first study to estimate the trophic position of *M. californica* using stable isotopes. Our finding is consistent with previous stomach content analyses showing that this species primarily consumes mollusks and occupies an estimated trophic position of 3.3 (Jacobsen and Bennett, 2013).

The wide range in $\delta^{15}N$ isotopic values observed in the tissue of *U. halleri* (6.5‰ in muscle and 3.4‰ in skin) suggest a diet composed of prey with variable ^{15}N content and/or significant individual diet specialization. Previous stomach content analysis suggested that the diet of *U. halleri* is composed of mollusks, crustaceans, polychaetes, and fish (Babel, 1967; Jacobsen and Bennett, 2013; Valadez-Gonzalez et al., 2001). Our results show that these three prey groups have distinct $\delta^{15}N$ values in SDB (Table 2.1); thus, individuals feeding on different proportion of each prey group is likely the cause for the wide range of $\delta^{15}N$ values observed in the present study.

Variability in $\delta^{15}N$ values has been associated with a mixed diet elsewhere. In the Caribbean, the Southern stingray (*Dasyatis americana*) presented a $\delta^{15}N$ range of 3.42‰, which was explained by a generalist diet composed of soft bodied invertebrates, bivalves and crabs (Gilliam and Sullivan, 1993; Tilley et al., 2013). It is worth mentioning that reproductive behavior, growth rate, and starvation can confound interpretation of $\delta^{15}N$ variations. Lyons et al. (2017) suggested that starvation associated with reproductive behavior might have produced the increased blood $\delta^{15}N$ observed in adults of *U. halleri* compared to juveniles. Starvation is observed in adults during mating seasons when individuals rely on internal energy reserves to support metabolism (Lyons et al., 2017). The metabolism of internal reserves during starvation periods has been shown to increase $\delta^{15}N$ values in hair tissue of humans (Mekota et al., 2006), however, a recent study found the opposite effect in Whale sharks (*Rhincodon typus*) (Wyatt et al., 2019). These authors reported decreases in $\delta^{15}N$ values in captive and wild individuals associated with a high growth rate and starvation. In the present study, because the majority of sampled individuals were

juvenile, reproduction behavior is unlikely to explain isotopic variations. However, starvation and a fast growth rate are potential factors influencing the wide range in $\delta^{15}N$ isotopic values observed here.

Based on the potential prey groups reported by (Babel, 1967; Jacobsen and Bennett, 2013; Valadez-Gonzalez et al., 2001), our mixing models estimate that *U. halleri* in SDB feeds on a mixed diet with similar proportions of mollusks, crustaceans, and polychaetes (Fig. 2. 5). Such foraging behavior also resulted in the largest isotopic niche among our studied species (SEAc = 16.21). Our trophic position derived for this species (3.5) is similar to the estimate based on stomach content analysis (3.58) from the literature (Jacobsen and Bennett, 2013), and places this species in a similar trophic level as *M. californica* in SDB.

The interpretation of overlapping isotopic niches between sympatric species is generally due to resource partitioning and interspecific competition (Murillo-Cisneros et al., 2019; Shiffman et al., 2019; Vaudo and Heithaus, 2011). In the present study, we observed no overlaps in isotopic niche between *R. productus* and *M. californica* (Fig. 2. 3), which suggest these species do not directly compete for food resources besides sharing foraging habitats. Similar results were also observed in another foraging area along the Baja California Sur coast (Murillo-Cisneros et al., 2019). These authors interpreted the little overlap between these species as an indication of resource segregation. This interpretation is applicable to our results and corroborated by differences in diet (Gray et al., 1997; Valenzuela-Quiñonez et al., 2017), $\delta^{15}N$ values, and estimated trophic positions for these two species (Murillo-Cisneros et al., 2019).

In contrast, a high degree of overlap was observed between the isotopic niche of *U. halleri* and isotopic niches of the other two batoid species (Fig. 2. 3), suggesting that *U. halleri* competes for the same food resources with *M. californica* and *R. productus*. It is important to note that the isotopic niche of *U. halleri* was strongly influenced by two individuals with very low $\delta^{13}C$ values, which if removed would have produced a smaller overlap area. Regardless, this kind of inter-specific interaction has been reported for elasmobranch species elsewhere. For example, in a shark nursery area on the northeast coast of Queensland, Australia, seven juvenile sharks presented overlapping $\delta^{15}N$ values indicating that they were

feeding on prey with similar isotopic values (Kinney et al., 2011). For sympatric batoid species in the Mediterranean, two species from the genus *Raja* were observed to have overlapping isotopic niches and similar trophic positions (Yemışken et al., 2017). Another important aspect was observed for *M. californica* in the present study, when comparing isotopic niche between SDB and TB. We observed trophic plasticity in this species, as evidenced by a smaller isotopic niche area (SEAc) in SDB compared to TB (Tab. 2. 1) and separately supported by different proportions of prey contributions to the diet (Fig. 2. 5).

Considering that, in SDB, *M. californica* share habitats with multiple batoid species (Allen et al., 2002) while, in TB, this is the only batoid species known to commonly occur (Hopkins and Cech, 2003), the observed changes in isotopic niche area is an indication of diet plasticity and foraging adaptation for this species. In sharks, diet plasticity was observed in *Carcharhinus limbatus* and *C. acronotus* inhabiting the south coast of Florida where species isotopic niche and overlap changed among site of occurrence (Shiffman et al., 2019). Another example was observed in the Gulf of Mexico for the shark species *Rhizoprionodon terraenovae* (Drymon et al., 2012). These authors reported $\delta^{15}N$ values of the captured individuals varying between eastern and western regions, which was interpreted as an indication of change in diet. That interpretation was supported by trawl data demonstrating differences in fish and invertebrate biomass between these regions (Drymon et al., 2012). It is possible that dietary and foraging habitat plasticity is a common trait in elasmobranchs, allowing for co-existence of sympatric species that feed at similar trophic levels (Barría et al., 2018; Drymon et al., 2012; Kiszka et al., 2015).

Interpretation of $\delta^{15}N$ variation in consumers can provide important insights into trophic ecology and diet of predators. However, interpretation is not always straight-forward as variation in isotopic values can be confounded by factors other than prey choice, such as similarity in isotopic values among distinct prey species, prey's excretion mode, and fasting or starvation of consumers (Mekota et al., 2006; Newsome et al., 2007; Vanderklift and Ponsard, 2003). That is where the use of complementary chemical tracers, such

as mercury (Hg), can help the interpretation of isotopic variation and trophic interactions (McMeans et al., 2010).

4.3. Hg accumulation and contamination niche

A recent review shows that about a third of batoid species worldwide are at risk of toxicity effects from Hg exposure considering a Lowest Observed Adverse Effect Level (LOAEL) of 0.5 $\mu g.g^{-1}$ w. w. (Bezerra et al., 2019; Depew et al., 2012). This is alarming, considering these are mesopredators typically feeding on small fishes, zooplankton and benthic invertebrates (Ebert and Bizzarro, 2007; Jacobsen and Bennett, 2013). As mechanisms governing Hg bioaccumulation in elasmobranchs are not well understood, the present study contributes to a better understanding of this issue. The nearly sole pathway for Hg uptake in fish is through food intake (Bradley et al., 2017; Hall et al., 1997). Therefore, diet is one of the most important factors to explain differences in Hg accumulation in fish (Ferriss and Essington, 2014; Lacerda et al., 2014; Teffer et al., 2014). By pairing Hg concentrations with $\delta^{15}N$ and $\delta^{13}C$ values in our SIBER models, it was possible to distinguish species based on their contamination niches (Fig. 2. 4). Our results show that, in contrast to major overlaps in the isotopic niches (Fig. 2. 3), *M. californica* and *U. halleri* presented significant differences in Hg concentrations and non-overlapping contamination niches (Fig. 2. 4).

That finding suggests these species are in fact partitioning resources while sharing the foraging habitat. Differences in Hg concentration in batoid species in the present study result from differences in Hg concentrations of potential prey, where filter-feeding mollusks (the main prey item for *M. californica*) presented higher Hg levels than omnivorous crustaceans and polychaetes (Tab. 2. 1). Omnivorous teleosts presented the highest Hg levels among prey, which can explain the higher Hg levels found in *R. productus*. Such associations between Hg concentration and food preference has been reported for many marine taxa, including batoids (Bezerra et al., 2019), sharks (McMeans et al., 2010), and teleost fishes (Bank et al., 2007; Cai et al., 2007). For batoids, a meta-analysis of trace element contamination found that diet was one of the factors to better explain Hg contamination in species worldwide (Bezerra et al.,

2019). These authors found significantly lower Hg accumulation in batoids feeding mainly on zooplankton compared to species with other food preferences, such as crustaceans, mollusks and fish. However, diet is not the only factor governing Hg accumulation in marine organisms. Animal size/age (Moura et al., 2020; Rodriguez et al., 2020) and geographical location (Lacerda et al., 2014; Le Bourg et al., 2019; Bezerra et al. 2019) are also important under different scenarios.

Hg accumulates in fish if there is a positive net balance between uptake and elimination processes, and this process is generally evidenced by greater Hg levels in larger/older individuals compared to smaller/younger ones (Bradley et al., 2017). Many examples exist of Hg concentration increasing with animal size in elasmobranchs (Cai et al., 2007; Taylor et al., 2014). However, this is not always the case as negative correlations between Hg concentration and size (De Carvalho et al., 2014; de Pinho et al., 2002; Rumbold et al., 2014), and the absence of significant correlation (Le Croizier et al., 2020; McMeans et al., 2010; Moura et al., 2020) have also been reported for elasmobranchs. In the present study, we found no significant correlation between Hg concentration and animal size in any of the studied species. We attributed this to the fact that the majority of our specimens were juvenile and, thus, they all had similar Hg assimilation efficiencies. In life stages with fast growth rates, such as the juvenile, size changes at a faster pace compared to Hg assimilation, which is known as the 'growth dilution effect' (Dang and Wang, 2012). This is generally why Hg increases with size is not detected when analyzing juvenile fish populations. Similar results have been reported for juvenile populations of *Aetobatos narinari* along the northeastern coast of Brazil (Moura et al., 2020), and *Carcharhinus albimarginatus* in the northeast Pacific Ocean (Le Croizier et al., 2020).

Geographical location is another important factor that influences Hg accumulation in elasmobranchs from the legacy effect in Hg background contamination. Mercury enters the food web through assimilation by filter-feeding organisms and primary producers (Mason et al., 1996). Therefore, changes in local Hg background can have a significant effect on Hg levels in upper trophic level consumers. We found higher Hg levels in *M. californica* from TB compared to SDB despite similarities in body size, diet and

estimated trophic position (Tab. 2.1). We attributed this to the influence of distinct Hg background levels between these areas. The Tomales Bay watershed is predominantly rural with relatively low human impacts, but with a history of Hg mining activities that contributes to current elevated concentrations in sediments and biota throughout the estuary (Johnson et al., 2009; Whyte and Kirchner, 2000). Past Hg impairment assessments reported Hg levels exceeding U.S. EPA criterion of 0.3 $\mu g.g^{-1}$ w.w. (USEPA, 2001) for several sport fishes, including *Paralichthys californicus*, *Triakis semifasciata*, *Mustelus henlei*, S*quatina californica*, and *M. californica* (OEHHA, 2004; Ridolfi et al., 2010). A decade later, Hg levels in *M. californica* are still above this threshold as evidenced by the present study. San Diego Bay is also impacted by elevated Hg contamination (Bay et al., 2016) and, currently, both SDB and TB have active safety advisories limiting consumption of many fish species, including elasmobranchs (OEHHA, 2018, 2009).

5. Conclusions

We presented here a description of trophic interactions among three sympatric batoid species in a foraging and nursery habitat along the Southern California coast. By using Hg as a complementary dietary tracer, it was possible to separate overlapping isotopic niches and to describe ecological niches of these organisms. We observed isotopic niche plasticity in *M. californica,* as indicated by changes in SEAc when comparing SDB and TB. This finding is consistent with previous studies reporting diet variation in this species.

We partially rejected our first hypothesis and concluded that *M. californica* and *U. halleri* presented distinct $\delta^{15}N$ isotope values, even while sharing the available food resources as generalist mesopredators. This was evidenced by overlapping areas of isotopic niches and similar estimated trophic positions. We did not reject our second hypothesis and concluded that differences in Hg levels observed in batoids in SDB were consistent with species-specific diet differences, where *M. californica* (mainly feeding on filter-feeding mollusks) presented higher Hg levels compared to *U. halleri* (mixed diet of mollusk, crustaceans and polychaetes), and lower compared to *R. productus* (piscivorous diet). Differences in Hg

background levels between SDB and TB were reflected in *M. californica*, but not in the potential prey samples. The reason for that is not entirely clear and demands further investigations with a more extensive prey sampling effort also focusing on areas outside the bay to fully characterize the diet Hg pool in *M. californica*, given their great swimming capacity and known seasonality of occurrence in both areas.

Finally, we partially rejected our third hypothesis and concluded that although no significant differences were observed in trophic position and isotopic values ($\delta^{15}N$ and $\delta^{13}C$) in *M. californica* between SDB and TB we did observe differences in isotopic niche (represented by SEAc) with a smaller area in SDB compared to TB. That was interpreted as an indication of trophic plasticity in feeding behavior/diet for this species facilitating co-existence with other batoid species and reducing competition for food. This study demonstrates the benefit of using multiple biogeochemical tracers in Hg and stable isotopes (^{13}C and ^{15}N) to understand the trophic ecology of elasmobranch fishes.

Table 2.1 – Sample size (n), disc width (cm), mean Hg ± standard deviation (μg.g^{-1} d.w.), $\delta^{13}C$ and $\delta^{15}N$ isotopic values (‰), Standard Ellipse Area (SEAc), and estimated trophic position (TP) in batoid species collected in San Diego Bay (SDB) and Tomales Bay (TB).

Species	n	Disc width ± SD (min - max)		Hg ± SD (min – max)	$\delta^{15}N$ ± SD (min – max)	$\delta^{13}C$ ± SD (min – max)	Total area (TA)	$\delta^{15}N$ range	$\delta^{13}C$ range	[a]SEAc	TP_{post}	TP_{hussey}
San Diego Bay												
Myliobatis californica	26	62.7 ± 8.3 (50.5 – 84.5)	Muscle	1.14 ± 0.33 (0.68 – 1.88)	15.25 ± 0.76 (13.2 – 16.7)	-17.24 ± 0.80 (-18.8 – -15.6)	4.47	3.5	3.2	1.20	3.1	3.4
			Skin	-	14.63 ± 0.64 (12.8 – 15.9)	-15.93 ± 0.62 (-16.9 – -14.5)		3.1	2.4			
Rhinobatos productus	4	112.6 ± 17.9* (89.0 – 131.1)	Muscle	1.86 ± 0.65 (1.23 – 2.45)	17.63 ± 0.65 (16.7 – 18.2)	-16.14 ± 2.36 (-18.1 – -12.9)	3.49	1.5	5.2	6.34	3.8	4.2
			Skin	-	16.70 ± 2.47 (14.3 – 19.3)	-16.56 ± 2.17 (-18.6 – -14.0)		5.9	4.6			
Urobatis halleri	10	13.9 ± 1.1 (12.4 – 16.0)	Muscle	0.54 ± 0.16 (0.29 – 0.83)	16.46 ± 1.74 (13.4 – 19.9)	-16.17 ± 2.64 (-21.3 – -14.2)	28.09	6.5	7.1	16.21	3.5	3.8
			Skin	-	16.08 ± 0.98 (14.4 – 17.8)	-15.09 ± 2.90 (-20.9 – -11.7)		3.4	9.2			
Gymnura marmorata	1	29.9	Muscle	-	16.34	-14.83					3.3	3.5
			Skin	-	16.65	-16.26						
Tomales Bay												
Myliobatis californica	15	66.2 ±7.2 (56.4 – 80.0)	Muscle	1.59 ± 0.42 (0.91 – 2.26)	15.11 ± 1.11 (13.9 – 17.5)	-14.86 ± 1.14 (-17.4 – -13.0)	10.31	3.6	4.4	4.31	2.8	3.0
			Skin	-	15.02 ± 0.98 (13.9 – 16.8)	-14.07 ± 1.2 (-16.9 – -11.9)		2.9	5.0			

* Total length. [a] For $\delta^{13}C$ and $\delta^{15}N$ pair.

Table 2.2 – Species, sample size (n), Hg (µg.g^{-1} d.w.), and $\delta^{13}C$ and $\delta^{15}N$ values (‰) in the Food web at San Diego Bay and Tomales Bay.

Species	n*	Hg ± SD (min – max)	$\delta^{15}N$ ± SD (min – max)	$\delta^{13}C$ ± SD (min – max)
Tomales Bay				
Omnivorous crustaceans	3	0.03 ± 0.01 (0.02 – 0.04)	12.33 ± 1.27 (10.9 – 13.3)	-14.47 ± 3.87 (-16.7 – -10.0)
Filter-feeding mollusks	12	0.16 ± 0.04 (0.11 – 0.23)	12.53 ± 0.58 (11.4 – 13.4)	-20.81 ± 1.55 (-22.8 – -18.9)
Polychaete	3	0.11 ± 0.03 (0.08 – 0.14)	13.05 ± 0.93 (12.1 – 14.0)	-14.53 ± 2.74 (-17.2 – -11.8)
Primary producer - Eelgrass	1	0.02	9.86	-21.04
Primary producer - Algae	1	0.06	10.10	-11.40
San Diego Bay				
Omnivorous teleosts	4[d]	0.15 ± 0.05 (0.08 – 0.18)	15.89 ± 1.62 (14.7 – 18.2)	-14.85 ± 3.0 (-19.1 – -12.3)
Omnivorous crustaceans	6	0.04 ± 0.03[a] (0.02 – 0.07)	12.65 ± 1.45 (9.9 – 13.8)	-14.55 ± 3.97 (-19.1 – -10.1)
Filter-feeding mollusks	12	0.12 ± 0.04 (0.04 – 0.18)	11.21 ± 0.74 (10.3 – 13.0)	-19.08 ± 0.85 (-21.1 – -17.9)
Herbivorous mollusks	4[e]	-	12.43 ± 0.94 (11.0 – 13.0)	-6.51 ± 1.86 (-8.1 – -4.3)
Polychaete	5	0.05[b]	14.71 ± 1.27 (12.8 – 16.1)	-15.68 ± 1.54 (-17.3 – -13.8)
Primary producer - Eelgrass	48	0.02 ± 0.01[c] (0.01 – 0.02)	10.01 ± 1.12 (7.9 – 12.3)	-11.73 ± 1.74 (-16.4 – -9.3)
Primary producer - Algae	62	-	11.93 ± 1.85 (8.6 – 18.2)	-17.35 ± 4.07 (-31.8 – -9.7)

*Composite sample unless otherwise noted. [a] n = 3. [b] n = 1. [c] n = 2. [d, e] individual samples.

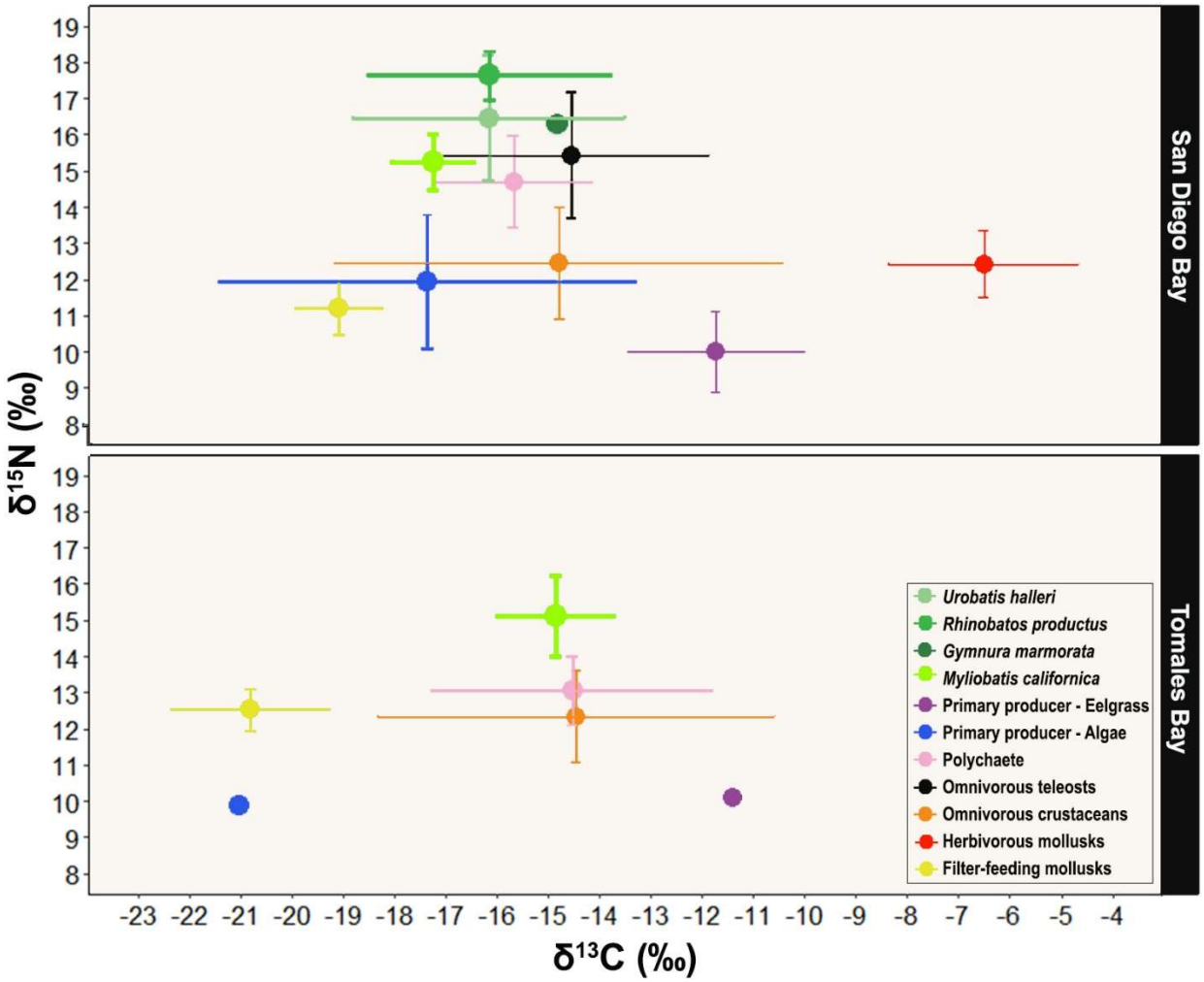

Figure 2.1 – Food-web isotopic space represented by mean ± SD of $\delta^{15}N$ and $\delta^{13}C$ in San Diego Bay (top) and Tomales Bay (bottom). ***This figure fits as a single-column image***

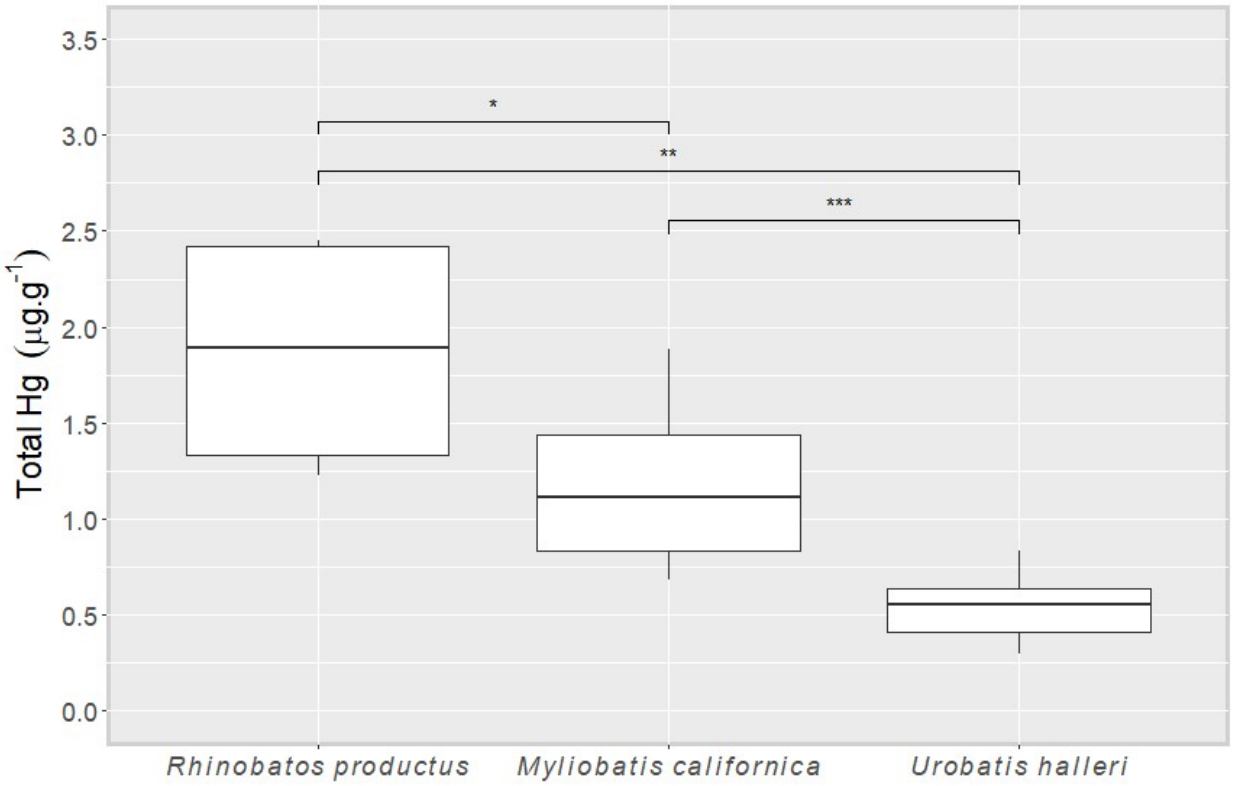

Figure 2.2 – Boxplot (median, 25th and 75th percentiles, and 1.5 * IQR whiskers) of Hg concentration in batoid species from San Diego Bay. Asterisks represent significant differences: Pairwise Wilcoxon post-hoc test, *$p \leq 0.05$, ** $p \leq 0.01$, *** $p \leq 0.001$. ***This figure fits as a single-column image***

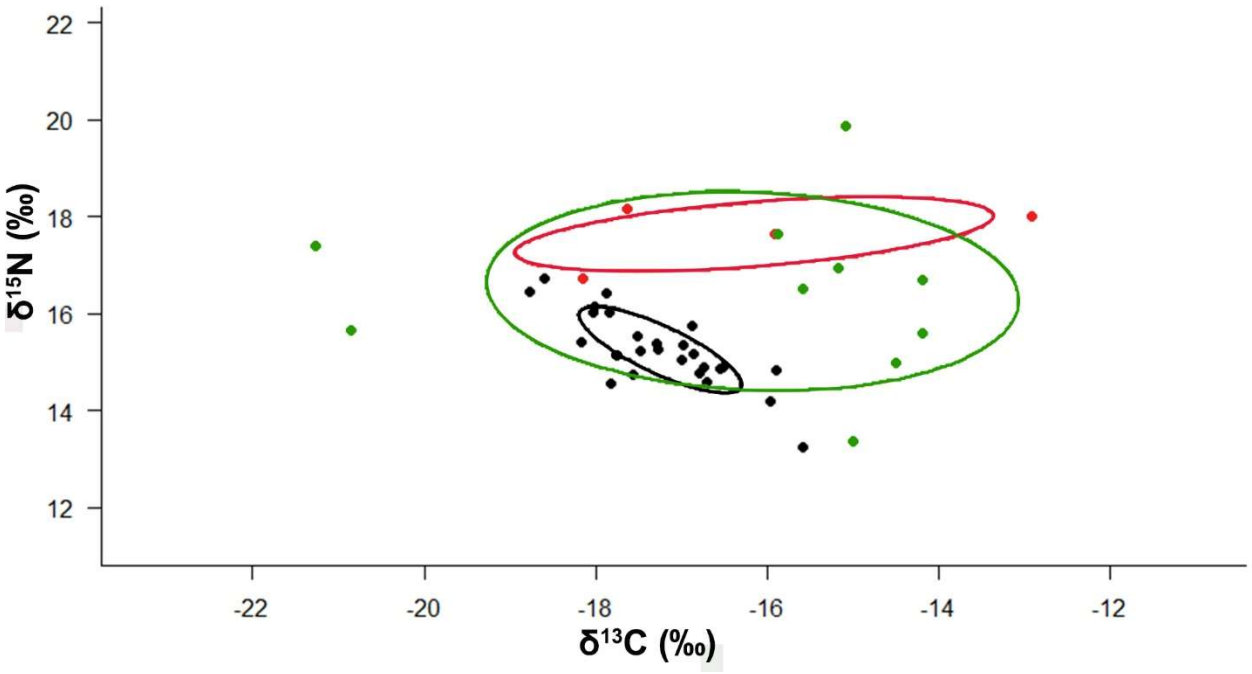

Figure 2.3 – Isotopic niche occupied by sympatric batoid species in San Diego Bay (SDB). Green ellipse: *U. halleri*; Red ellipse: *R. productus*; and Black ellipse: *M. californica*. ***This figure fits as a single-column image***

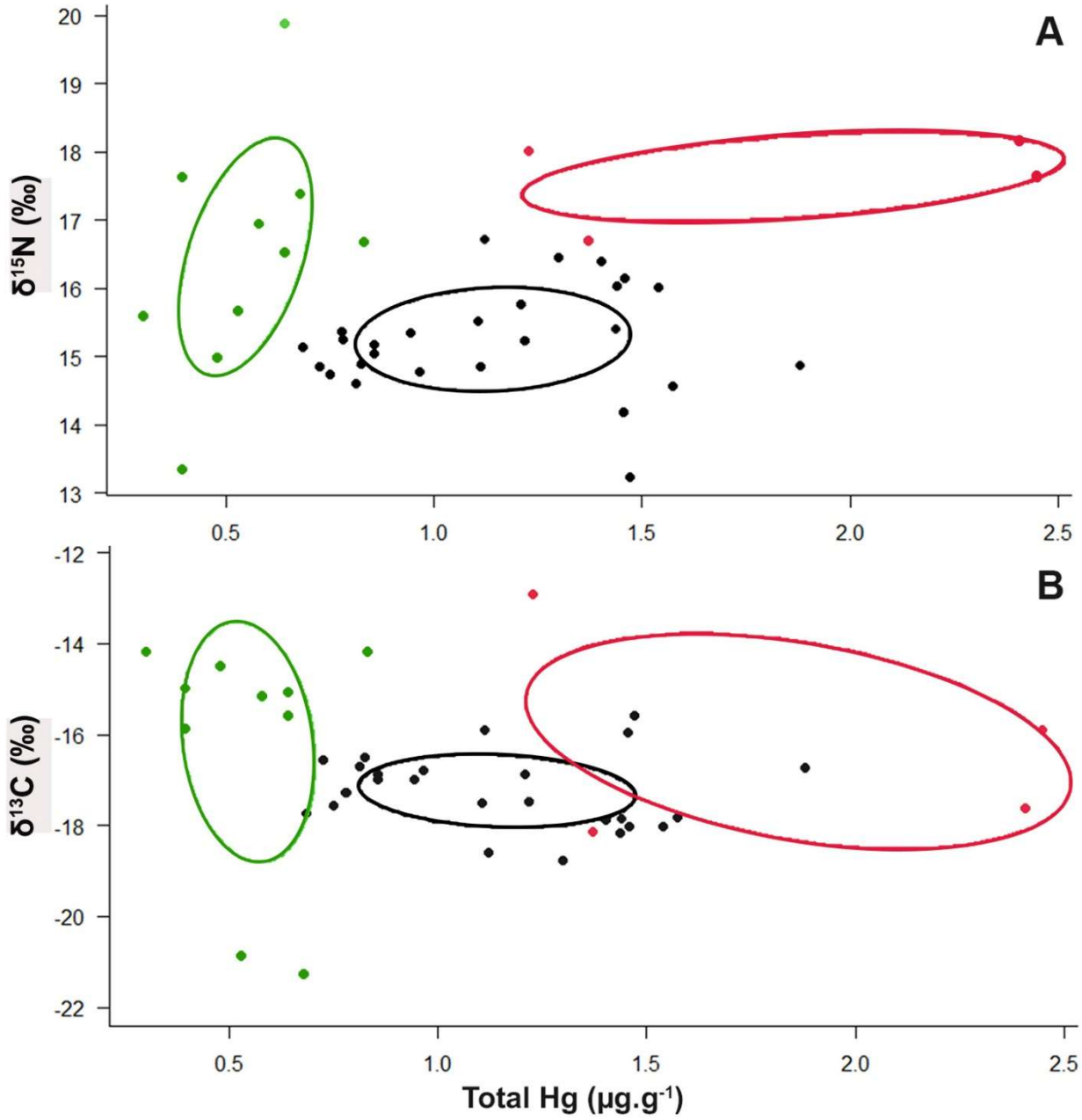

Figure 2.4 – Contamination niches [Total Hg vs. $\delta^{15}N$ (A) and Total Hg vs. $\delta^{13}C$ (B)] occupied by sympatric batoid species in San Diego Bay (SDB). Green ellipse: *U. halleri*; Red ellipse: *R. productus*; and Black ellipse: *M. californica*. ***This figure fits as a single-column image***

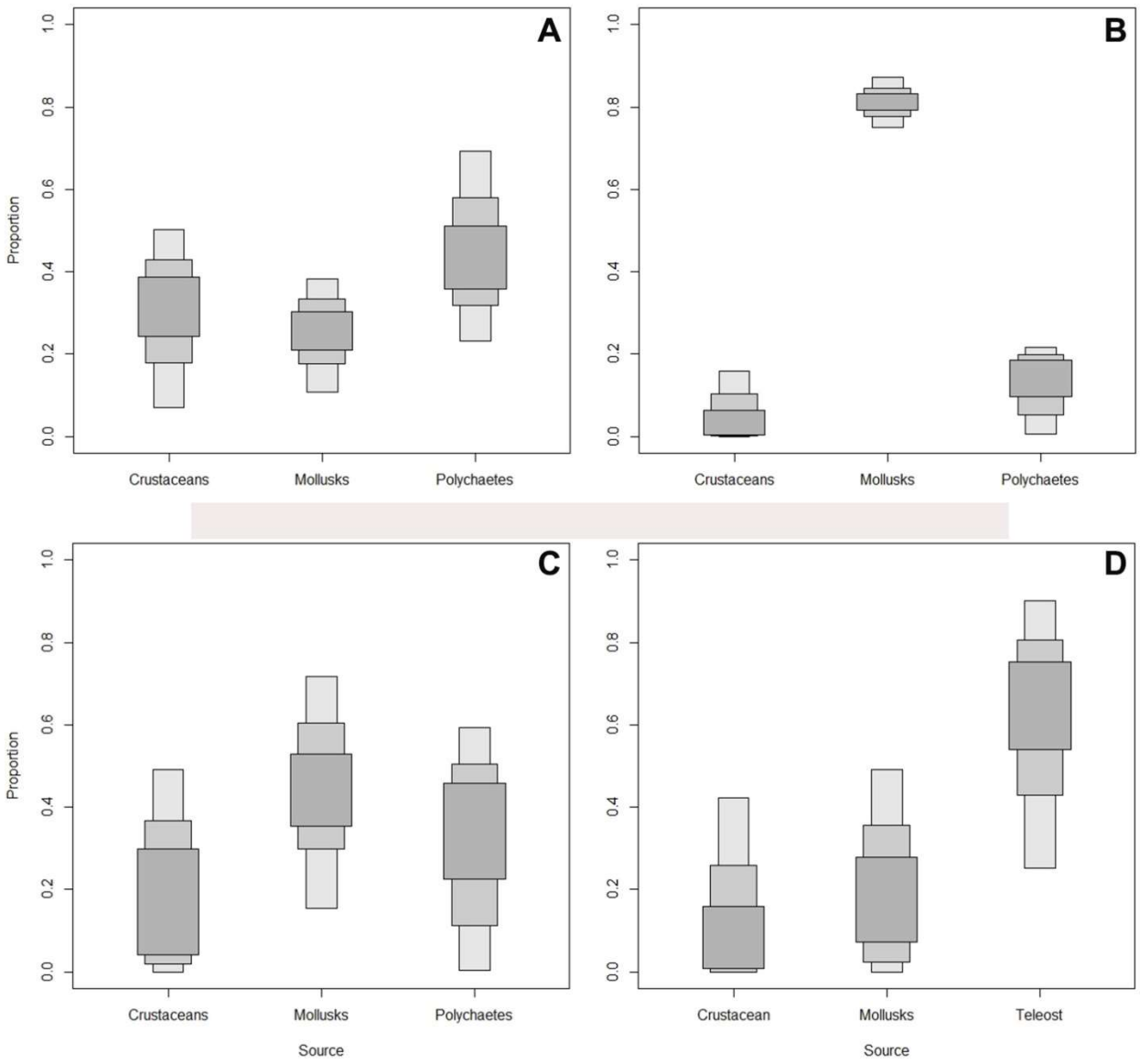

Figure 2.5 – Diet proportion of batoid species. (A) *M. californica* in TB, (B) *M. californica* in SDB, (C) *U. halleri* in SDB, (D) *R. productus* in SDB. ***This figure fits as a single-column image***

References

Ackerman, J.T., Kondratieff, M.C., Matern, S.A., Cech, J.J., 2000. Tidal influence on spatial dynamics of leopard sharks, Triakis semifasciata, in Tomales Bay, California. Environ. Biol. Fishes 58, 33–43. https://doi.org/10.1023/A:1007657019696

Allen, L.G., Findlay, A.M., Phalen, C.M., 2002. Structure and Standing Stock of the Fish Assemblages of San Diego Bay, California from 1994 to 1999. Bull. South. Calif. Acad. Sci. 101, 49–85.

Babel, J.S., 1967. Reproduction, life history, and ecology of the round stingray, Urolophus halleri Cooper. Fish Bull. 1–104.

Bank, M.S., Chesney, E., Shine, J.P., Maage, A., Senn, D.B., 2007. Mercury bioaccumulation and trophic transfer in sympatric snapper species from the gulf of Mexico. Ecol. Appl. 17, 2100–2110. https://doi.org/10.1890/06-1422.1

Barría, C., Navarro, J., Coll, M., 2018. Trophic habits of an abundant shark in the northwestern Mediterranean Sea using an isotopic non-lethal approach. Estuar. Coast. Shelf Sci. 207, 383–390. https://doi.org/10.1016/j.ecss.2017.08.021

Bay, S.M., Greenstein, D.J., Parks, A.N., Zeeman, C.Q.T., 2016. Assessment of Bioaccumulation in San Diego Bay. Technical report 953. https://doi.org/10.1017/CBO9781107415324.004

Bearhop, S., Adams, C.E., Waldron, S., Fuller, R.A., Macleod, H., 2004. Determining trophic niche width: A novel approach using stable isotope analysis. J. Anim. Ecol. 73, 1007–1012. https://doi.org/10.1111/j.0021-8790.2004.00861.x

Bezerra, M.F., Lacerda, L.D., Lai, C., 2019. Trace metals and persistent organic pollutants contamination in batoids (Chondrichthyes : Batoidea): A systematic review *. Environ. Pollut. 248, 684–695. https://doi.org/10.1016/j.envpol.2019.02.070

Bouillon, S., Connolly, R.M., Gillikin, D.P., 2011. Use of Stable Isotopes to Understand Food Webs and

Ecosystem Functioning in Estuaries. Treatise Estuar. Coast. Sci. 143–173. https://doi.org/10.1016/B978-0-12-374711-2.00711-7

Bradley, M.A., Barst, B.D., Basu, N., 2017. A review of mercury bioavailability in humans and fish. Int. J. Environ. Res. Public Health 14. https://doi.org/10.3390/ijerph14020169

Cai, Y., Rooker, J.R., Gill, G.A., Turner, J.P., 2007. Bioaccumulation of mercury in pelagic fishes from the northern Gulf of Mexico. Can. J. Fish. Aquat. Sci. 64, 458–469. https://doi.org/10.1139/f07-017

Campos, B.R., Fish, M.A., Jones, G., Riley, R.W., Allen, P.J., Klimley, P.A., Cech, J.J., Kelly, J.T., 2009. Movements of brown smoothhounds, Mustelus henlei, in Tomales Bay, California. Environ. Biol. Fishes 85, 3–13. https://doi.org/10.1007/s10641-009-9462-y

Carlisle, A.B., Kim, S.L., Semmens, B.X., Madigan, D.J., Jorgensen, S.J., Perle, C.R., Anderson, S.D., Chapple, T.K., Kanive, P.E., Block, B.A., 2012. Using stable isotope analysis to understand the migration and trophic ecology of northeastern Pacific white sharks (Carcharodon carcharias). PLoS One 7. https://doi.org/10.1371/journal.pone.0030492

Chikaraishi, Y., Ogawa, N.O., Kashiyama, Y., Takano, Y., Suga, H., Tomitani, A., Miyashita, H., Kitazato, H., Ohkouchi, N., 2009. Determination of aquatic food-web structure based on compound-specific nitrogen isotopic composition of amino acids. Limnol. Oceanogr. Methods 7, 740–750. https://doi.org/10.4319/lom.2009.7.740

Cortés, E., 2002. Incorporating uncertainty into demographic modeling: Application to shark populations and their conservation. Conserv. Biol. 16, 1048–1062. https://doi.org/10.1046/j.1523-1739.2002.00423.x

Dang, F., Wang, W.X., 2012. Why mercury concentration increases with fish size? Biokinetic explanation. Environ. Pollut. 163, 192–198. https://doi.org/10.1016/j.envpol.2011.12.026

Das, K., Beans, C., Holsbeek, L., Mauger, G., Berrow, S.D., Rogan, E., Bouquegneau, J.M., 2003. Marine

mammals from northeast atlantic: Relationship between their trophic status as determined by δ13C and δ15N measurements and their trace metal concentrations. Mar. Environ. Res. 56, 349–365. https://doi.org/10.1016/S0141-1136(02)00308-2

De Carvalho, G.G.A., Degaspari, I.A.M., Branco, V., Canário, J., De Amorim, A.F., Kennedy, V.H., Ferreira, J.R., 2014. Assessment of total and organic mercury levels in blue sharks (Prionace glauca) from the south and southeastern Brazilian coast. Biol. Trace Elem. Res. 159, 128–134. https://doi.org/10.1007/s12011-014-9995-6

de Pinho, A.P., Guimarães, J.R.D., Martins, A.S., Costa, P.A.S., Olavo, G., Valentin, J., 2002. Total mercury in muscle tissue of five shark species from Brazilian Offshore waters: Effects of feeding habit, sex, and length. Environ. Res. 89, 250–258. https://doi.org/10.1006/enrs.2002.4365

Deheyn, D.D., Latz, M.I., 2006. Bioavailability of metals along a contamination gradient in San Diego Bay (California, USA). Chemosphere 63, 818–834. https://doi.org/10.1016/j.chemosphere.2005.07.066

Depew, D.C., Basu, N., Burgess, N.M., Campbell, L.M., Devlin, E.W., Drevnick, P.E., Hammerschmidt, C.R., Murphy, C.A., Sandheinrich, M.B., Wiener, J.G., 2012. Toxicity of dietary methylmercury to fish: Derivation of ecologically meaningful threshold concentrations. Environ. Toxicol. Chem. 31, 1536–1547. https://doi.org/10.1002/etc.1859

Di Beneditto, A.P.M., Bittar, V.T., de Rezende, C.E., Camargo, P.B., Kehrig, H.A., 2013. Mercury and stable isotopes δ15N and δ13C) as tracers during the ontogeny of Trichiurus lepturus. Neotrop. Ichthyol. 11, 211–216. https://doi.org/10.1590/s1679-62252013000100024

Drymon, J.M., Powers, S.P., Carmichael, R.H., 2012. Trophic plasticity in the Atlantic sharpnose shark (Rhizoprionodon terraenovae) from the north central Gulf of Mexico. Environ. Biol. Fishes 95, 21–35. https://doi.org/10.1007/s10641-011-9922-z

Dulvy, N.K., Fowler, S.L., Musick, J. a, Cavanagh, R.D., Kyne, M., Harrison, L.R., Carlson, J.K., Davidson, L.N.K., Sonja, V., 2014. Extinction risk and conservation of the world ' s sharks and rays. Elife 1–35. https://doi.org/10.7554/eLife.00590

Ebert, D., Bizzarro, J.J., 2007. Standardized diet compositions and trophic levels of skates (Chondrichthyes: Rajiformes: Rajoidei). Dev. Environ. Biol. Fishes 80, 221–237. https://doi.org/10.1007/s10641-007-9227-4

Ebert, D.A., Compagno, L.J. V, 2007. Biodiversity and systematics of skates (Chondrichthyes: Rajiformes: Rajoidei). Environ. Biol. Fishes 80, 111–124. https://doi.org/10.1007/s10641-007-9247-0

Farrugia, T.J., Espinoza, M., Lowe, C.G., 2011. Abundance, habitat use and movement patterns of the shovelnose guitarfish (*Rhinobatos productus*) in a restored southern California estuary. Mar. Freshw. Res. 62, 648–657. https://doi.org/10.1071/MF10173

Ferriss, B.E., Essington, T.E., 2014. Does trophic structure dictate mercury concentrations in top predators? A comparative analysis of pelagic food webs in the Pacific Ocean. Ecol. Modell. 278, 18–28. https://doi.org/10.1016/j.ecolmodel.2014.01.029

Fowler, S.L., Cavanagh, R.D., Camhi, M., Burgess, G.H., Cailliet, G.M., Fordham, S. V, Simpfendorfer, C. a, Musick, J. a, 2005. Sharks, rays and chimaeras: the status of the chondrichthyan fishes, National Wildlife. https://doi.org/10.2305/IUCN.CH.2005.SSC-AP.9.en

Frisk, M.G., 2010. Life History Strategies of Batoids, in: Carrier, J.C., Musick, J.A., Heithaus, M.R. (Eds.), Sharks And Their Relatives II: Biodiversity, Adaptive Physiology, And Conservation. CRC Press, pp. 283–316. https://doi.org/10.1201/9781420080483

García-Rodríguez, A., Hernández-Herrera, A., Galván-Magaña, F., Ceballos-Vázquez, B.P., Pelamatti, T., Tovar-Ávila, J., 2020. Estimation of the size at sexual maturity of the bat ray (Myliobatis

californica) in northwestern Mexico through a multi-model inference. Fish. Res. 231, 105712. https://doi.org/10.1016/j.fishres.2020.105712

Gilliam, D., Sullivan, K.M., 1993. Diet and feeding habits of the southern stingray Dasyatis americana in the central Bahamas. Bull. Mar. Sci. 52, 1007–1013.

Gray, A.E., Mulligan, T.J., Hannah, R.W., 1997. Food habits, occurrence, and population structure of the bat ray, *Myliobatis californica*, in Humboldt Bay, California. Environ. Biol. Fishes 49, 227–238.

Hale, L.F., Lowe, C.G., 2008. Age and growth of the round stingray Urobatis halleri at Seal Beach, California. J. Fish Biol. 73, 510–523. https://doi.org/10.1111/j.1095-8649.2008.01940.x

Hall, B.D., Bodaly, R.A., Fudge, R.J.P., Rudd, J.W.M., Rosenberg, D.M., 1997. Food as the dominant pathway of methylmercury uptake by Fish. Water. Air. Soil Pollut. 100, 13–24. https://doi.org/10.1023/A:1018071406537

Heupel, M.R., Carlson, J.K., Simpfendorfer, C.A., 2007. Shark nursery areas: Concepts, definition, characterization and assumptions. Mar. Ecol. Prog. Ser. 337, 287–297. https://doi.org/10.3354/meps337287

Hobson, K.A., Clark, R.G., 1992. ASSESSING AVIAN DIETS USING STABLE ISOTOPES I: TURNOVER OF 13C IN TISSUES Canadian Wildrife Service, Prairie and Northern Wildlife Centre, I1 5 Perimeter Road. Condor 94, 181–188.

Hopkins, T.E., Cech, J.J., 2003. The influence of environmental variables on the distribution and abundance of three elasmobranchs in Tomales Bay, California. Environ. Biol. Fishes 66, 279–291. https://doi.org/10.1023/A:1023907121605

Hussey, N.E., Brush, J., McCarthy, I.D., Fisk, A.T., 2010. δ15N and δ13C diet-tissue discrimination factors for large sharks under semi-controlled conditions. Comp. Biochem. Physiol. - A Mol. Integr. Physiol. 155, 445–453. https://doi.org/10.1016/j.cbpa.2009.09.023

Hussey, N.E., Olin, J.A., Kinney, M.J., McMeans, B.C., Fisk, A.T., 2012. Lipid extraction effects on stable isotope values (δ13C and δ15N) of elasmobranch muscle tissue. J. Exp. Mar. Bio. Ecol. 434–435, 7–15. https://doi.org/10.1016/j.jembe.2012.07.012

IUCN, 2021. The IUCN Red List of Threatened Species. Version 2021-1. https://www.iucnredlist.org. Downloaded on 7 May 2021.

Jackson, A.L., Inger, R., Parnell, A.C., Bearhop, S., 2011. Comparing isotopic niche widths among and within communities: SIBER - Stable Isotope Bayesian Ellipses in R. J. Anim. Ecol. 80, 595–602. https://doi.org/10.1111/j.1365-2656.2011.01806.x

Jacobsen, I.P., Bennett, M.B., 2013. A comparative analysis of feeding and trophic level ecology in stingrays (Rajiformes; Myliobatoidei) and electric rays (Rajiformes: Torpedinoidei). PLoS One 8, e71348. https://doi.org/10.1371/journal.pone.0071348

Jirik, K.E., Lowe, C.G., 2012. An elasmobranch maternity ward: Female round stingrays Urobatis halleri use warm, restored estuarine habitat during gestation. J. Fish Biol. 80, 1227–1245. https://doi.org/10.1111/j.1095-8649.2011.03208.x

Johnson, B.E., Esser, B.K., Whyte, D.C., Ganguli, P.M., Austin, C.M., Hunt, J.R., 2009. Mercury accumulation and attenuation at a rapidly forming delta with a point source of mining waste. Sci. Total Environ. 407, 5056–5070. https://doi.org/10.1016/j.scitotenv.2009.05.025

Kennish, M.J., 2002. Environmental threats and environmental future of estuaries. Environ. Conserv. 29, 78–107. https://doi.org/10.1017/S0376892902000061

Kinney, M.J., Hussey, N.E., Fisk, A.T., Tobin, A.J., Simpfendorfer, C.A., 2011. Communal or competitive? Stable isotope analysis provides evidence of resource partitioning within a communal shark nursery. Mar. Ecol. Prog. Ser. 439, 263–276. https://doi.org/10.3354/meps09327

Kiszka, J.J., Aubail, A., Hussey, N.E., Heithaus, M.R., Caurant, F., Bustamante, P., 2015. Plasticity of

trophic interactions among sharks from the oceanic south-western Indian Ocean revealed by stable isotope and mercury analyses. Deep. Res. Part I Oceanogr. Res. Pap. 96, 49–58. https://doi.org/10.1016/j.dsr.2014.11.006

Lacerda, L.D., Costa, B.G.B.C., Lopes, D.N., Oliveira, K., Bezerra, M.F., Bastos, W.R., 2014. Mercury in indigenous, introduced and farmed fish from the semiarid region of the Jaguaribe River Basin, NE Brazil. Bull. Environ. Contam. Toxicol. 93. https://doi.org/10.1007/s00128-014-1263-0

Layman, C.A., Arrington, D.A., Montaña, C.G., Post, D.M., 2007. Can Stable Isotope Ratios Provide for Community-Wide Measures of Trophic Structure? Ecology 88, 42–48. https://doi.org/10.1890/0012-9658(2007)88[42:CSIRPF]2.0.CO;2

Le Bourg, B., Kiszka, J.J., Bustamante, P., Heithaus, M.R., Jaquemet, S., Humber, F., 2019. Effect of body length, trophic position and habitat use on mercury concentrations of sharks from contrasted ecosystems in the southwestern Indian Ocean. Environ. Res. 169, 387–395. https://doi.org/10.1016/j.envres.2018.11.024

Le Croizier, G., Lorrain, A., Schaal, G., Ketchum, J., Hoyos-Padilla, M., Besnard, L., Munaron, J.M., Le Loc'h, F., Point, D., 2020. Trophic resources and mercury exposure of two silvertip shark populations in the Northeast Pacific Ocean. Chemosphere 253. https://doi.org/10.1016/j.chemosphere.2020.126645

Le Croizier, G., Schaal, G., Point, D., Le Loc'h, F., Machu, E., Fall, M., Munaron, J.M., Boyé, A., Walter, P., Laë, R., Tito De Morais, L., 2019. Stable isotope analyses revealed the influence of foraging habitat on mercury accumulation in tropical coastal marine fish. Sci. Total Environ. 650, 2129–2140. https://doi.org/10.1016/j.scitotenv.2018.09.330

Lenihan, H., Oliver, J., Stephenson, M., 1990. Changes in hard bottom communities related to boat mooring and tributyltin in San Diego Bay a natural experiment . Mar. Ecol. Prog. Ser. 60, 147–159. https://doi.org/10.3354/meps060147

Logan, J.M., Lutcavage, M.E., 2010. Stable isotope dynamics in elasmobranch fishes. Hydrobiologia 644, 231–244. https://doi.org/10.1007/s10750-010-0120-3

Lyons, K., Carlisle, A.B., Lowe, C.G., 2017. Influence of ontogeny and environmental exposure on mercury accumulation in muscle and liver of male Round Stingrays. Mar. Environ. Res. 130, 30–37. https://doi.org/10.1016/j.marenvres.2017.07.004

MacNeil, M.A., Drouillard, K.G., Fisk, A.T., 2006. Variable uptake and elimination of stable nitrogen isotopes between tissues in fish. Can. J. Fish. Aquat. Sci. 63, 345–353. https://doi.org/10.1139/f05-219

Maloney, N.J., Chan, K.M., 1859. Hydrography of harbors, lagoons and sloughs., in: Dailey, M.D., Hill, B., Lansing, N. (Eds.), A Summary of Knowledge of the Southern California Coastal Zone and Offshore Areas. Southern California Ocean Studies Consortium, Long Beach, p. 352.

Marcus, L., Virtue, P., Nichols, P.D., Ferreira, L.C., Pethybridge, H., Meekan, M.G., 2019. Stable Isotope Analysis of Dermis and the Foraging Behavior of Whale Sharks at Ningaloo Reef, Western Australia. Front. Mar. Sci. 6, 1–11. https://doi.org/10.3389/fmars.2019.00546

Mason, R.P., Reinfelder, J.R., Morel, F.M.M., 1996. Uptake, toxicity, and trophic transfer of mercury in a coastal diatom. Environ. Sci. Technol. 30, 1835–1845. https://doi.org/10.1021/es950373d

Matern, S.A., Cech, J.J., Hopkins, T.E., 2000. Diel movements of bat rays, Myliobatis californica, in Tomales Bay, California: Evidence for behavioral thermoregulation? Environ. Biol. Fishes 58, 173–182. https://doi.org/10.1023/A:1007625212099

McMeans, B.C., Svavarsson, J., Dennard, S., Fisk, A.T., 2010. Diet and resource use among Greenland sharks (Somniosus microcephalus) and teleosts sampled in Icelandic waters, using d13C, d15N, and mercury. Can. J. Aquat. Sci. 67, 1428–1438. https://doi.org/10.1139/F10-072

Mekota, A.M., Grupe, G., Ufer, S., Cuntz, U., 2006. Serial analysis of stable nitrogen and carbon isotopes

in hair: Monitoring starvation and recovery phases of patients suffering from anorexia nervosa. Rapid Commun. Mass Spectrom. 20, 1604–1610. https://doi.org/10.1002/rcm.2477

Moura, V.L., Rabelo, J.N., Bezerra, M.F., Silva, G.B.D., Faria, V.V., Rezende, C.E., Bastos, W.R., Lacerda, L.D.D., 2020. Ecological and biological factors associated to mercury accumulation in batoids (Chondrichthyes: Batoidea) from northeastern Brazil. Mar. Pollut. Bull. 161. https://doi.org/10.1016/j.marpolbul.2020.111761

Murillo-Cisneros, D.A., O'Hara, T.M., Elorriaga-Verplancken, F.R., Curiel-Godoy, P., Sánchez-González, A., Marmolejo-Rodríguez, A.J., Marín-Enríquez, E., Galván-Magaña, F., 2019. Trophic assessment and isotopic niche of three sympatric ray species of western Baja California Sur, Mexico. Environ. Biol. Fishes 102, 1519–1531. https://doi.org/10.1007/s10641-019-00923-1

Newsome, S.D., Martinez del Rio, C., Bearhop, S., Phillips, D.L., 2007. A niche for isotopic ecology. Front. Ecol. Environ. 5, 429–436. https://doi.org/10.1890/060150.1

OEHHA, 2018. Health Advisory and Guidelines for Eating Fish From San Diego Bay (San Diego County). California Environmental Protection Agency's Office of Environmental Health Hazard Assessment (OEHHA).

OEHHA, 2009. Update of California Sport Fish Advisories. California Environmental Protection Agency's Office of Environmental Health Hazard Assessment (OEHHA).

OEHHA, 2004. Health Advisory Guidelines for Consumption ofFish and Shellfish from Tomales Bay (Marin County). OEHHA: Sacramento, CA. Off. Environ. Heal. Hazard Assess.

Parnell, A.C., Inger, R., Bearhop, S., Jackson, A.L., 2010. Source partitioning using stable isotopes: Coping with too much variation. PLoS One 5, 1–5. https://doi.org/10.1371/journal.pone.0009672

Peterson, B.J., Fry, B., 1987. Stable Isotopes In Ecosystem Studies. Annu. Rev. Ecol. Syst. 18, 293–320. https://doi.org/10.1146/annurev.ecolsys.18.1.293

Peterson, S.H., Ackerman, J.T., Costa, D.P., 2015. Marine foraging ecology influences mercury bioaccumulation in deep-diving northern elephant seals. Proc. R. Soc. B Biol. Sci. 282, 1–9. https://doi.org/10.1098/rspb.2015.0710

Pinzone, M., Damseaux, F., Michel, L.N., Das, K., 2019. Stable isotope ratios of carbon, nitrogen and sulphur and mercury concentrations as descriptors of trophic ecology and contamination sources of Mediterranean whales. Chemosphere 237, 124448. https://doi.org/10.1016/j.chemosphere.2019.124448

Post, D.M., 2002. Using stable isotopes to estimate trophic position: models, methods, and assumptions. Ecology 83, 703–718. https://doi.org/10.1890/0012-9658(2002)083[0703:USITET]2.0.CO;2

Post, D.M., Layman, Æ.C.A., Arrington, D.A., Takimoto, Æ.G., Quattrochi, J., Montan, Æ.C.G., 2007. Getting to the fat of the matter : models , methods and assumptions for dealing with lipids in stable isotope analyses 179–189. https://doi.org/10.1007

Quezada-Romegialli, C., Jackson, A.L., Hayden, B., Kahilainen, K.K., Lopes, C., Harrod, C., 2018. tRophicPosition, an r package for the Bayesian estimation of trophic position from consumer stable isotope ratios. Methods Ecol. Evol. 9, 1592–1599. https://doi.org/10.1111/2041-210X.13009

Ridge, R.M., 1963. Food habits of the bat ray, Myliobatis californica, from Tomales Bay, California. University of California, Berkeley.

Ridolfi, K., Grenier, L., Melwani, A., McKee, L., Allen, R., Collins, J., 2010. Impairment Assessment for Mercury in Tomales Bay, CA. ACS/Watersheds/Conservation Biol. Contrib. No. 614. Spons. by San Fr. Bay Water Qual. Control Board.

Rodriguez, C.A.B., de Lacerda, L.D., Bezerra, M.F., Moura, V.L., de Rezende, C.E., Bastos, W.R., 2020. Influence of size on total mercury (THg), methyl mercury (MeHg), and stable isotopes of N and C in green turtles (Chelonia mydas) from NE Brazil. Environ. Sci. Pollut. Res. 27, 20527–20537.

https://doi.org/10.1007/s11356-020-08623-5

Rumbold, D., Wasno, R., Hammerschlag, N., Volety, A., 2014. Mercury Accumulation in Sharks From the Coastal Waters of Southwest Florida. Arch. Environ. Contam. Toxicol. 67, 402–412. https://doi.org/10.1007/s00244-014-0050-6

Scheuhammer, A., Braune, B., Man, H., Frouin, H., Krey, A., Letcher, R., Loseto, L., Noël, M., Ostertag, S., Ross, P., Wayland, M., 2015. Recent progress on our understanding of the biological effects of mercury in fi sh and wildlife in the Canadian Arctic. Sci. Total Environ. 509–510, 91–103. https://doi.org/10.1016/j.scitotenv.2014.05.142

Shiffman, D.S., Kaufman, L., Heithaus, M., Hammerschlag, N., 2019. Intraspecific differences in relative isotopic niche area and overlap of co-occurring sharks. Aquat. Ecol. 5. https://doi.org/10.1007/s10452-019-09685-5

Slotton, D.G., Ayers, S.M., Suchanek, T.H., D, W.R., Liston, A.M., 2004. Mercury bioaccumulation and trophic transfer in the Cache Creek Watershed, California, in relation to diverse aqueous mercury exposure conditions. Rep. CALFED Bay-Delta Agency 137. https://doi.org/10.5433/1679-0359.2014v35n3p1221

Smith, S. V., Hollibaugh, J.T., Dollar, S.J., Vink, S., 1991. Tomales bay metabolism: C N P stoichiometry and ecosystem heterotrophy at the land-sea interface. Estuar. Coast. Shelf Sci. https://doi.org/10.1016/0272-7714(91)90055-G

Smith, S. V, Hollibaugh, J.T., 1997. Annual cycle and interannual variability of ecosystem metabolism in a temperate climate embayement. Ecol. Monogr. 67, 509–533. https://doi.org/10.2307/2963468

Talent, L.G., 1985. The occurrence, seasonal distribution, and reproductive condition of elasmoranch fishes in Elkhorn Slough, California. Calif. Fish Game 71, 210–219.

Talent, L.G., 1982. Food habits of the grey smooth-hound, Mustelus californicus, the brown smooth-

hound, Mustelus henlei, the shovelnose guitarfish, Rhinobatos productus, and the bat ray, Myliobatis californica, in Elkhorn Slough, California. Calif. Fish Game 68, 224–234.

Taylor, D.L., Kutil, N.J., Malek, A.J., Collie, J.S., 2014. Mercury bioaccumulation in cartilaginous fishes from Southern New England coastal waters: Contamination from a trophic ecology and human health perspective. Mar. Environ. Res. 99, 20–33. https://doi.org/10.1016/j.marenvres.2014.05.009

Teffer, A.K., Staudinger, M.D., Taylor, D.L., Juanes, F., 2014. Trophic influences on mercury accumulation in top pelagic predators from offshore New England waters of the northwest atlantic ocean. Mar. Environ. Res. 101, 124–134. https://doi.org/10.1016/j.marenvres.2014.09.008

Thorne, L.H., Fuirst, M., Veit, R., Baumann, Z., 2021. Mercury concentrations provide an indicator of marine foraging in coastal birds. Ecol. Indic. 121, 106922. https://doi.org/10.1016/j.ecolind.2020.106922

Tiktak, G.P., Butcher, D., Lawrence, P.J., Norrey, J., Bradley, L., Shaw, K., Preziosi, R., Megson, D., 2020. Are concentrations of pollutants in sharks, rays and skates (Elasmobranchii) a cause for concern? A systematic review. Mar. Pollut. Bull. 160, 111701. https://doi.org/10.1016/j.marpolbul.2020.111701

Tilley, A., López-Angarita, J., Turner, J.R., 2013. Diet reconstruction and resource partitioning of a Caribbean marine mesopredator using stable isotope Bayesian modelling. PLoS One 8, 1–10. https://doi.org/10.1371/journal.pone.0079560

UN Environment, 2019. Global Mercury Assessment 2018. UN Environment Programme, Chemicals and Health Branch Geneva, Switzerland. Geneva, Switzerland.

US EPA, 2007. Method 7473 (SW-846): Mercury in Solids and Solutions by Thermal Decomposition, Amalgamation, and Atomic Absorption Spectrophotometry. Methods 1–17.

USEPA, 2001. Water Quality Criterion for the Protection of Human Health : Methylmercury Final. US

Environ. Prot. Agency, Washington, DC EPA-823-R-, 303.

Valadez-Gonzalez, C., Anguilar-Palomino, B., Hernandez-Vazquez, S., 2001. Feeding habits of the round stingray Urobatis halleri (Cooper, 1863) (Chonrichthyes: Urolophidae) from the continental shelf of Jalisco and Colima, Mexico. Ciencias Mar. 27, 91–104. https://doi.org/10.7773/cm.v27i1.375

Valenzuela-Quiñonez, F., Galván-Magaña, F., Ebert, D.A., Aragón-Noriega, E.A., 2017. Feeding habits and trophic level of the shovelnose guitarfish (Pseudobatos productus) in the upper Gulf of California. J. Mar. Biol. Assoc. United Kingdom 1–10. https://doi.org/10.1017/S0025315417000832

Vanderklift, M.A., Ponsard, S., 2003. Sources of variation in consumer-diet δ15N enrichment: A meta-analysis. Oecologia 136, 169–182. https://doi.org/10.1007/s00442-003-1270-z

Vaudo, J., Heithaus, M.R., 2011. Dietary niche overlap in a nearshore elasmobranch mesopredator community. Mar. Ecol. Prog. Ser. 425, 247–260. https://doi.org/10.3354/meps08988

Vaudo, J.J., Heithaus, M.R., 2012. High-Trophic-Level Consumers: Elasmobranchs, Treatise on Estuarine and Coastal Science. Elsevier Inc. https://doi.org/10.1016/B978-0-12-374711-2.00617-3

Villavicencio-Garayzar, C.J., 1993. Biología reproductiva de Rhinobatos productus (Pisces: Rhinobatidae), en Bahía Almejas, Baja California Sur, México. Rev. Biol. Trop. 41, 777–782. https://doi.org/10.1063/1.3615285

Whyte, D.C., Kirchner, J.W., 2000. Assessing water quality impacts and cleanup effectiveness in streams dominated by episodic mercury discharges. Sci. Total Environ. 260, 1–9. https://doi.org/10.1016/S0048-9697(00)00537-4

Wiener, J.G., Krabbenhoft, D.P., Heinz, G.H., Scheuhammer, A.M., 2003. Ecotoxicology of mercury, in: Hoffman, D., Rattner, B., Burton, G., Cairns, J. (Eds.), Handbook of Ecotoxicology. Boca Raton, FL. Lewis Publishers, pp. 409–63. https://doi.org/10.1201/9781420032505

Wyatt, A.S.J., Matsumoto, R., Chikaraishi, Y., Miyairi, Y., Yokoyama, Y., Sato, K., Ohkouchi, N.,

Nagata, T., 2019. Enhancing insights into foraging specialization in the world's largest fish using a multi-tissue, multi-isotope approach. Ecol. Monogr. 89. https://doi.org/10.1002/ecm.1339

Yeakel, J.D., Bhat, U., Elliott Smith, E.A., Newsome, S.D., 2016. Exploring the Isotopic Niche: Isotopic Variance, Physiological Incorporation, and the Temporal Dynamics of Foraging. Front. Ecol. Evol. 4, 429–432. https://doi.org/10.3389/fevo.2016.00001

Yemışken, E., Forero, M.G., Megalofonou, P., Eryilmaz, L., Navarro, J., 2017. Feeding habits of three Batoids in the Levantine Sea (north-eastern Mediterranean Sea) based on stomach content and isotopic data. J. Mar. Biol. Assoc. United Kingdom 1–8. https://doi.org/10.1017/S002531541700073X

CHAPTER 2 – Supplementary material

Table S2.1 – Paired t test performed.

Test	Variable	Species	Location	Source of Variance	df	t value	*p* value
Paired t test							
	$\delta^{13}C$	*M. californica*	TB	tissue	14	-5.23	**<0.001**
	$\delta^{13}C$	*M. californica*	SDB	tissue	25	-12.25	**<0.001**
	$\delta^{15}N$	*M. californica*	SDB	tissue	25	7.51	**<0.001**
	$\delta^{13}C$	*R. productus*	SDB	tissue	3	0.197	0.86
	$\delta^{15}N$	*R. productus*	SDB	tissue	3	0.80	0.48
	$\delta^{15}N$	*U. halleri*	SDB	tissue	9	0.535	0.61

Table S2.2 – Non-parametric Analysis of Variance performed.

Test	Variable	Species	Location	Source of Variance	n	df	Coefficient	*p* value
Mann-Whitney								
	$\delta^{15}N$	*M. californica*	TB	size_class	15	-	25	0.86
	$\delta^{15}N$	*M. californica*	TB	sex	15	-	18	0.43
	$\delta^{13}C$	*U. halleri*	SDB	tissue	10	-	13	0.16
Paired Wilcoxon	$\delta^{15}N$	*M. californica*	TB	tissue	15	-	67	0.7197
	$\delta^{13}C$	*All*	SDB	tissue	40	-	153	**<0.001**
	$\delta^{15}N$	*All*	SDB	tissue	40	-	692	**<0.001**
Kruskal-Wallis								
	THg	*All*	SDB	species	40	2	22.4	**<0.001**
Post-hoc Wilcoxon pairwise								
	M. californica : U. halleri		SDB	species	-	-	-	**<0.001**
	M. californica :R. productus		SDB	species	-	-	-	**0.04**
	R. productus :U. halleri		SDB	species	-	-	-	**0.004**
	$\delta^{15}N$	*All*	SDB	species	40	2	14.5	**<0.001**
Post-hoc Wilcoxon pairwise								
	M. californica : U. halleri		SDB	species	-	-	-	**0.02**
	M. californica :R. productus		SDB	species	-	-	-	**<0.001**
	R. productus :U. halleri		SDB	species	-	-	-	0.08

*bold number indicate a significant *p* value

Table S2.3 – Parametric Analysis of Variance performed.

Test	Variable	Species	Location	Source of Variance	df	SS	F	*p* value
ANOVA								
	THg	*M. californica*	-	location	1, 39	1.956	14.8	**<0.001**
	$\delta^{13}C$	*M. californica*	-	location	1, 39	54.22	61.32	**<0.001**
	$\delta^{15}N$	*M. californica*	-	location	1, 39	0.19	0.23	0.632
	$\delta^{13}C$	*M. californica*	TB	Size_class	1, 13	0.002	0.001	0.973
	THg	*M. californica*	TB	Size_class	1, 13	0.003	0.01	0.897
	$\delta^{13}C$	*M. californica*	TB	Sex	1, 13	1.597	1.24	0.285
	THg	*M. californica*	TB	Sex	1, 13	0.018	0.09	0.77
	$\delta^{13}C$	*R. productus*	SDB	Sex	1, 2	0.08	0.009	0.93
	$\delta^{15}N$	*R. productus*	SDB	Sex	1, 2	0.003	0	0.985
	THg	*R. productus*	SDB	Sex	1, 2	0.454	1.09	0.40
	$\delta^{13}C$	-	SDB	species	2, 37	10.7	2.06	0.14

*bold number indicate a significant *p* value

Table S2.4 – Parametric and non-parametric correlation tests performed.

Method	Species	Location	Variable pair	df	r	*p* value
Spearman						
	M. californica	SDB	THg vs size_cm	24	-0.03	0.88
	M. californica	SDB	$\delta^{13}C$ vs size_cm	24	0.13	0.52
	M. californica	SDB	$\delta^{15}N$ vs size_cm	24	-0.34	0.087
	M. californica	TB	THg vs $\delta^{15}N$	13	0.35	0.21
	M. californica	TB	$\delta^{13}C$ vs $\delta^{15}N$	13	0.01	0.96
	M. californica	TB	$\delta^{15}N$ vs size_cm	13	-0.26	0.34
	U. halleri	SDB	THg vs $\delta^{13}C$	8	-0.22	0.54
	U. halleri	SDB	$\delta^{13}C$ vs size_cm	8	-0.33	0.34
	U. halleri	SDB	$\delta^{13}C$ vs $\delta^{15}N$	8	-0.45	0.19
Pearson						
	M. californica	SDB	THg vs $\delta^{15}N$	24	0.10	0.62
	M. californica	SDB	THg vs $\delta^{13}C$	24	-0.14	0.48
	M. californica	SDB	$\delta^{13}C$ vs $\delta^{15}N$	24	-0.80	**<0.001**
	M. californica	TB	THg vs size_cm	13	-0.30	0.28
	M. californica	TB	THg vs $\delta^{13}C$	13	-0.26	0.34
	M. californica	TB	$\delta^{13}C$ vs size_cm	13	0.10	0.71
	U. halleri	SDB	THg vs size_cm	8	-0.29	0.42
	U. halleri	SDB	THg vs $\delta^{15}N$	8	0.45	0.18
	U. halleri	SDB	$\delta^{15}N$ vs size_cm	8	0.013	0.97
	R. productus	SDB	THg vs size_cm	2	-0.82	0.18
	R. productus	SDB	THg vs $\delta^{15}N$	2	0.40	0.59
	R. productus	SDB	THg vs $\delta^{13}C$	2	-0.38	0.62
	R. productus	SDB	$\delta^{15}N$ vs size_cm	2	-0.45	0.54
	R. productus	SDB	$\delta^{13}C$ vs $\delta^{15}N$	2	0.49	0.51
	R. productus	SDB	$\delta^{13}C$ vs size_cm	2	-0.12	0.88

*bold number indicate a significant *p* value.

CHAPTER 3 – Trophodynamics of mercury in estuarine food webs in California Coast

M.F. Bezerra

1. Introduction

Contaminant bioaccumulation assessments of chemicals are crucial to understand how pollutants accumulate and affect organisms (Schäfer et al. 2015). Bioaccumulation is the process where concentration of a chemical is higher in the organism compared to its ambient environment, while biomagnification is the process of increasing chemical concentrations in organisms along the food-web (Gobas and Morrison 2000).

Hg is a pervasive and highly toxic pollutant with natural and anthropogenic sources (UNEP 2013). In global oceans, about 2/3 of the Hg historically emitted through anthropogenic sources resides on waters shallower than 1,000 m, which was estimated to represent three-fold of the naturally emitted Hg presented in oceans' surface waters (Lamborg et al. 2014). In coastal ecosystems, inorganic Hg (Hg(II)) originates from sedimentation and soil formation processes and can be transformed into organic Hg (MeHg) through bacterial metabolism processes (Hammerschmidt and Fitzgerald 2006b, Mason et al. 2012, Lamborg et al. 2014). The mercury biogeochemical cycle involves complex transformation of several Hg chemical species among environmental compartments (e.g. soil, water, air and biota). In general, elemental Hg (Hg(0)) is the most abundant Hg species in the atmosphere due to its high volatility and chemical stability. Photo-oxidation processes in the atmosphere transform Hg(0) to Hg(II) cations, which is readily deposited on land and/or water bodies. Once in aquatic systems most of Hg is in the reduced form Hg(II). When partitioning to suspended solids, Hg(II) can form insoluble compounds, such as HgS and $HgCl_2$, that can sink to the sediment. Once in the sediment, bacteria-mediated processes can methylate Hg(II) forming MeHg, which is the most toxic Hg compound to aquatic biota and humans (Morel et al. 1998, Schneider et al. 2013, UNEP 2013).

Traditionally, pollutants' risk assessment employs measures of bioaccumulation using bioconcentration factor, bioaccumulation factor (BAF), biota- sediment accumulation factor (BSAF), and biomagnification factor (BMF). These are generally estimated in laboratories, providing key information of the factors controlling rates of bioaccumulation that take into account chemical properties of the pollutant and biotic characteristics (e.g. habitat, diet, etc.) of the contaminated organism (Borgå et al. 2012). However, as

these measures often do not corroborate with community-level estimates in the field (e.g. Van Geest et al., (2010), there has been a recent trend towards the use of Trophic Magnification Factors (TMF) to assess biomagnification of pollutants across different food webs (Burkhard et al. 2013, Walters et al. 2016). TMF are estimated by the regression between pollutant levels in organisms of the same food web and their relative trophic positions. The slope of this regression line is used to assess the system with a TMF > 1 indicating biomagnification of the pollutant in the food web. This approach has been widely used to assess mercury (Hg) biomagnification worldwide (Gobas and Morrison 2000, Borgå et al. 2012, Lavoie et al. 2013).

Factors influencing Hg biomagnification includes physical (e.g. latitude, temperature), chemical (e.g. pH, dissolved organic carbon - DOC) and bio-ecological processes (e.g. growth rate, species diversity and length of the food chain) (Watras et al. 1998, Hammerschmidt and Fitzgerald 2006a, DeForest et al. 2007). However, there is no consensus regarding which are the key variables controlling the rate of Hg biomagnification in aquatic ecosystems (Lavoie et al. 2013). In a worldwide Hg biomagnification meta-analysis, Lavoie et al., (2013), using TMF as a measure of Hg biomagnification, found that latitude and Hg deposition were two of the most important variables describing its variation across the freshwater and marine ecosystems. As this assessment was conducted at a global scale, including observations from the tropical, temperate, and polar ecosystems, it is not clear if these relationships would still hold at regional scales.

This study uses data collected in San Diego Bay (SDB) and Tomales Bay (TB) to assess spatial and temporal variations in Hg levels among different taxa, to examine Hg bioaccumulation across multiple trophic levels, and to quantify Hg biomagnification at a regional scale. Specifically, we aim to describe and compare Hg bioaccumulation and biomagnification between two estuaries in Californica coast by asking (1) Do Hg levels in marine biota vary temporally and spatially in SDB and TB, and (2) Are there differences across trophic levels ? (3) Which factors better describe Hg concentrations in SDB and TB food webs across multiple years?

2. Methods

2.1. *Study site description*

San Diego Bay - SDB (32.72° N, 117.2° W), Southern California, is a natural, semi-enclosed embayment extending approximately 25 km from the head to the mouth. It has been extensively impacted by human activities, such as dredging, filling and industries discharges (Lenihan et al. 1990), and is a highly polluted environment, especially by legacy heavy metals, due to a history of military and recreational boating, as well as urban runoff (Deheyn and Latz 2006, Gassel et al. 2013).

Assessment of sediment toxicity in the bay found that areas nearby naval shipyard, commercial shipping, and small boat operations exceeded established probable effect levels (PEL), and effects range median (ERM) for mercury (>0.69 $\mu g.g^{-1}$ and > 0.71 $\mu g.g^{-1}$, respectively) and other heavy metals (Fairey et al. 1998). Due to elevated Hg and PCBs levels, a health advisory was published by the California Office of Environmental Health Hazard Assessment (OEHHA) in 2013 concerning the consumption of fish from SDB (Gassel et al. 2013). These guidelines placed upper trophic level fishes (i.e. Leopard Sharks; Gray smooth hound sharks) in the "not be consumed by women and children" category. In contrast, Komoroske et al., (2011) found low Hg concentrations in blood and carapace fragments (mean of 1.01 ng g^{-1} and 47.5 ng g^{-1}, respectively) of green turtles foraging in SDB, which are known to be predominantly herbivores feeding at low trophic levels. These previous findings suggest that, in addition to physical factors such as the discharging history by local sources that define background levels, understanding the trophic ecology of aquatic organisms and their interactions is at least equally crucial for assessing Hg bioaccumulation and biomagnification.

SDB is home to a large number of marine organisms. In an extensive survey, 78 fish species were identified, with the most abundant species being the Northern Anchovy (*Engraulis mordax*), Topsmelt (*Atherinops affinis*) and Slough Anchovy (*Anchoa delicatissima*). The Round Stingray (U*robatis halleri*) was considered the second most important species in terms of individual number, body weight, and frequency of occurrence; and, together with the Bat-ray (*Myliobatis californica*), they represent over 30% of total fish biomass in the bay (Allen et al. 2002). Other batoid species also occur, including the Butterfly

Ray (*Gymnura marmorata*), Shovelnose Guitarfish (*Rhinobatos productus*), Diamond Stingray (*Dasyatis dipterurus*) and Banded Guitarfish (*Zapteryx exasperata*) (Allen et al. 2002).

Tomales Bay – TB (38.2° N, 122.93° W), Central California, is a narrow and relatively shallow small estuary located in Marin County. A diverse system, TB has intertidal, subtidal and benthic habitats, salt and freshwater marshes, mudflats and dunes. Shallow sand bars with seagrass beds dominates the bottom of lower bay zones, where tidal exchange and upwelling provide nutrients and control physicochemical water characteristics. In the inner zones, runoff, evaporation and rainfall are the major drivers of water properties where mud flats sustain benthic macro-algae communities (Smith et al. 1991, Smith and Hollibaugh 1997, TBWC 2003).

Although TB's watershed is predominantly rural with relatively low human impacts this area is blitzed by legacy Hg from historical mining activities. Recent Hg concentration measurements in upper trophic level fishes exceeds EPA safe limits (< 0.3 ppm) and is highest in Brown Smooth-hound Shark (1.31 ppm) and Leopard Shark (1.09 ppm), followed by Bat-ray (0.56 ppm) and Pacific Angelshark (0.43) (CRWQCB, 2012; Johnson et al., 2009).

2.2. *Data collection*

To assess Hg bioaccumulation and temporal/spatial variation, we compiled Hg concentration and biometric data from six independent reports conducted in TB and SDB. Data from these reports were made available to the public by the Californica Department of Fish and Wildlife, and includes the NOAA Mussel Watch Program (1986 - 2010), Environmental Monitoring and Assessment Program (1999), the RWB9 San Diego Bay Oyster and lobster Studies (2015 to 2019), the California State Mussel Watch Program (1980 - 2004), and the Statewide Coast Sportfish SF Bay Regional Monitoring for Water Quality (1993 - 2009). From this large dataset, we selected species occurring in both locations and/or with at least ten observations across multiple years. Bioaccumulation relationships per species and location were created using linear regressions between total Hg (THg) concentration and animal size. To assess temporal and spatial variation in Hg accumulation data were grouped into year, decade, and region at each study site. Chosen species include the Common Mussel (*Mytillus* sp.), the California Spiny Lobster

(*Panulirus interruptus*), the Shiner Perch (*Cymatogaster aggregate*), the Black Surfperch (*Embiotoca jacksoni*), the White Seaperch (*Phanerodon furcatus*), the Kelp Bass (*Paralabrax clathratus*), the Spotted Sand Bass (*Paralabrax maculatofasciatus*), the Barred Sand Bass (*Paralabrax nebulifer*), the California Halibut (*Paralichthys californicus*), the Smooth-hound Sharks (*Mustelus californicus* and *Mustelus henlei*), the Pacific Angelshark (*Squatina californica*), the Leopard Shark (*Triakis semifasciata*), the Bat-ray (*M. californica*), and the Round Stingray (*U. halleri*).

To assess Hg biomagnification, we collected organisms from 2016 to 2019 composing the food web of the Bat-ray (*Myliobatis californica*) in each study area using multiple methods, such as entanglement nets, beach seine, and hook and line for fish and elasmobranch species, and hand tools for benthic invertebrates and primary producers. Sampled species includes *M. californica*, mollusks of the orders Mytilida and Veneridae, decapoda crustaceans of the genus *Carcinus* and *Crangon*, polychaetes, and the primary producers *Zostera marina* and macroalgae of the genus *Ulva*. Muscle tissues in *M. californica* were collected by a non-lethal method using 6mm diameter biopsy punches from the dorsal area of both "wings". Animals were released in good health condition after each sampling procedure. Inverterbate species were collected and analyzed as whole organisms. Disc width, weight and sex (identified by presence/absence of claspers in males) were recorded for each *M. californica* individual. All samples were kept on ice in the field and stored frozen (- 20 ºC) in the laboratory. In the laboratory, all samples were freeze-dried for 24h – 48h and homogenized using a porcelain mortar and pestle. For benthic invertebrates and primary producers, composite samples were obtained by pooling multiple individuals into the following groups: Mollusca, Crustacea, Polychaete, and Primary producer. We also included isotopic ratios of $\delta^{13}C$ and $\delta^{15}N$ in primary producers and invertebrates from San Diego Bay using the NOAA SWFSC database in order to characterize the food web isotopic baseline for the Hg biomagnification assessment.

2.3. Chemical analysis

Total mercury (THg) concentrations were determined using a dedicated Perkin Elmer Flow Injection Mercury System (FIMS) and Direct Mercury Analyzer (DMA-80 Milestone, Inc.), according to Slotton et

al., (2004) and the EPA Method 7473 (US EPA 2007), respectively. Calibration curves (n = 3) with an overall range varying from 0.5 to 200 ng Hg were established with a mean linearity coefficient (R^2) of 0.9998 ± 0.0001. We assured analytical quality (i.e. accuracy and reproducibility) of Hg measurements by using analytical blanks (every 10 samples) and certified reference materials (NRC DORM-3, BCR-463, NRC DOLT-4) in every analysis batch. Total Hg recovery ranged from 97.6% to 101.8% (100.8 ± 1.4%, n = 6) for BCR-463, 101.7% to 103.7% (102.5 ± 0.8%, n = 6) for NRC DOLT-4, and 88.0% to 97.7% (91.2 ± 3.7%, n = 12) for NRC DORM-3. The limit of detection is 0.002 $\mu g.g^{-1}$ dry weight (d.w.). All Hg concentrations are expressed as $\mu g.g^{-1}$ d.w.

Isotopic determination in muscle tissues consisted of approximately 1.0 mg of tissue material loaded into sterilized tin capsules and analyzed by a continuous-flow isotope-ratio mass spectrometer in the Stable Isotope Laboratory at the University of Florida, Gainesville USA. All samples were analyzed for their $\delta^{15}N$, and %N values. A Carlo Erba NA 1500 Elemental Analyzer system interfaced via a ConFlo II device (Finningan MAT) to a Thermo Electron DeltaV Ad- vantage gas IRMS was used. Prior to exiting the elemental analyzer, combustion gas was measured using a thermal conductivity detector to determine percent compositions. USGS40 standards (9.52 % N, 40.82% C) were used for calibration. Sample stable isotope ratios relative to the isotope standard are expressed in the following conventional delta (δ) notation in parts per thousand (‰).

$$\delta = [(R_{Sample}/R_{standard}) - 1] \times 1000 \quad (1)$$

where R_{sample} and $R_{standard}$ are the corresponding ratios of heavy to light isotopes ($^{15}N/^{14}N$) in the sample and international standard (Air for nitrogen and Vienna Pee Dee Belemnite for carbon), respectively.

2.4. *Data analysis*

Linear regressions between THg vs. animal size was conducted to assess bioaccumulation in organisms from both study areas. Generalized linear models (GLM) were performed to determine the effects of factors (e.g. region, animal size, year, species, and genus) on THg concentrations. We also tested for differences in THg concentration among factors using the size normalized THg concentrations (hereafter THg_{norm}). THg concentration was divided by total length of each individual, and then, standardized to the

sample mean by multiplying by the location-specific mean length for the species (total length data are provided in Tab. 3. 1) (Scudder Eikenberry et al. 2015). Variables THg and THg_{norm} were log transformed to improve normality and homogeneity of variance. To select the best model we used the "stepAIC" function in the MASS R package that is based upon the Akaike Information Criterion (AIC) (Bentzen et al. 2016).

For Hg biomagnification assessment, parametric and non-parametric Analysis of Variance (ANOVA) was conducted using THg and THg_{norm} as dependent variables to test for differences among factors. Parametric assumptions of the data were tested using Shapiro Wilks and Levene's test. We used $\delta^{15}N$ as a proxy for trophic position and then applied linear regressions to estimate biomagnification using the following equation:

$$\log_{10}[Hg] = \delta^{15}N(b) + a \quad (1)$$

where the slope (b) is an indicator of biomagnification potential used to calculate the Trophic Magnification Factor (TMF) (Borgå et al. 2012) according to the following equation:

$$TMF = 10^{b} \quad (2)$$

If the slope is significant and positive (TMF > 0), Hg biomagnification is considered happening in the food web (Conder et al. 2012). Biomagnification was also assessed using linear regression of Log_{10}[THg] vs. trophic level (TL) of organisms. TL was calculated from $\delta^{15}N$ values according to the following equation:

$$TL_{consumer} = (\delta^{15}N_{consumer} - \delta^{15}N_{baseline})/ \Delta^{15}N + \lambda \quad (3)$$

where λ is the trophic level of the baseline organism (TL = 2 for primary consumers – filter-feeding mollusks), $TL_{consumer}$ is the trophic level of the target consumer, and $\delta^{15}N_{consumer}$ and $\delta^{15}N_{baseline}$ are $\delta^{15}N$ values of the target consumer and the baseline organism, respectively. Trophic discrimination factors ($\Delta^{15}N = \delta^{15}N_{consumer} - \delta^{15}N_{prey}$) used include the elasmobranch-specific value of 2.29 ± 0.22 ‰ reported by Hussey et al., (2010) applied for *M. californica*, and the more generally used value of 3.4 ± 0.98 ‰ reported by Post (2002) applied elsewhere. The *M. californica*'s food web in both study areas was composed by tertiary consumers (*M. californica*), secondary consumers (polychaetes, *Carcinus* sp. and

Crangon sp.), primary consumers (*Mytillus* sp. for both location; and *Chione* sp. for SDB), and primary producers (*Zostera. marina* for both locations; and *Ulva* sp. for TB). All statistical analyses and plots were performed using R version 3.4.3 (R Core Team, 2017). Statistical significance was defined as $p < 0.05$.

3. *Results*

3.1. Temporal variation in Hg contamination

In SDB, Hg data in mussels ranged from years 1985 to 2020 (n = 106). THg concentrations did not vary significantly across decades or years (Kruskal-Wallis, W_{decade} =, $W_{year} = 5.2$, $p > 0.09$) (Fig. 3. 1). We also employed a size normalized THg concentrations (THg_{norm}) to remove the effect of size on Hg concentration. THg_{norm} were found to not vary significantly across decades and years (Kruskal-Wallis, $W_{decade} = 5.97$, $W_{year} = 21.4$, $p > 0.11$). In contrast, when treating year as a continuous variable, a linear regression showed a significant negative association between year and THg ($p = 0.02$). In TB, Hg data in mussels ranged from years 1979 to 2019 (n = 78). THg concentrations were found to differ significantly among decades and years (Kruskal-Wallis, $W_{decade} = 14.7$, $W_{year} = 41.9$, $p < 0.005$) with THg levels in the 2010s (0.16 ± 0.04 $\mu g.g^{-1}$) significantly lower compared to 1990s (0.21 ± 0.06 $\mu g.g^{-1}$) and 2000s (0.24 ± 0.1 $\mu g.g^{-1}$) (Wilcoxon, $p < 0.04$) (Fig. 3. 1). In contrast, THg_{norm} did not vary among decades or years ($p > 0.52$). When treating year as a continuous variable, a linear regression showed no significant association between year and THg ($p = 0.29$). For the Shiner Perch, 27 individuals were collected including years 2001 (n= 1), 2002 (n = 3), 2009 (n = 22), and 2018 (n = 1) in SDB. Fish size differed significantly among years (Kruskal-Wallis, $W = 9.96$, $p = 0.02$). In contrast, size normalized THg concentrations (THg_{norm}) did not vary significantly among years (ANOVA, $F_{3, 23} = 0.52$, $p = 0.67$). Similarly, a linear regression showed no significant trend in Hg contamination among the four sampled years comprising a 17 years period ($p = 0.17$). In TB, 19 individuals were collected including years 1998 (n = 2), 1999 (n = 4), 2001 (n = 2), and 2009 (n = 11). Fish size differed significantly among years (ANOVA, $F_{3, 15} = 8.0$, $p = 0.002$). In contrast, size normalized THg concentrations (THg_{norm}) were found to not vary significantly among

years (ANOVA, $F_{3, 15} = 1.47$, $p = 0.26$). Similarly, a linear regression showed no significant trend in Hg contamination among the four sampled years comprising a 11 years period ($p = 0.18$).

For Bat-ray, 26 individuals were collected including years 2016 (n = 13) and 2019 (n = 13) in SDB. Animal size did not vary between years. In contrast, THg and THg_{norm} concentrations were significantly greater in 2016 (1.4 ± 0.2 $\mu g.g^{-1}$) compared to 2019 (0.9 ± 0.1 $\mu g.g^{-1}$) (t test, $t = 7.2$, $p < 0.001$) (Fig. 3. 2). In TB, 30 individuals were collected including years 1998 (n = 1), 1999 (n = 2), 2001 (n = 12), 2018 (n = 2), and 2019 (n = 13). Animal size in 1990s (29.6 ± 11.4 cm) were significantly smaller compared to 2000s (60.6 ± 6.19 cm) and 2010s (66.2 ± 7.17 cm) (Wilcoxon pairwise post-hoc, $p < 0.02$). THg_{norm} concentrations were significantly greater in 1990s (4.98 ± 1.1 $\mu g.g^{-1}$) compared to 2000s (1.92 ± 0.64 $\mu g.g^{-1}$) and 2010s (0.54 ± 0.76 $\mu g.g^{-1}$) (Wilcoxon pairwise post-hoc, $p < 0.008$) (Fig. 3. 2). For the California Halibut six individuals were collected in 1999 (n = 4), 2002 (n = 1), and 2018 (n = 1) in SDB. In TB, 15 individuals were collected in 1998 (n = 2), 1999 (n = 1), and 2001 (n = 12). For barred bass (*P. nebulifer*), 21 individuals were collected in 1999 (n = 4), 2002 (n = 5), and 2009 (n = 12) in SDB. Fish size in 1999 (20.3 ± 9.6 cm) was significantly different compared to 2009 (37.1 ± 6.6 cm) (Wilcoxon pairwise post-hoc, $p = 0.039$). No difference in fish size was found when comparing 2002 with 2009, and 2002 with 1999 ($p > 0.2$). In contrast, THg_{norm} concentrations did not differ among years (ANOVA, $F_{2, 18} = 0.226$, $p = 0.8$). For spotted bass (*P. maculatofasciatus*), 82 individuals were collected in 1999 (n = 4), 2000 (n = 2), 2001 (n = 18), 2002 (n= 1), 2009 (n = 24), and 2018 (n = 33). Fish size differed significantly among years (Kruskal-Wallis, $W = 21.9$, $p < 0.001$). THg_{norm} concentrations were significantly lower in 2018 (0.61 ± 0.3 $\mu g.g^{-1}$) compared to 2001 (0.91 ± 0.2 $\mu g.g^{-1}$) (Tukey HSD post-hoc, $p = 0.0004$). No significant differences were observed for THg_{norm} among other years ($p > 0.07$). When treating year as a continuous variable, a linear regression showed a significant association of year with THg_{norm} ($p < 0.001$) (Fig. 3. 3). For the Round Stingray (U. *halleri*), 28 individuals were collected in 2001 (n = 10), and 2017 (n = 17) in SDB. Animal size differed significantly between 2001 (17.3 ± 1.9 cm) and 2017 (13.9 ± 1.1 cm) (t test, $t = 5.88$, $p = 3.3e\text{-}6$). Similarly, THg_{norm} concentrations were significantly greater in 2001 (1.1 ± 0.2 $\mu g.g^{-1}$) compared to 2017 (0.6 ± 0.2 $\mu g.g^{-1}$) (t test, $t = 5.01$, $p < 0.001$).

3.2. Site differences *in Hg contamination*

For the mussel (*Mytillus* sp.), animal size did not differ significantly between SDB (5.7 ± 0.6 cm) and TB (5.1 ± 1.3 cm) (Wilcoxon, p = 0.053). In contrast, THg concentration was on average greater in SDB (0.26 ± 0.14 $ug.g^{-1}$) compared to TB (0.21 ± 0.1 $ug.g^{-1}$) (p = 0.002). For the Shiner Perch (*C. aggregata*), size was greater in SDB (11.7 ± 1.2 cm) compared to TB (9.1 ± 2.4 cm) (t test, t = 4.46, p < 0.001). In contrast, average THg_{norm} concentration was significantly greater in TB (0.28 ± 0.08 $\mu g.g^{-1}$) compared to SDB (0.22 ± 0.08 $\mu g.g^{-1}$) (t test, t = -2.17, p = 0.03). For the Smooth-hound Sharks (*Mustelus* sp.), animal size was greater in TB (86.6 ± 4.03 cm) compared to SDB (72.1 ± 9.28 cm) (Wilcoxon, p < 0.001). Similarly, THg_{norm} concentrations were significantly greater in TB (4.95 ± 1.04 $\mu g.g^{-1}$) compared to SDB (1.81 ± 0.68 $\mu g.g^{-1}$) (Wilcoxon, p < 0.001). For the Bat-ray (*M. californica*), comparisons were limited to the 2010 decade. Animal size did not differ between SDB (62.7 ± 8.3 cm) and TB (60.3 ± 12.8 cm) (Wilcoxon, p = 0.1). In contrast, average THg was significantly greater in TB (1.59 ± 0.42 $\mu g.g^{-1}$) compared to SDB (1.14 ± 0.33 $\mu g.g^{-1}$) (t test, t = -3.61, p = 0.001). For the halibut (*P. californicus*), fish size was significantly greater in TB (66 ± 8.6 cm) compared to SDB (35 ± 20.2 cm) (Wilcoxon, p = 0.003). Similarly, THg_{norm} concentrations was significantly greater in TB (0.7 ± 0.2 $\mu g.g^{-1}$) compared to SDB (0.4 ± 0.11 $\mu g.g^{-1}$) (Wilcoxon, p = 0.001). For Leopard Sharks (*T. semifasciata*), animal size did not differ between SDB (95.1 ± 23.4 cm) and TB (102 ± 10.9 cm) (t test, t = -0.62, p = 0.56). Similarly, THg concentrations were significantly greater in TB (4.0 ± 0.9 $\mu g.g^{-1}$) compared to SDB (3.1 ± 2.6 $\mu g.g^{-1}$) (t test, t = -0.82, p = 0.45). For the California Halibut, we pooled data from all years at each location to compare fish size and THg concentrations. Fish size was significantly greater in TB (66 ± 8.6 cm) compared to SDB (35 ± 20.2 cm) (Wilcoxon, p = 0.003). Similarly, THg_{norm} was significantly greater in TB (0.72 ± 0.2 $\mu g.g^{-1}$) compared to SDB (0.41 ± 0.1 $\mu g.g^{-1}$) (Wilcoxon, p = 0.002).

3.3. Spatial variation in THg within each study area

We analyzed only *Mytillus* sp. as this is the only sessile organism with contamination data ranging various parts of the bay within each study site. For SDB, no significant difference in average THg concentrations was observed among areas (North bay – 0.27 ± 0.2 $\mu g.g^{-1}$; Central bay – 0.24 ± 0.1 $\mu g.g^{-1}$;

South bay – 0.18 ± 0.1 $\mu g.g^{-1}$) (Kruskal-Wallis, W = 3.36, p = 0.19). For TB, THg levels differed significantly between various parts of the bay (Wilcoxon, W = 0.92, p = 0.0002) with greater THg in the outer bay (0.26 ± 0.08 $\mu g.g^{-1}$) compared to the inner bay area (0.17 ± 0.05 $\mu g.g^{-1}$).

3.4. Hg bioaccumulation relationships

Linear regressions between animal size (total length) and THg concentration are shown in Table 3. 2. A significant and positive association was observed for the Shiner Perch (both locations $p < 0.04$), the Smooth-hound Sharks (both locations, $p < 0.03$), the Kelp Bass (SDB, $p = 0.02$), the Round Stingray (SDB, $p < 0.001$), the Barred bass (SDB, $p < 0.001$), the California Halibut (SDB, $p = 0.01$), the Pacific Angelshark (TB, $p = 0.018$), the spotted bass (SDB, $p < 0.001$), and the Leopard Shark (both location, $p < 0.012$). For all other species, the association between THg and size was not statistically significant.

3.5. Factors associated with THg variation

Variation in THg was assessed separately at each site (Tab. 3. 2). The initial model included all factors (e.g. species, region, decade, genus, and year), interaction terms, and one dependent variable (e.g. log[THg], or $log[THg_{norm}]$). Animal size was also included as a covariate for the log[THg] model. For SDB, the best model describing log[THg] variation included species, region, animal size, year; and the interaction terms species*region, and species*animal size (AIC = 249.9, Adjusted-R^2 = 0.76, $F_{48, 323}$ = 21.9, p-value < 0.001). We ran models including size normalized THg concentrations ($Log[THg_{norm}]$) to correct for the effect of animal size in Hg concentrations. The best model describing $log[THg_{norm}]$ variation included species, region, and year (AIC = 197.0, Adjusted-R^2 = 0.70, $F_{37, 344}$ = 24.3, p-value < 0.001).

For TB, the best model describing log[THg] variation included species, region, animal size, year, and the interaction terms species*animal size and animal size*year (AIC = 177.6, Adjusted-R^2 = 0.97, $F_{28, 99}$ = 103.6, p-value < 0.001). The best model describing $log[THg_{norm}]$ variation included species, year, and the interaction term species*year (AIC = 154.4, Adjusted-R^2 = 0.95, $F_{22, 105}$ = 101.6, p-value < 0.001).

3.6. ***Total Hg biomagnification***

Trophic levels (calculated using eq. 3) of organisms ranged from 1.5 ± 0.3 in primary producers to 3.2 ± 0.3 in batoids for SDB, and from 1.2 ± 0.1 in primary producers to 3.1 ± 0.5 in batoids for TB (Tab. 3. 3). $\delta^{15}N$ values ranged from 15.2 ± 0.8 ‰ in batoids to 10.0 ± 1.1 ‰ in primary producers for SDB, and from 15.1 ± 1.1 ‰ in batoids to 10.0 ± 0.2 ‰ in primary producers for TB (Tab. 3. 3). Average $\delta^{15}N$ values in SDB (all species groups) was significantly different compared to TB (ANOVA, $F_{1,125} = 59.5$, $p < 0.001$). There was a significant interaction between location and species groups ($F_{4,125} = 3.01$, $p = 0.02$). For comparisons between SDB and TB within a group, no significant difference was found (e.g. TB-batoids:SDB-batoids, TB-crustacean:SDB-crustacea, TB-mollusca:SDB-mollusca, TB-polychaete:SDB-polychaete, and TB-primary producers:SDB-primary producers) (Tukey HSD posthoc, $p > 0.05$). For comparisons among groups within each location, $\delta^{15}N$ values in batoids were higher compared to all other groups for SDB ($p < 0.001$) and TB ($p < 0.04$), except compared to polychaete in SDB ($p > 0.05$). $\delta^{15}N$ values in polychaetes were higher compared to crustacea, Mollusca and primary producers for SDB ($p < 0.05$) but not significantly different in TB ($p > 0.05$) (Fig. 3. 4). No significant differences were found for $\delta^{15}N$ values between crustacean and mollusca groups in SDB ($p > 0.05$) and among crustacea, Mollusca, and polychaete in TB ($p > 0.05$) (Fig. 3. 4).

Total Hg ranged from 1.1 ± 0.3 $\mu g.g^{-1}$ in batoids to 0.02 ± 0.01 $\mu g.g^{-1}$ in primary producers for SDB, and from 1.6 ± 0.4 $\mu g.g^{-1}$ in batoids to 0.04 ± 0.03 $\mu g.g^{-1}$ in primary producers for TB (Tab. 3. 3). Average concentration of THg in SDB (all species groups) was not significantly different from TB (ANOVA, $F_{1,72} = 0.42$, $p = 0.52$). A positive and significant association was found between THg concentration and $\delta^{15}N$ values for SDB ($R^2 = 0.75$, $p < 0.001$) and TB ($R^2 = 0.7$, $p < 0.001$) (Fig. 3. 5). Trophic magnification factor (TMF, eq. 2) for SDB and TB was 1.82 and 1.99, respectively.

4. Discussion

Since 1888 and until 1960s, San Diego Bay was a disposal site for untreated domestic and industrial sewage discharges. By 1964, domestic sewage disposal had been eliminated and beginning in 1972, through the U.S. Clean Water Act, pollution control programs were implemented creating regulatory standards for the protection of residents and wildlife (Fairey et al. 1996). These standards improved

conditions in the Bay, but more than 25 years later toxicity from heavy metals and Persistent Organic Pollutants (POPs) was still pervasive in San Diego Bay especially in areas of industrial and shipping activities (Fairey et al. 1998). Currently, much of the San Diego Bay shoreline is listed on the Clean Water Act section 303(d) List of Water Quality Limited Segments for elevated levels of heavy metals in the marine sediment (CRWQCB 2012b). Specifically, recent Hg concentrations reported for sediments in San Diego Bay ranged from 0.26 $\mu g.g^{-1}$ in the Central region to 0.44 $\mu.g^{-1}$ in the North region (Bay et al. 2016). Although these levels are within the range in which toxicity effects would occasionally occur (Long et al. 1995), a decline in Hg levels is observed compared to values reported during 1990s (Fairey et al. 1998). However, Hg levels in sediment do not always reflect accumulation in biota because bioavailability of Hg is dependent on factors, such as chemical speciation, complexation, and methylation processes (Benoit et al. 1999). In the present study, we found contrasting results regarding temporal variations in Hg contamination in the biota of San Diego Bay. Significant decline trends in THg_{norm} were observed over a period of more than 10 years in *P. clathratus*, *U. halleri, P. maculatofasciatus,* and *Mytillus* sp. (THg only) ($p < 0.002$, Fig. 3. 3). In contrast, no significant trend was observed for C. aggregata*, and P. californicus* ($p > 0.28$, Fig. 3. 6). Our results suggest that Hg loads in the biota of San Diego Bay is slowly declining over time, but this trend is not consistent among all studied species. Tomales Bay is within the California Coast Range mercury mineral belt and is impacted by the legacy of historic Hg and gold mining, as well as runoff water coming from the highly mercury-mineralized rocks (Whyte and Kirchner 2000). In a landmark Hg contamination episode during 1982, this estuary received a significant amount of poorly sorted Hg-rich sediment originated from a dam failure in a Hg mine site within the Tomales Bay watershed (Whyte and Kirchner 2000). The discharge of mine waste into the Walker Creek, one of the two major streams flowing into the estuary, continued until 1999 when remediation of the mine site was concluded (Smelser and Whyte 2001). Between 1998 and 2003, the average Hg concentrations in sediments at the Walker Creek Delta ranged from 0.9 to 3.1 $\mu g.g^{-1}$, whereas other areas within the estuary ranged from 0.05 to 0.5 $\mu g.g^{-1}$ (Johnson et al. 2009). Since the remediation, cleaner sediment is burying the mining waste accumulated at the Delta, but Tomales Bay is still listed on

the Clean Water Act section 303(d) List of Water Quality Limited Segments for elevated levels of Hg (CRWQCB 2012a). In the present study, we found contrasting results regarding temporal variation in Hg contamination in the Tomales Bay. A significant decline trend in THg_{norm} over a period of more than 10 years was observed in *M. californica* ($p = 0.004$). In contrast, a non-significant trend was observed in *T. semifasciata*, *M. henlei, C. aggregate*, and *Mytillus sp.* ($p > 0.19$). Our results suggest that Hg loads in biota still reflect legacy contamination in Tomales Bay. Interestingly, when analyzing Hg loads in mussels (Fig. 3. 1), we observe greater Hg concentrations between 1997 and 2002, corresponding to the period affected by the mine dam failure. The most recent data collected in 2019 showed a lower Hg concentration level that is comparable to the period prior the contamination episode during 1982.

A previous study assessing Hg contamination trends using mussels in California also found inconsistent patterns in concentrations from 1980 to 2010 (Melwani et al. 2013). These authors reported that for one site (Coronado Bridge) in San Diego Bay a significant decline in Hg contamination was observed between 1989 (0.18 $\mu g.g^{-1}$ on average) and 2007 (0.07 $\mu g.g^{-1}$ on average), while no significant trend was observed in another site (Shelter Island) during a similar time period (1980 to 2010). They also found no significant trend for Tomales Bay from 1980 to 2010 (Melwani et al. 2013), which is consistent with our findings.

In regards to spatial variation in Hg contamination, we observed no significant variation in Hg levels in *Mytillus sp.* among the three major estuarine regions (e.g. north, central, and south). This result is similar to previous findings on Hg contamination in plankton, fish, and invertebrates from San Diego Bay (Bay et al. 2016). These authors found no significant differences in Hg concentrations among regions. They collected sport and forage fish species, and benthic invertebrates, including mollusk and crustaceans, between 2013 and 2015. Differences among regions were only observed for Hg levels in sediments and polychaetes and were greater in the central region compared to north and south (Bay et al. 2016). As stated previously, metal concentration in the sediment is not always reflected in biota (Benoit et al. 1999). An example of this is differences between the heavy metal contamination gradients and the accumulation in benthic biota found in San Diego Bay (Deheyn and Latz 2006). These authors reported an increasing

gradient in 15 elements (Hg not included) in sediment from the mouth to the back of the estuary. However, accumulation of these elements measured in transplanted brittles stars were similar throughout the estuary (Deheyn and Latz 2006). Their finding highlights the importance of using multiple organisms to assess spatial and temporal variation in contamination.

In the present study, we found a greater concentration of THg in *Mytillus* sp. in the outer region compared to inner region of Tomales Bay. The outer region is characterized by shallow sand bars with seagrass beds dominating the bottom, and where tidal exchange and upwelling control physicochemical characteristics. In the inner zones, runoff, evaporation and rainfall are the major drivers of water properties (Smith et al. 1991, Smith and Hollibaugh 1997, TBWC 2003). The inner region of Tomales Bay is also characterized by the presence of mud-flats, increased concentrations of organic matter, greater water residence time, and higher temperatures which all can favor Hg methylation by sulfate-reducing bacteria (Marvin-DiPasquale and Agee 2003). However, the outer region is where the Walker Creek Delta is located which also present a relatively large intertidal mudflat that can favor Hg methylation. Previous studies have found similar results with transplanted mussels presenting greater Hg level in the Walker Creek Delta compared to areas in the back of the estuary (Johnson et al. 2009).

4.1. Hg bioaccumulation

Hg bioaccumulation is common in aquatic organisms as Hg uptake is strongly correlated with diet (Hall et al. 1997). We found significant and positive association of THg and animal size in the majority of studied species, indicating bioaccumulation of this pollutant (Tab. 3. 2). Positive association of Hg with body size is often reported for fishes with carnivore and piscivore feeding habits, and/or occupying upper trophic levels (Cai et al. 2007). Although increasing Hg concentrations with body length is generally expected, other factors such as sexual dimorphism and ontogenetic changes in diet can mask this association driving differences in bioaccumulation patterns (Stacy and Lepak 2012).

In the present study, Hg was positively associated with fish size in species with carnivorous diets and occupying a tertiary consumer level in the trophic web (e.g. *M. californicus, U. halleri, S. californica, P. californicus, T. semifasciata, P. clathratus, P. nebulifer, P. maculatofasciatus*) (Tab. 3. 2), but also in *C.*

aggregata which feeds on zooplankton and bethic invertebrates (Miller and McGowan 2013). Fish size range is also important when assessing Hg vs. body size relationships. For example, *P. californicus* in SDB presented a positive and significant relationship, but not in TB (Tab. 3. 2). This is mainly attributed to the size range of individuals in TB (55.9 – 87.6 cm) comprising only adults, while in SDB (20.6 – 62.3 cm) juvenile and adults occurred. Similarly, for *P. interruptus* the sampled population included only adults (6.1 – 8.5 cm) and, thus, were too narrow in range. Previous studies have found a positive and significant relationship between Hg concentration and body size for this species (Loflen et al. 2018). It is worth to mention that for some species in our dataset (i.e. Mytillus sp.), Hg concentration data spanned over several decades, which added additional variability outside of the THg-size relationship.

4.2. Factors associated with THg variation

Generalized linear models designed for each study area showed that the factors that better explained THg variation were species, year, and region (Tab. 3. 4). In TB, the best model explained 95% of THg variation and included factors such as species, year, and the interaction term species*year. We interpreted this interaction term as an effect of an unbalanced design, in which not all the species occurred in all sampled years. In SDB, the best model included the same factors in addition to region, and explained 70% of THg variation. Interestingly, the effect of region was not significant in any of our models, but it was still important in describing Hg variation in this location. As discussed previously, the temporal and spatial variation observed in both study sites were accounted for in the best models. Body size was less consistent, mostly due to narrow size ranges in our samples, but still a significant factor, which highlights the importance of using size standardization for THg concentration when comparing different species, locations, and years.

4.3. ***Total Hg biomagnification***

M. californica food webs in San Diego Bay and Tomales Bay had similar structure being composed of primary producers and consumers, secondary consumers and tertiary consumers. On average, THg levels were not different between SDB and TB, and Hg biomagnification was observed on both food webs (Fig. 3. 7). The slope from the linear regression between Log[THg] and $\delta^{15}N$ values is an indicator of

biomagnifying potential in the food web (Lavoie et al. 2013). The similar trophic magnification slope (b) in TB (b = 0.34) and SDB (b = 0.30) suggest that Hg biomagnifying potential is similar between both locations. In fact, average Hg levels were not significantly different between SDB and TB, except for batoids in TB that was greater compared to SDB (Fig. 3. 7). That is likely why the Trophic magnification factor estimated for TB (TMF = 1.99) is slightly greater compared to SDB (TMF = 1.82).

Overall, we expected to find similar TMFs between SDB and TB as these areas share several similarities regarding factors affecting Hg biomagnification. Both areas are classified as low-inflow estuaries, which means that in these estuaries salinity gradient, estuarine circulation, (e.g. water residence time, and mixing rates) and the supply of nutrients depend mostly on the daily tide oscillations (Largier et al. 1997). These are all important aspects controlling physicochemical parameters and Hg transport and fate in the estuary, which also affect biomagnification process (Lavoie et al. 2013). As seen previously, food web composition was very similar between SDB and TB. As properties of organisms composing the food web is a major factor, having similar food web structure may also explain why the two estuaries having similar TMFs (Borgå et al. 2012). Latitude has been shown to be an important factor to explain variation of TMF in food webs worldwide (Lavoie et al. 2013), with higher latitudes (polar and temperate) presenting a greater biomagnification potential compared to lower tropical latitudes. The fact that, in the present study, both estuaries are located within the temperate latitude range also contributes to the similar TMF between food webs. The biggest difference between these estuaries is the source input of Hg. In SDB, Hg contamination has diffuse sources (e.g. atmospheric deposition, and urban/industrial runoff), while in TB a major portion of Hg entering the system comes from past mining activities in the watershed (Johnson et al. 2009, CRWQCB 2012b).

When comparing TMFs estimated in the present study with other food webs worldwide, the estimated values for SDB and TB are higher compared to tropical food webs. In a study conducted in contaminated and pristine areas in Brazil, the authors reported TMFs ranging from 1.19 to 1.67 (Bisi et al. 2012). Despite the fact that these tropical food webs included large marine mammals, such as the Guiana dolphin (*Sotalia guianensis*), the TMFs estimated for SDB and TB were still higher. It is worth mentioning that

these values are within the range reported for marine ecosystems in temperate (1.66 ± 1.29) and polar (1.62 ± 1.17) regions worldwide as reported by Lavoie et al., (2013). According to these authors, there are no consensus about the main variables affecting Hg biomagnification across aquatic systems. The greater TMFs found for sites in the present study compared to tropical ecosystems can be a result of large-scale latitudinal differences. For example, growth rate in fish can increase with temperatures, due to a faster metabolism and trophic transfer efficiency (O'Gorman et al. 2016), which can modulate Hg concentrations resulting in reduced accumulation as the fish grows (i.e. growth dilution) (Simoneau et al. 2005). Also, fish from colder environments has shown slower excretion rates which can facilitate Hg accumulation in temperate aquatic ecosystems compared to tropical ones (Trudel and Rasmussen 1997). Other factors known to affect Hg biomagnification includes physicochemical characteristics of the system, such as dissolved organic carbon, Hg deposition, and total phosphorus (Lavoie et al. 2013). Although we did not measure these factors, it is possible that they are also contributing to differences in TMFs between sits in the present study compared to tropical sites. We suggest these factors to be taken into account in future studies.

5. Conclusion

In the present study, we found that Hg trophodynamics in these two temperate systems are mainly controlled by species type, trophic level, and body size, with a large effect of temporal variability. Hg levels are relatively high in both locations as reported previously in the literature and a decline trend over time was observed for several fish species. The small scale of latitude variation was not sufficient to produce differences in TMFs, and the values estimated in the present study are within the range observed for other temperate sites. Our results contribute to the understanding of Hg bioaccumulation and biomagnification by providing empirical data to describe factors associated with these processes in two temperate coastal ecosystems.

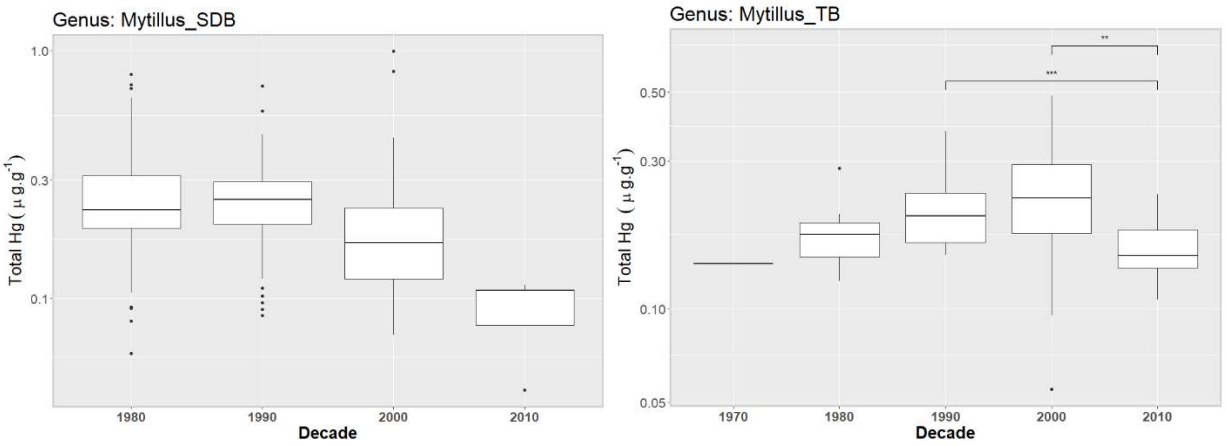

Figure 3. 1 – Boxplot of THg in mussels in SDB (left) and TB (right) across multiple decades. Significance symbols: ***p = 0.0001, **p = 0.001.

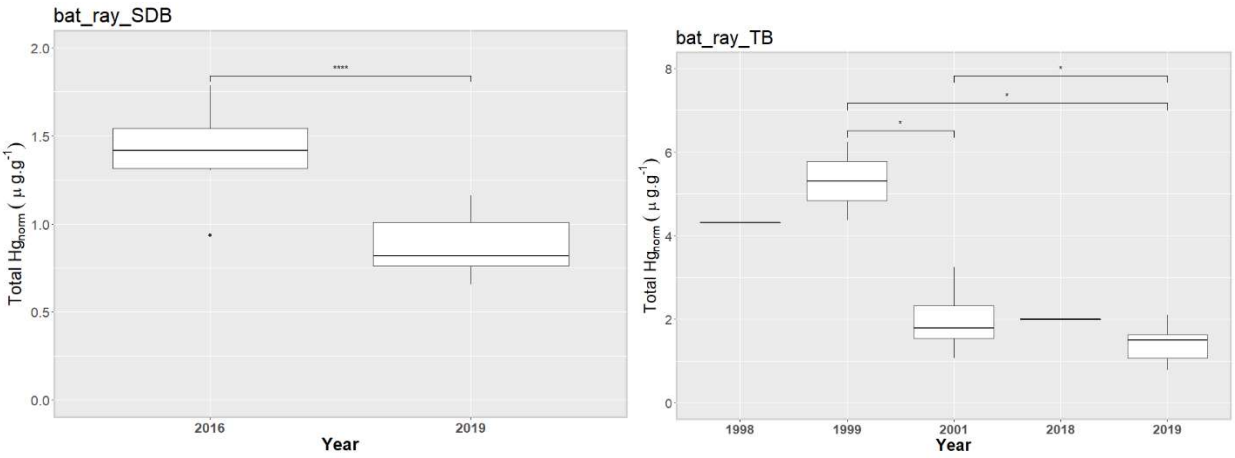

Figure 3. 2 - Boxplot of THg in Bat-ray in SDB (left) across two years. Significance symbols: ***p = 0.0001, **p = 0.001, *p = 0.01.

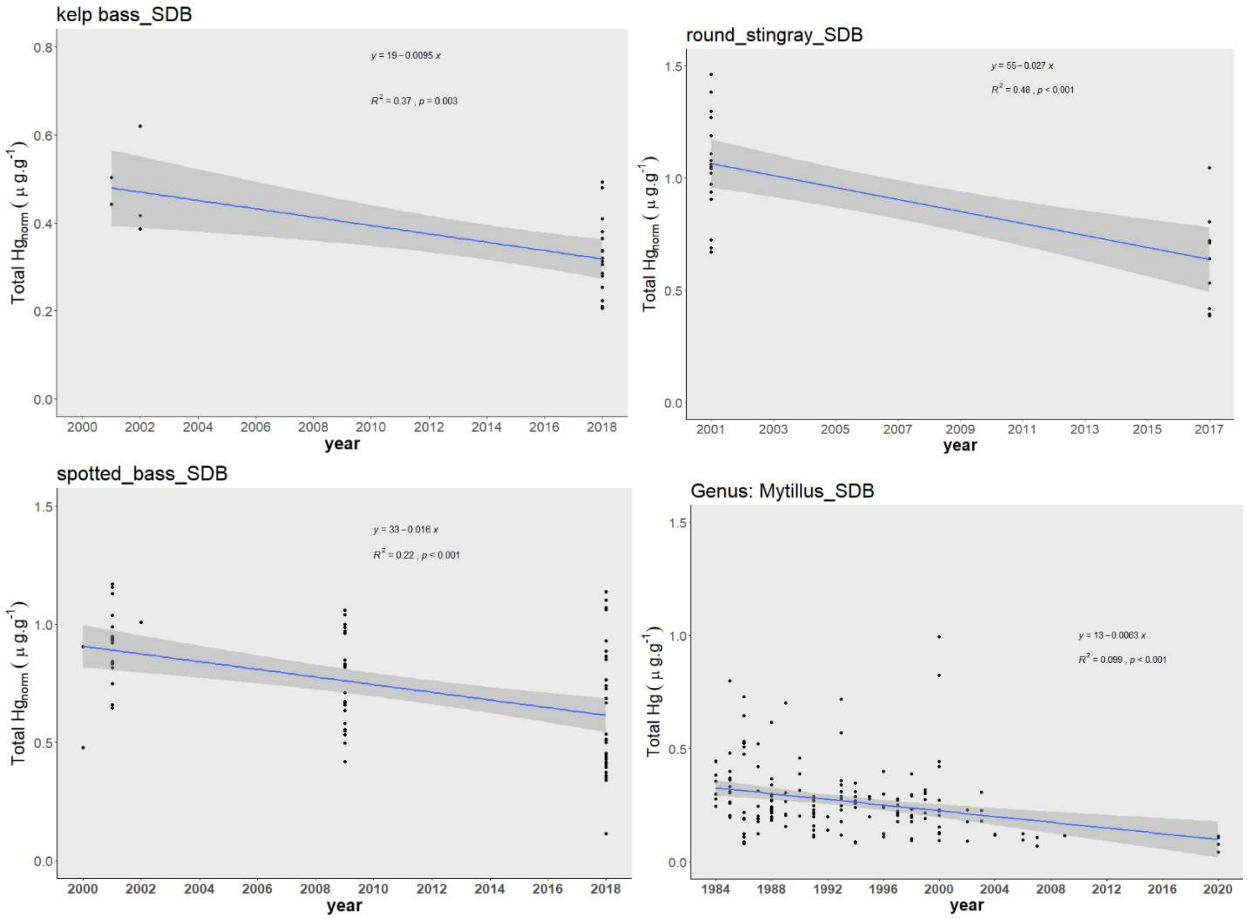

Figure 3. 3 – Significant trend lines in Total THg_{norm} for 4 studied species over more than a 10 year period in SDB.

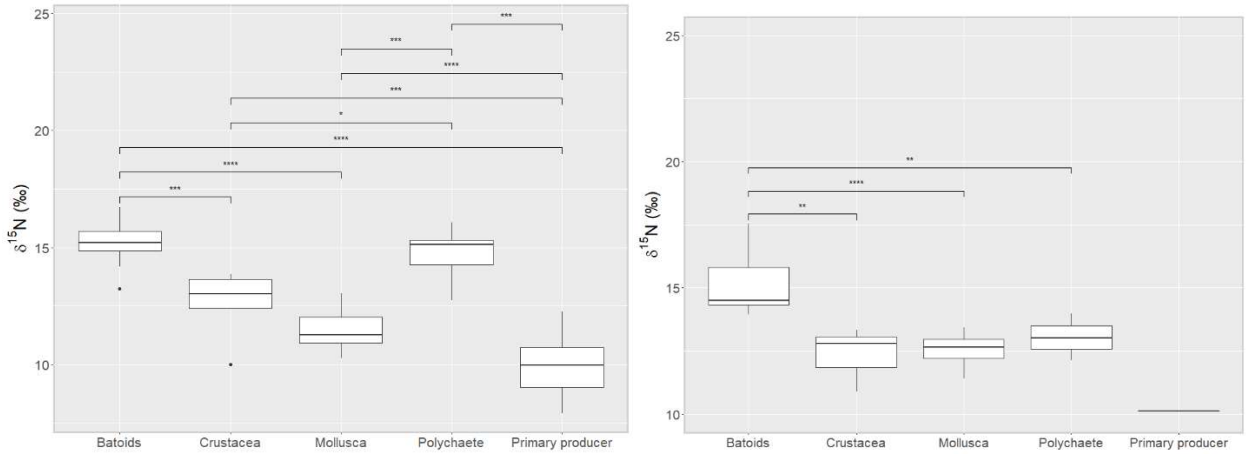

Figure 3. 4 – Boxplot of $\delta^{15}N$ values among groups in SDB (left) and TB (right).

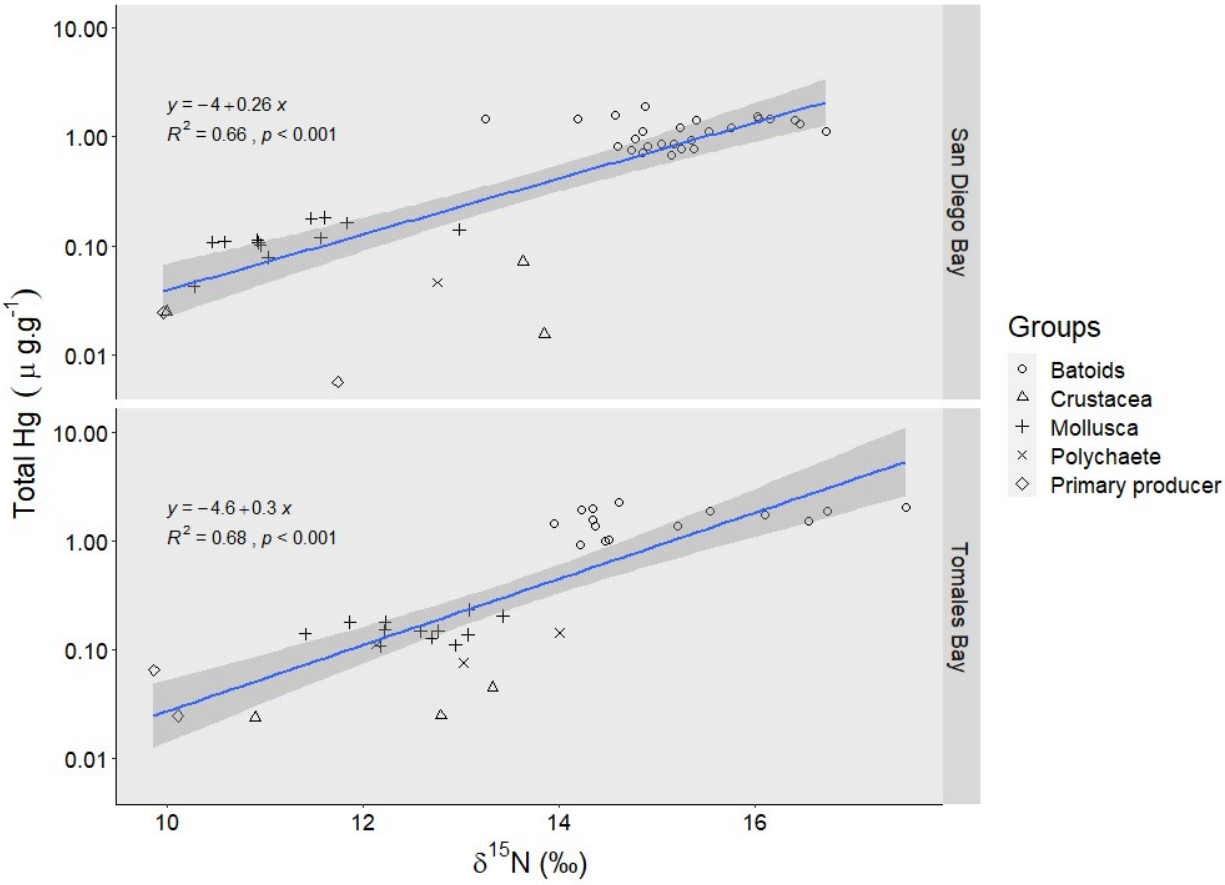

Figure 3. 5 – Linear regression of Log[THg] ppm dw vs. $\delta^{15}N$ in SDB and TB food webs.

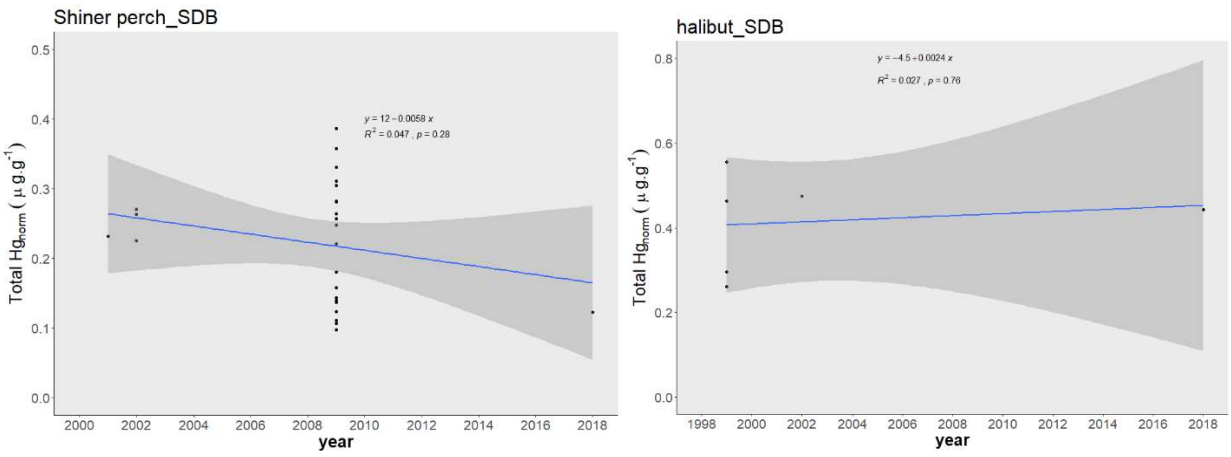

Figure 3. 6 – Non-significant trend lines in Total THg_{norm} for 2 studied species in SDB

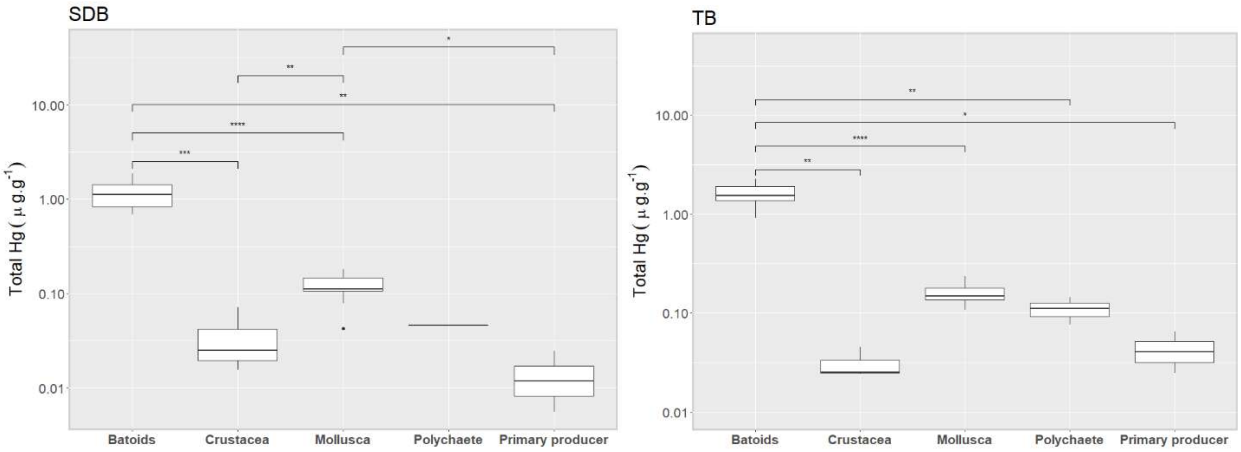

Figure 3. 7 – Boxplot of THg among groups in SDB (left) and TB (right).

Table 3. 1 – Biometric data, year range, and sample size of target species from SDB and TB.

Species	Common name	n	location	Year range	Size (cm)	Feeding habit
Cymatogaster aggregata	Shiner Perch	27	Sdb	2001 – 2018	11.7 ± 1.2 (9.3 – 15.8)	Zooplankton (and benthic invertebrates)[a]
Cymatogaster aggregata	Shiner Perch	19	tb	1998 - 2009	9.1 ± 2.4 (5.4 – 13.2)	Zooplankton (and benthic invertebrates)[a]
Embiotoca jacksoni	Black Surfperch	13	sdb	1999 - 2002	20.6 ± 6.1 (10.8 – 28.4)	invertebrates, primarily amphipods[b]
Mustelus californicus	Gray Smooth-hound Shark	20	sdb	2002 – 2009	72.1 ± 9.3 (58.6 – 92.4)	Crabs[c]
Mustelus henlei	Brown Smooth-hound Shark	16	Tb	1998 – 2009	86.6 ± 4.0 (79 – 92.4)	Crabs and fish[d]
Myliobatis californica	Bat-ray	26	Sdb	2016 – 2019	62.7 ± 8.3 (50.5 – 84.5)	Polychaete, molllusk
Myliobatis californica	Bat-ray	30	Tb	1998 – 2019	60.3 ± 12.8 (18.8 – 80)	Polychaete, molllusk
Mytillus sp.	Common Mussel	78 (16)*	Tb	1979 – 2019	5.0 ± 1.3 (2.5 – 7.0)	Filter feeding
Mytillus sp.	Common Mussel	207 (108)*	Sdb	1980 – 2020	5.6 ± 0.65 (2.5 – 7.1)	Filter feeding
Panulirus interruptus	California Spiny Lobster	19	Sdb	2013 – 2015	7.4 ± 0.5 (6.1 – 8.5)	Crustaceans and mollusks[e]
Paralabrax clathratus	Kelp Bass	22	Sdb	2001 – 2018	29.3 ± 3.9 (20.5 – 35.2)	
Paralabrax maculatofasciatus	Spotted Sand Bass	82	Sdb	1999 – 2018	30 ± 4.8 (19 – 40.3)	Decapods and fishes[f]
Paralabrax nebulifer	Barred Sand Bass	21	Sdb	1999 – 2009	33.2 ± 9 (15.3 – 49.7)	Crustaceans, mollusks, and epibenthic fishes[g]
Paralichthys californicus	California Halibut	15	Tb	1998 – 2001	66 ± 8.6 (55.9 – 87.6)	Epibenthic fishes and crustaceans[h]
Paralichthys californicus	California Halibut	6	SDB	1999 – 2018	35 ± 20.2 (20.7 – 62.3)	Epibenthic fishes and crustaceans[h]
Phanerodon furcatus	White Seaperch	11	Tb	2009	11.9 ± 2.7 (10.3 – 19.7)	Amphipods and mollusks[i]
Squatina californica	Pacific Angelshark	21	Tb	1999 – 2001	103.1 ± 3.7 (93 – 109)	Demersal fishes[j]
Triakis semifasciata	Leopard Shark	22	Tb	1999 - 2009	101.8 ± 10.8 (90 – 121.5)	Crustaceans and fishes[l]
Triakis semifasciata	Leopard Shark	5	SDB	2002	95.1 ± 23.4 (72 – 134.2)	Crustaceans and fishes[l]
Urobatis halleri	Round Stingray	28	Sdb	2001 – 2017	16.1 ± 2.3 (12.4 – 21.2)	Mollusks

* sample size of individuals with shell length information. [a] Odenweller 1975. [b] Schmitt and Holbrook (1984). [c] Talent (1982). [d] Pantoja-Echevarría et al., (2020). [e] Castañeda-Fernández et al., (2005). [f] Mendoza-carranza et al., (2000). [g] Roberts et al. (1984). [h] Plummer et al. (1983). [i] Ellison et al. (1979). [j] Escobar-Sánchez et al. (2006). [l] Russo, (1975).

Table 3. 2 – Linear regressions between THg ($ug.g^{-1}$) and animal size (cm) assessing bioaccumulation of Hg in SDB and TB food webs.

	Location	n	Slope	Intercept	R^2	P value
Common Mussels	SDB	207	0.039	0.016	0.016	0.19
	TB	78	0.040	-0.99	0.22	0.07
Shiner Perch	SDB	27	0.030	-0.13	0.16	**0.04**
	TB	19	0.045	-0.12	0.67	**<0.001**
Smooth-hound Sharks	SDB	20	0.009	-0.45	0.23	**0.03**
	TB	16	0.020	-1.1	0.55	**<0.001**
Round Stingray	SDB	28	0.050	-0.96	0.43	**<0.001**
Kelp Bass	SDB	22	0.020	-1.1	0.25	**0.018**
Barred bass	SDB	21	0.018	-0.99	0.62	**<0.001**
California Halibut	SDB	6	0.013	-0.92	0.84	**0.01**
	TB	15	0.004	-0.46	0.10	0.25
Pacific Angelshark	SDB	21	0.020	-1.8	0.26	**0.018**
Leopard Shark	SDB	5	0.012	-0.73	0.91	**0.012**
	TB	22	0.007	-0.11	0.54	**<0.001**
Black surf perch	SDB	13	-0.021	0.1	0.18	0.15
Bat-ray	SDB	26	0.002	-0.12	0.027	0.43
	TB	30	-0.004	0.45	0.12	0.06
California Spiny Lobster	SDB	19	0.011	-0.19	<0.001	0.9
Spotted Bass	SDB	82	0.018	-0.99	0.62	**<0.001**
White Seaperch	TB	11	0.018	-0.99	0.31	0.074

Table 3. 3 – Average ± Standard Deviation (range, n size) of Trophic level (TL) (calculated using eq), Total Hg, and $\delta^{15}N$ in *M. californica* food webs from San Diego Bay and Tomales Bay.

	Species group	TL	Total Hg ($\mu g.g^{-1}$) d.w	$\delta^{15}N$ (‰)
San Diego Bay				
	Batoids	3.2 ± 0.3 (2.3 – 3.8, 26)	1.1 ± 0.3 (0.7 – 1.9, 26)	15.2 ± 0.8 (13.2 – 16.7, 26)
	Crustacea	2.3 ± 0.4 (1.6 – 2.7, 6)	0.04 ± 0.03 (0.02 – 0.07, 3)	12.5 ± 1.4 (9.9 – 13.8, 6)
	Polychaete	2.9 ± 0.4 (2.4 – 3.3, 5)	0.05 (1)	14.7 ± 1.3 (12.8 – 16.1, 5)
	Mollusca	2.0 ± 0.3 (1.6 – 2.4, 16)	0.12 ± 0.04 (0.04 – 0.18, 12)	11.5 ± 0.9 (10.2 – 13.0, 16)
	Primary producer	1.5 ± 0.3 (0.9 – 2.2, 47)	0.02 ± 0.01 (0.08 – 0.18, 2)	10.0 ± 1.1 (7.2 – 12.3, 47)
Tomales Bay				
	Batoids	3.1 ± 0.5 (2.6 – 4.2, 15)	1.6 ± 0.4 (0.9 – 2.2, 15)	15.1 ± 1.1 (13.9 – 17.5, 15)
	Crustacea	1.9 ± 0.4 (1.5 – 2.2, 3)	0.03 ± 0.01 (0.02 – 0.04, 3)	12.3 ± 1.3 (10.9 – 13.3, 3)
	Polychaete	2.2 ± 0.3 (1.9 – 2.4, 3)	0.11 ± 0.03 (0.08 – 0.14, 3)	13.0 ± 0.9 (12.1 – 14.0, 3)
	Mollusca	2.0 ± 0.2 (1.7 – 2.3, 12)	0.16 ± 0.04 (0.1 – 0.2, 12)	12.5 ± 0.6 (11.4 – 13.4, 12)
	Primary producer	1.2 ± 0.1 (1.2 – 1.3, 2)	0.04 ± 0.03 (0.04 – 0.06, 2)	10.0 ± 0.2 (9.9 – 10.1, 2)

Table 3. 4 – Best generalized linear models for variation of log[THg], and log[THg_{norm}] in SDB and TB.

Models	**location**	**AIC**	**df**	**F**	**R^2**	**P value**
Log[THg_{norm}] ~ species + region + year	SDB	197	37, 344	24.3	0.70	<0.0001
Log[THg_{norm}] ~ species + year + species*year	TB	151.4	22, 105	101.6	0.95	<0.0001

References

Allen, L. G., A. M. Findlay, and C. M. Phalen. 2002. Structure and Standing Stock of the Fish Assemblages of San Diego Bay, California from 1994 to 1999. Bulletin Southern California Academy of Sciences 101:49–85.

Bay, S. M., D. J. Greenstein, A. N. Parks, and C. Q. T. Zeeman. 2016. Assessment of Bioaccumulation in San Diego Bay. Technical report 953.

Benoit, J. M., C. C. Gilmour, R. P. Mason, and A. Heyes. 1999. Erratum: Sulfide controls on mercury speciation and bioavailability to methylating bacteria in sediment pore waters (Environmental Science and Technology (1999) 33 (951-957)). Environmental Science and Technology 33:1780.

Bentzen, R., J. M. Castellini, R. Gerlach, C. Dykstra, and T. O'Hara. 2016. Mercury concentrations in Alaska Pacific halibut muscle relative to stable isotopes of C and N and other biological variables. Marine Pollution Bulletin 113:110–116.

Bisi, T. L., G. Lepoint, A. D. F. Azevedo, P. R. Dorneles, L. Flach, K. Das, O. Malm, and J. Lailson-Brito. 2012. Trophic relationships and mercury biomagnification in Brazilian tropical coastal food webs. Ecological Indicators 18:291–302.

Borgå, K., K. A. Kidd, D. C. G. Muir, O. Berglund, J. M. Conder, F. A. P. C. Gobas, J. Kucklick, O. Malm, and D. E. Powellkk. 2012. Trophic magnification factors: Considerations of ecology, ecosystems, and study design. Integrated Environmental Assessment and Management 8:64–84.

Burkhard, L. P., K. Borgaìš, D. E. Powell, P. Leonards, D. C. G. Muir, T. F. Parkerton, and K. B. Woodburn. 2013. Improving the quality and scientific understanding of trophic magnification factors (TMFs). Environmental Science and Technology 47:1186–1187.

Cai, Y., J. R. Rooker, G. A. Gill, and J. P. Turner. 2007. Bioaccumulation of mercury in pelagic fishes from the northern Gulf of Mexico. Canadian Journal of Fisheries and Aquatic Sciences 64:458–469.

Conder, J. M., F. A. P. C. Gobas, K. Borgå, D. C. G. Muir, and D. E. Powell. 2012. Use of trophic magnification factors and related measures to characterize bioaccumulation potential of chemicals. Integrated Environmental Assessment and Management 8:85–97.

CRWQCB, C. R. W. Q. C. B. 2012a. Total Maximum Daily Load (TMDL) for Mercury in Tomales Bay. Staff Report. California Regional Water Quality Control Board. San Francisco Bay Region.

CRWQCB, C. R. W. Q. C. B. 2012b. Cleanup and Abatement Order, Shipyard Sediment Site, San Diego Bay, National Steel and Shipbuilding Co., BAE Systems San Diego Ship Repair, Inc., City of San Diego, Campbell Industries, San Diego Gas and Electric, United States Navy, and San Diego Unified.

DeForest, D. K., K. V. Brix, and W. J. Adams. 2007. Assessing metal bioaccumulation in aquatic environments: The inverse relationship between bioaccumulation factors, trophic transfer factors and exposure concentration. Aquatic Toxicology 84:236–246.

Deheyn, D. D., and M. I. Latz. 2006. Bioavailability of metals along a contamination gradient in San Diego Bay (California, USA). Chemosphere 63:818–834.

Ellison, J. P., C. Terry, and J. S. Stephens. 1979. Food resource utilization among five species of embiotocids at King Harbor, California, with preliminary estimates of caloric intake. Marine Biology 52:161–169.

Escobar-Sánchez, O., L. A. Abitia-Cárdenas, and F. Galván-Magaña. 2006. Food habits of the Pacific angel shark Squatina californica in the southern Gulf of California, Mexico. Cybium 30:91–97.

Fairey, R., C. Bretz, S. Lamerdin, J. Hunt, B. Anderson, S. Tudor, C. J. Wilson, F. LaCaro, M. Stephenson, M. Puckett, and E. Long. 1996. CHEMISTRY, TOXICITY AND BENTHIC COMMUNITY CONDITIONS IN SEDIMENTS OF THE SAN DIEGO BAY REGION. Santa Cruz, CA.

Fairey, R., C. Roberts, M. Jacobi, S. Lamerdin, R. Clark, J. Downing, E. Long, J. Hunt, B. Anderson, J. Newman, R. Tjeerdema, M. Stephenson, and C. Wilson. 1998. Assessment of sediment toxicity and chemical concentrations in the San Diego Bay region, California, USA. Environmental Toxicology & Chemistry/ SETAC 17:1570–1581.

Gassel, M., R. K. Brodberg, and K. Bangia. 2013. Health Advisory and Guidelines for Eating Fish From San Diego Bay (San Diego County). Special Report from the Office of Environmental Health Hazard Assessment California Environmental Protection Agency. San Diego, California.

Van Geest, J. L., D. G. Poirier, P. K. Sibley, and K. R. Solomon. 2010. Measuring bioaccumulation of contaminants from field-collected sediment in freshwater organisms: A critical review of laboratory methods. Environmental Toxicology and Chemistry 29:2391–2401.

Gobas, F., and H. Morrison. 2000. Bioconcentration and biomagnification in the aquatic environment. Pages 189–231 *in* R. Boethling and D. Mackay, editors. Handbook of property estimation methods for chemicals, environmental and health sciences. Boca Raton (FL): CRC.

Hall, B. D., R. A. Bodaly, R. J. P. Fudge, J. W. M. Rudd, and D. M. Rosenberg. 1997. Food as the dominant pathway of methylmercury uptake by Fish. Water, Air, and Soil Pollution 100:13–24.

Hammerschmidt, C. R., and W. F. Fitzgerald. 2006a. Methylmercury in freshwater fish linked to atmospheric mercury deposition. Environmental Science and Technology 40:7764–7770.

Hammerschmidt, C. R., and W. F. Fitzgerald. 2006b. Methylmercury cycling in sediments on the continental shelf of southern New England. Geochimica et Cosmochimica Acta 70:918–930.

Hussey, N. E., J. Brush, I. D. McCarthy, and A. T. Fisk. 2010. δ15N and δ13C diet-tissue discrimination factors for large sharks under semi-controlled conditions. Comparative Biochemistry and Physiology - A Molecular and Integrative Physiology 155:445–453.

Johnson, B. E., B. K. Esser, D. C. Whyte, P. M. Ganguli, C. M. Austin, and J. R. Hunt. 2009. Mercury

accumulation and attenuation at a rapidly forming delta with a point source of mining waste. Science of the Total Environment 407:5056–5070.

Komoroske, L. M., R. L. Lewison, J. a Seminoff, D. D. Deheyn, and P. H. Dutton. 2011. Pollutants and the health of green sea turtles resident to an urbanized estuary in San Diego, CA. Chemosphere 84:544–552.

Lamborg, C. H., C. R. Hammerschmidt, K. L. Bowman, G. J. Swarr, K. M. Munson, D. C. Ohnemus, P. J. Lam, L.-E. Heimbürger, M. J. a. Rijkenberg, and M. a. Saito. 2014. A global ocean inventory of anthropogenic mercury based on water column measurements. Nature 512:65–68.

Largier, J. L., J. T. Hollibaugh, and S. V. Smith. 1997. Seasonally hypersaline estuaries in Mediterranean-climate regions. Estuarine, Coastal and Shelf Science 45:789–797.

Lavoie, R. A., T. D. Jardine, M. M. Chumchal, K. A. Kidd, and L. M. Campbell. 2013. Biomagnification of mercury in aquatic food webs: A worldwide meta-analysis. Environmental Science and Technology 47:13385–13394.

Lenihan, H., J. Oliver, and M. Stephenson. 1990. Changes in hard bottom communities related to boat mooring and tributyltin in San Diego Bay a natural experiment . Marine Ecology Progress Series 60:147–159.

Loflen, C. L., T. Buck, A. Bonnema, and W. A. Heim. 2018. Pollutant bioaccumulation in the California spiny lobster (Panulirus interruptus) in San Diego Bay, California, and potential human health implications. Marine Pollution Bulletin 128:585–592.

Long, E. R., D. D. Macdonald, S. L. Smith, and F. D. Calder. 1995. Incidence of adverse biological effects within ranges of chemical concentrations in marine and estuarine sediments. Environmental Management 19:81–97.

Marvin-DiPasquale, M., and J. L. Agee. 2003. Microbial Mercury Cycling in Sediments of the San

Francisco Bay-Delta. Estuaries 26:1517–1528.

Mason, R. P., A. L. Choi, W. F. Fitzgerald, C. R. Hammerschmidt, C. H. Lamborg, A. L. Soerensen, and E. M. Sunderland. 2012. Mercury biogeochemical cycling in the ocean and policy implications. Environmental research 119:101–17.

Melwani, A. R., J. A. Davis, D. Gregorio, J. Jin, M. Stephenson, K. Maruya, D. Crane, and G. Lauenstein. 2013. Mussel Watch Monitoring in California: Long-term Trends in Coastal Contaminants and Recommendations for Future Monitoring:67.

Miller, E. F., and J. A. McGowan. 2013. Faunal shift in southern california's coastal fishes: A new assemblage and trophic structure takes hold. Estuarine, Coastal and Shelf Science 127:29–36.

Morel, F. M. M., A. M. L. Kraepiel, and M. Amyot. 1998. The chemical cycle and bioaccumulation of mercury. Annual Review of Ecology and Systematics:543–566.

O'Gorman, E. J., Ó. P. Ólafsson, B. O. L. Demars, N. Friberg, G. Guðbergsson, E. R. Hannesdóttir, M. C. Jackson, L. S. Johansson, Ó. B. McLaughlin, J. S. Ólafsson, G. Woodward, and G. M. Gíslason. 2016. Temperature effects on fish production across a natural thermal gradient. Global change biology 22:3206–3220.

Plummer, K. M., E. E. Demartini, and D. A. Roberts. 1983. The feeding habits and distribution of juvenile-small adult California halibut (Paralichthys californicus) in coastal waters off northern San Diego County. California Cooperative Oceanic Fisheries Investigations Reports 24:194–201.

Post, D. M. 2002. Using stable isotopes to estimate trophic position: models, methods, and assumptions. Ecology 83:703–718.

Roberts, D. A., E. E. Demartini, and K. M. Plummer. 1984. The feeding habits of juvenile-small adult barred sand bass (Paralabrax nebulifer) in nearshore waters off northern San Diego County. California Cooperative Oceanic Fisheries Investigations Reports 25:105–111.

Russo, R. A. 1975. Observations on the food habits of leopard sharks (Triakis semifasciata) and brown smoothhounds (Mustelus henlei). California Fish and Game 61:95–103.

Schäfer, S., G. Buchmeier, E. Claus, L. Duester, P. Heininger, A. Körner, P. Mayer, A. Paschke, C. Rauert, G. Reifferscheid, H. Rüdel, C. Schlechtriem, C. Schröter-Kermani, D. Schudoma, F. Smedes, D. Steffen, and F. Vietoris. 2015. Bioaccumulation in aquatic systems: Methodological approaches, monitoring and assessment. Environmental Sciences Europe 27.

Schneider, L., W. Maher, A. Green, and R. C. Vogt. 2013. Mercury contamination in reptiles: An emerging problem with consequences For wild life and human health. Pages 173–232 *in* K.-H. Kim and R. J. C. Brown, editors. Mercury: sources, applications and health impacts. Nova Science Publishers.

Scudder Eikenberry, B. C., K. Riva-Murray, C. D. Knightes, C. A. Journey, L. C. Chasar, M. E. Brigham, and P. M. Bradley. 2015. Optimizing fish sampling for fish-mercury bioaccumulation factors. Chemosphere 135:467–473.

Simoneau, M., M. Lucotte, S. Garceau, and D. Laliberté. 2005. Fish growth rates modulate mercury concentrations in walleye (Sander vitreus) from eastern Canadian lakes. Environmental Research 98:73–82.

Slotton, D. G., S. M. Ayers, T. H. Suchanek, W. R. D, and A. M. Liston. 2004. Mercury bioaccumulation and trophic transfer in the Cache Creek Watershed, California, in relation to diverse aqueous mercury exposure conditions. Report for the CALFED Bay-Delta Agency:137.

Smelser, M., and D. Whyte. 2001. Remediation of the Gambonini Mercury Mine, Marin County, California. Engineering Geology Practice in Northern California, California Division of Mines and Geology Bulletin.

Smith, S. V., J. T. Hollibaugh, S. J. Dollar, and S. Vink. 1991. Tomales bay metabolism: C N P

stoichiometry and ecosystem heterotrophy at the land-sea interface.

Smith, S. V, and J. T. Hollibaugh. 1997. Annual cycle and interannual variability of ecosystem metabolism in a temperate climate embayement. Ecological monographs 67:509–533.

Stacy, W. L., and J. M. Lepak. 2012. Relative influence of prey mercury concentration, prey energy density and predator sex on sport fish mercury concentrations. Science of the Total Environment 437:104–109.

TBWC. 2003. Tomales Bay Watershed Stewardship Plan: A Framework for Action. Tomales Bay Watershed Council Report. 137p.

Trudel, M., and J. B. Rasmussen. 1997. Modeling the elimination of mercury by fish. Environmental Science and Technology 31:1716–1722.

UNEP. 2013. Global Mercury Assessment 2013: Sources, Emissions, Releases and Environmental Transport. UNEP Chemicals Branch, Geneva, Switzerland.

US EPA. 2007. Method 7473 (SW-846): Mercury in Solids and Solutions by Thermal Decomposition, Amalgamation, and Atomic Absorption Spectrophotometry. Methods:1–17.

Walters, D. M., T. D. Jardine, B. S. Cade, K. A. Kidd, D. C. G. Muir, and P. Leipzig-Scott. 2016. Trophic Magnification of Organic Chemicals: A Global Synthesis. Environmental Science and Technology 50:4650–4658.

Watras, C. J., R. C. Back, S. Halvorsen, R. J. M. Hudson, K. A. Morrison, and S. P. Wente. 1998. Bioaccumulation of mercury in pelagic freshwater food webs. Science of the Total Environment 219:183–208.

Whyte, D. C., and J. W. Kirchner. 2000. Assessing water quality impacts and cleanup effectiveness in streams dominated by episodic mercury discharges. Science of the Total Environment 260:1–9.